The ecological role of the fish-derived kairomone 5α-cyprinol sulfate in shaping *Daphnia* vertical migration and risk perception



Doctoral thesis

for

the award of the doctoral degree

of the Faculty of Mathematics and Natural Sciences

of the University of Cologne

submitted by

Johanna Ahlers

Köln, 2025

Reviewers:

Prof. Dr. Eric von Elert

Prof. Dr. Patrick Fink

Table of Contents

Abstract **1**

General Introduction **3**

Chapter 1: Mesocosm experiments validate induction of *Daphnia* vertical migration by the fish-derived kairomone 5α-cyprinol sulfate **9**

1.1 Abstract 9
1.2 Introduction 10
1.3 Methods 11
1.4 Results 14
1.5 Discussion 22
1.6 Author contribution statement 25
1.7 Acknowledgements 25
1.8 References 26
1.9 Supporting information 31

Chapter 2: "Landscape of fear" in diel vertical migration: 5-alpha-cyprinol sulfate shapes the temporal and spatial dynamics of the perceived risk of predation in *Daphnia* **60**

2.1 Abstract 60
2.2 Introduction 61
2.3 Methods 64
2.4 Results 69
2.5 Discussion 76
2.6 Author contribution statement 82
2.7 Acknowledgements 83
2.8 References 84
2.9 Supporting information 90

Chapter 3: "Signals in flux: Investigating the seasonal turnover of the cyprinid kairomone 5α-cyprinol sulfate" **95**

3.1 Abstract 95
3.2 Introduction 96
3.3 Methods 99
3.4 Results 107
3.5 Discussion 116
3.6 Author contribution statement 122
3.7 Acknowledgements 122
3.8 References 124
3.9 Supporting information 129

General Discussion **132**

General References **139**

Declaration for the Doctoral Thesis ..... Fehler! Textmarke nicht definiert.

List of Publications **145**

Acknowledgements **146**

Abstract

In freshwater ecosystems, predator-prey interactions shape trophic relationships, nutrient dynamics, and species distributions. As key herbivorous zooplankton and while also serving as prey for planktivorous fish, *Daphnia* link primary production to higher trophic levels. In response to predation, *Daphnia* exhibit a range of inducible defenses triggered by chemical cues, so-called kairomones. One of the most prominent behavioral defenses is diel vertical migration (DVM), a daily movement through the water column that helps reduce predation risk. During this cycle, *Daphnia* descend to cooler, darker depths at daybreak and return to surface waters after dusk. While DVM has long been recognized as a predator-avoidance strategy, the identity of the chemical signal driving this response remained unknown until recently. The bile salt 5α-cyprinol sulfate (CPS), excreted by cyprinid fish, was identified as the kairomone responsible for inducing DVM in *Daphnia magna*. However, its ecological relevance under natural conditions and its role in shaping zooplankton behavior in the field had yet to be confirmed. The aim of this dissertation was to investigate the ecological role, distribution, and dynamics of CPS in natural lake ecosystems. Specifically, I addressed three questions: (1) Can CPS alone induce DVM in *Daphnia* under natural conditions? (2) How do spatial and temporal variations in CPS concentration define a chemical landscape of fear? (3) What determines the production and degradation of CPS in aquatic environments? In the first study, a mesocosm experiment was conducted in a natural lake to test whether purified CPS can trigger DVM in a field-derived *Daphnia* community. Exposure to nanomolar concentrations of CPS caused a significant downward shift in daytime vertical distribution. The response was dose-dependent and reversible, confirming that CPS is a behaviorally active infochemical in natural conditions. Chemical analysis using high-performance liquid chromatography–mass spectrometry (HPLC-MS) verified that these concentrations are within the range observed in the lake, validating the

ecological relevance of CPS as a kairomone. The second study explored diel and seasonal CPS dynamics in Lake Klostersee and investigated how this chemical cue contributes to a spatially and temporally variable landscape of fear. CPS concentrations varied markedly with depth and time, likely peaking during periods of increased fish activity. Bioassays with *Daphnia longispina* clones revealed genotypic variation in sensitivity to CPS, with individual thresholds differing by several orders of magnitude. These results show that even within a single population, prey interpret the same chemical landscape differently, resulting in diverse behavioral outcomes. The third study examined the production and degradation of CPS under controlled and natural conditions. Laboratory feeding experiments demonstrated that CPS excretion was closely linked to fish feeding intensity and not to fish size. In parallel, degradation experiments revealed rapid microbial breakdown of CPS in lake water, with temperature strongly accelerating the process. A temperature-dependent model predicted that more than 80% of CPS can be degraded within 24 hours under summer conditions. These findings indicate that CPS is a short-lived signal, reflecting real-time predator activity rather than long-term predator presence. Taken together, the three studies demonstrate that CPS functions as a powerful, transient, and ecologically relevant kairomone in freshwater systems. CPS not only induces DVM in *Daphnia* but also creates a dynamic chemical landscape of fear that varies in time and space and is interpreted differently by genetically diverse prey. The results establish CPS as a key link between predator behavior and ecosystem function, offering new insights into chemically mediated interactions and their role in structuring freshwater food webs.

General Introduction

Aquatic ecosystems are complex and dynamic environments shaped by a multitude of biotic and abiotic interactions (Brönmark and Hansson 2012). Among these, predator-prey relationships are mediated not only through direct trophic links but also by nuanced chemical signals that transmit information across species boundaries (Rajchard 2013; von Elert and Pohnert 2000). In freshwater systems, chemical cues play a critical role in modulating prey responses, influencing behavior, morphology, and life-history strategies (Dodson 1988; Weider and Pijanowska 1993; Tollrian 1995). One of the most ecologically important classes of these cues are kairomones, compounds released by predators that, while not beneficial to the emitter, can trigger adaptive responses in prey (Brown et al. 1970). Chemical communication is particularly favored in freshwater environments such as lakes and ponds, where low water flow, stable stratification, and limited light penetration reduce the reliability of visual cues. These conditions make chemical cues more persistent and detectable, allowing prey organisms like *Daphnia* to assess predation risk with high accuracy (Kats and Dill 1998; Hahn et al. 2019).

A major breakthrough in aquatic chemical ecology has been the identification of 5α-cyprinol sulfate (CPS) as a biologically active kairomone that induces diel vertical migration (DVM) in *Daphnia*, a genus of freshwater crustaceans central to lake food webs (Hahn et al. 2019). Prior to this, isolating and identifying a specific fish kairomone had remained elusive due to the complexity of aquatic chemical mixtures and the minute concentrations of active compounds (von Elert and Loose 1996; von Elert and Pohnert 2000). The discovery of CPS not only filled a longstanding knowledge gap but also provided the first chemically characterized, field-relevant fish kairomone.

CPS, a bile salt excreted through the gills and gut of cyprinid fishes, acts as a potent chemical signal linking predator metabolism to prey behavior and ecosystem processes (Polkinghorne et al. 2001; Brant et al. 2013). Its identification has opened new experimental frontiers, allowing the manipulation of predator-induced fear in situ (Hahn and von Elert 2022). Advances in analytical chemistry, particularly liquid chromatography–mass spectrometry (LC-MS), now allow for the quantification of CPS at nanomolar to picomolar concentrations, facilitating the real-time mapping of predator-induced landscapes of fear.

Chemical signaling in aquatic environments exemplifies a broader ecological principle: interactions are often mediated not by direct contact but by information exchange through molecules (Pohnert et al. 2007; Brönmark and Hansson 2012). This insight aligns aquatic research with broader developments in chemical ecology and evolutionary biology, where infochemicals are recognized as key drivers of adaptation and speciation (Müller et al. 2020). As climate change alters predator-prey dynamics and affects the physical and chemical properties of aquatic environments, understanding the role and resilience of chemically mediated cues becomes increasingly important for predicting ecosystem responses (Draper and Weissburg 2019; Roggatz et al. 2022).

Freshwater crustaceans of the genus *Daphnia* hold a pivotal position in freshwater ecosystems (Ebert 2022). Particularly large-bodied species act as keystone organisms, simultaneously exerting strong top-down control on algal primary producers and serving as a crucial food source for planktivorous fish (Ogorelec et al. 2021). As both consumer and prey, *Daphnia* experiences intense predation pressure, especially from fish, which has been shown to drive rapid evolutionary changes in life-history and morphological traits (de Meester et al. 1999; Cousyn et al. 2001). This predation pressure manifests through two distinct pathways:

consumptive effects, where predators reduce prey abundance through direct mortality, and non-consumptive effects, where the mere presence or chemical cues of predators induce adaptive changes in prey phenotypes. Early work focused primarily on consumptive effects, such as size-selective predation and its consequences for survival and community structure (Brooks and Dodson 1965; Gliwicz 1986). More recently, however, research has emphasized the importance of non-consumptive effects, showing that predator cues alone can induce profound behavioral, morphological, and developmental responses which in itself, without consumptive effects, can result in rapid evolutionary responses on the community level (Scrosati 2021, Zhang et al. 2022). Owing to its diverse and well-characterized inducible defenses, *Daphnia* has become a model organism for studying such predator-induced plasticity, particularly in response to fish-derived chemical signals (Lass and Spaak 2003; Diel et al. 2020; Engel et al. 2014). These inducible defenses include alterations in life-history traits, body shape, and behavior (Miner et al. 2012; Tollrian 1995; Boersma et al. 1998). Among them, diel vertical migration is one of the most extensively studied behavioral adaptations (Stich and Lampert 1981). It is part of the largest synchronized daily animal movement on Earth (Brierley 2014), with *Daphnia* populations in lakes shifting tens of meters between sunlit, food-rich surface layers at night and the cold, dark hypolimnion during the day. This migration reflects a finely tuned trade-off between optimizing growth and avoiding visual predators (Loose and Dawidowicz 1994). While multiple factors, such as ultraviolet radiation, can influence DVM patterns, the primary driver in predator-prey contexts is fish-released kairomones (Stich and Lampert 1981; Rose et al. 2012). These cues, in combination with changes in light intensity, signal risk to *Daphnia*, triggering a descent into deeper waters that serve as refuges from predation (Hahn et al. 2019; Hahn and von Elert 2022; Ahlers and Hahn et al. 2024).

The ecological significance of diel vertical migration (DVM) lies in its capacity to influence population dynamics and drive cascading effects across food webs. By altering the spatial and temporal distribution of zooplankton, this behavior influences primary production, nutrient cycling, carbon transport, algal community composition, and even fish recruitment (Reichwaldt and Stibor 2005; Haupt et al. 2010). It effectively couples benthic and pelagic processes and restructures the vertical organization of lake ecosystems (Hays 2003). DVM therefore provides an exceptional model for linking individual-level decision-making with large-scale ecosystem functioning. Understanding the chemical cues that trigger this migration is critical for unraveling the mechanistic basis of predator-prey interactions and their cascading ecological effects.

Comparable ecosystem-wide consequences of fear-driven behavior have long been recognized in terrestrial systems, where prey adjust their spatial patterns in response to predation risk. This gave rise to the concept of a "landscape of fear," which describes how non-lethal predator effects shape prey behavior, habitat use, and ultimately ecosystem structure (Laundré et al. 2001). Notably, the concept finds a powerful aquatic analogue in the spatial and temporal distribution of CPS (Gaynor et al. 2019). Just as elk avoid wolf-dominated valleys, or rodents forage under cover to evade aerial predators, *Daphnia* respond to chemical gradients of risk in the water column. This cross-ecosystem parallel underscores the universality of fear as a shaping force in ecological communities.

Despite the central role of CPS in inducing DVM, fundamental questions remain about its ecological role, production dynamics, and spatial distribution. This dissertation addresses three central research objectives: (1) Can purified CPS alone trigger DVM in natural *Daphnia* communities under field conditions? (2) What are the spatial and temporal patterns of CPS

concentration in lakes, and how do these patterns contribute to a dynamic chemical landscape of fear? (3) What governs the production and degradation of CPS, and how are these processes shaped by environmental factors, especially temperature?

The thesis is structured around three empirical studies. Chapter 1 presents a mesocosm experiment conducted in a natural lake, in which CPS concentrations were manipulated in large in-lake enclosures, so called mesocosms. The vertical distribution of *Daphnia* was tracked to determine behavioral responses. Results showed that nanomolar concentrations of CPS reliably induced significant downward migration during the day. The response was dose-dependent and reversible, confirming that CPS is a behaviorally active kairomone under natural conditions and establishing an ecologically relevant concentration threshold.

Chapter 2 explores the spatial and temporal variability of CPS in Lake Klostersee. Using depth profiling and liquid chromatography–mass spectrometry (LC-MS), the study reveals strong vertical and temporal gradients in CPS concentration, with peak levels likely corresponding to periods of intense fish activity. Bioassays using locally collected *Daphnia* clones show significant variation in sensitivity to CPS, suggesting genotypic differences in risk perception among individuals. These findings support the concept of a shifting chemical landscape of fear, an environment where predation risk is experienced not uniformly, but as a mosaic that changes in space and time.

Chapter 3 examines the mechanisms that govern the production and degradation of CPS. Feeding trials reveal that CPS excretion scales with fish feeding rates, directly linking kairomone release to predator feeding activity. Degradation experiments demonstrate rapid microbial breakdown of CPS, with rates increasing significantly at higher temperatures. A Q10-

based model indicates that more than 80% of CPS can be degraded per day under warm conditions. This shows that CPS is a short-lived, dynamic signal that reflects real-time predator presence rather than serving as a persistent environmental cue.

In summary, this thesis provides a detailed and mechanistic understanding of how predator-released kairomones, specifically CPS, structure aquatic ecosystems by mediating prey behavior. It reveals that diel vertical migration in *Daphnia* is not merely a fixed response to the presence of predators but a flexible, context-dependent strategy shaped by the rapid flux of chemical information in the environment. By integrating behavioral assays, field experiments, and chemical analytics, this research advances a chemically explicit framework for studying predator-prey interactions. It underscores the importance of transient, non-consumptive effects in shaping ecological outcomes and offers new tools and perspectives for exploring the chemical dimensions of fear in aquatic food webs. The findings establish CPS as a central mediator of freshwater trophic dynamics, linking molecular-scale interactions to whole-ecosystem processes, and highlight *Daphnia* as a powerful model for understanding the role of inducible defenses in ecological and evolutionary contexts.

Chapter 1: Mesocosm experiments validate induction of *Daphnia* vertical migration by the fish-derived kairomone 5α-cyprinol sulfate

1.1 Abstract

The fish-derived bile salt 5α-cyprinol sulfate (CPS) has been identified as a kairomone inducing the predator avoidance behavior "diel vertical migration" (DVM) in *Daphnia magna* in response to fish. However, conclusions about the ecological significance of CPS have been derived from laboratory experiments only. Using a mesocosm approach, we investigate whether the role of CPS as a kairomone can be confirmed in the field. We demonstrate that CPS induces downward migration during daytime in a field-derived *Daphnia* community mainly consisting of *D. longispina* and *D. cucullata* within the experiment. In the study lake, the actual population of *D. longispina* shows a similar pattern of DVM, while concomitant quantification of CPS by HPLC-MS confirms that CPS in-situ concentrations are sufficiently high for induction of daytime downward migration of *D. longispina* in this oligo-mesotrophic lake. Together, these observations infer that CPS is a significant kairomone inducing DVM-like behavior in *Daphnia*.

1.2 Introduction

Infochemicals that mediate perception of predators by prey and which impart a benefit to the receiving organism while not being beneficial for the producer, are termed kairomones (Pohnert et al. 2007). Such chemical signaling has been well-established for inducible defenses in freshwater systems, in particular within predator-prey systems by planktivorous fish and prey organisms of the genus *Daphnia*. In response to kairomones from fish, *Daphnia* spp. deploy several inducible defenses against zooplanktivores including life history changes (e.g. earlier reproduction, smaller size at first reproduction; von Elert and Stibor 2006; Hahn and von Elert 2020), morphological defensive structures, (e.g. helmets; Laforsch and Tollrian 2004; Hahn and von Elert 2022), and diel vertical migration (DVM; Loose 1993a).

DVM in response to fish describes the daytime migration of zooplankton into the dark hypolimnion of a waterbody, which can serve as a refuge from visually-oriented predators (Ringelberg et al. 1991). During nighttime, zooplankton migrate back into the epilimnion. The metabolic costs associated with DVM (Loose and Dawidowicz 1994) are compensated by reduced predation losses (Lampert 1993). DVM contributes substantially to vertical nutrient transport (Haupt et al. 2009; Haupt et al. 2010) and to the biological carbon pump in marine systems (Brierley 2014), while also affecting foraging of planktivorous fish and distribution of phytoplankton biomass (Haupt et al. 2009; Reichwaldt and Stibor 2005).

Recently, a first fish-derived kairomone that induces DVM in *Daphnia magna* has been identified (Hahn et al. 2019). The only other identified kairomone perceived by *Daphnia* reported are fatty acids conjugated to the amino group of glutamine that are released by larvae of the insect Chaoborus (Weiss et al. 2018). In both cases kairomone identification was based on small-scale laboratory bioassays. For identification of the fish kairomone, DVM of a

D. magna clone was investigated in tubes of 1-m length in which the temperature stratification of a lake was simulated while the length of the water column and the temperature-, light- and food regime diverged from natural conditions (von Elert and Loose 1996). Using a clone of *D. magna*, the DVM-inducing kairomone was found to be the bile salt 5α-cyprinol sulfate (CPS), a compound exuded by various fish species (Hahn et al. 2019). *D. magna* mainly occurs in ponds where it may coexist with fish; however, DVM traditionally is described in lakes with smaller-sized *Daphnia* species (Larsson and Dodson 1993). Hence, it remains to be demonstrated that CPS also induces DVM in these smaller-sized *Daphnia* species. In addition, unfortunately little is known about the concentration and effect of CPS in nature.

Here, we conducted a field mesocosm experiment, in which we tracked the effect of purified CPS on the vertical distribution of a field-derived *Daphnia* community. We tested two different CPS concentrations to estimate CPS threshold concentrations for DVM induction and quantified CPS concentrations within the mesocosms over time to estimate its chemical stability. Subsequently, we measured vertical day- and nighttime distributions of *D. longispina* in the experimental lake and quantified concomitant CPS concentrations.

1.3 Methods

To test effects of CPS-addition on DVM, we performed a factorial mesocosm experiment during summer 2019 in the dimictic oligo-mesotrophic Lake Klostersee. This lake contains *D. cucullata* and *D. longispina* as the major *Daphnia* species (Seitz 1984; Ilić et al. 2021) and has zooplanktivorous cyprinid fish (for details see SI 1.1). In summer 2022, we determined vertical profiles of light, temperature, chlorophyll-a, as well as the day- and nighttime vertical distribution of *D. longispina* and CPS. To ensure that the chlorophyll profile from 2022 is

representative, such data was also collected during 2023. See Ahlers and Hahn et al. (2024) for all raw data used in this study.

Mesocosm experiment

In May 2019, lake plankton (< 250 µm) was enclosed in nine 12-m long bottom-sealed mesocosms (SI Figure 1). Thereafter, zooplankton was collected in Lake Klostersee with a plankton net (100-µm mesh) from 12 m to 0 m and inserted into the mesocosms. The experiment was started 33 days after establishment of the fish-free mesocosms to ensure degradation of any initially present fish kairomone. Then, on 11 June 2019, the mesocosms were amended with either CPS (1x or 10x concentrated) or control extract to initiate the experiment (SI Figure 1, for details see SI 1.2). Samples for quantification of CPS in the mesocosms were taken at 0-2 m and 9-11 m 48 h, 72 h and 120 h after CPS-addition (SI Figure 1, for details see SI 1.2)

Four vertical layers of the mesocosms (0-3, 3-6, 6-9 and 9-12 m) were sampled with 20-cm diameter closing plankton net (type Apstein, Pokorny-Netze GmbH, Czech Republic; 140 µm mesh size). To avoid disturbance of vertical gradients, sampling was initiated at the shallowest layer. Each of the nine mesocosms was sampled on 13 June 2019 during daytime (48 h after CPS) and nighttime (60 h after CPS) and on 14 June 2019 during daytime (72 h after CPS, see SI Figure 1). Zooplankton samples were fixed in 4 % (v:v) of formaldehyde and 4 % (w:v) saccharose; a dissecting microscope was used for taxa identification and counting. Treatment effects on vertical distributions were tested by PERMANOVAs, and effects on the share of the *Daphnia* community in different depth layers were tested by one-way ANOVA and posthoc tests (for details see SI 1.5). For analysis of nutritional and physical parameters see SI 1.6 and SI 1.7.

Vertical profiles in Lake Klostersee

On midday and midnight of 17, 18 and 19 August 2022, the layers 0-2, 2-4, 4-6, 6-8, 8-10 and 10-12 m were sampled in duplicate in the center of the lake, zooplankton was fixed, and *D. longispina* was counted as indicated above (2.1). Deeper strata were not sampled because of muddy sediments. The entire sample was counted for each duplicate before pooling data. A Cochran-Mantel-Haenszel test (software R, version 3.6.2) was performed to test for differences in vertical distribution of *D. longispina* among daytime and nighttime. At the same dates samples for CPS of were taken (for details see SI 1.8).

Vertical profiles of temperature were measured on 13 August 2015, 31 August 2016, 4 September 2019, 16 August 2022 and 12 August 2023. A vertical profile of light was measured on 17 August 2022 (see SI 1.7). R-package ggplot2 was used to fit an exponential model to the vertical profiles of light intensity and to apply geomline to connect data points of the vertical temperature profile.

On 17 August 2022 a 2-m long tube sampler was used to collect a vertical profile of chlorophyll-a. Samples of 2 L were stored at -20°C. After thawing, the samples were filtered onto GFF-filters and chlorophyll-a concentrations were determined spectrophotometrically (Tilzer 1983). On 12 August 2023 a vertical profile of chlorophyll-a was obtained using a Hydrolab HL4 OTT hydroMet multiprobe.

1.4 Results

Mesocosm study in 2019

In an earlier mesocosm study, the *Daphnia* community had been given several days to adapt to changes in fish abundance before vertical profiles of *Daphnia* were sampled (Loose 1993a; Loose 1993b). Accordingly, on 13 June 2019 we investigated daytime depth distributions at 48 h and 72 h after kairomone addition, while the nighttime profile was measured after 60 h

Table 1: Concentrations of 5α-cyprinol sulfate (CPS) in the experimental mesocosms 48 h after CPS addition during 2019. Concentrations represent means of two technical replicates.

	Control (nmol/L)	**1x CPS (nmol/L)**	**10x CPS (nmol/L)**
Epilimnion (0-2 m)	0.67	2.03	32.53
Hypolimnion (9-11 m)	0.22	0.44	6.66

(SI Figure 1). We found an effect of CPS on the daytime depth distribution of *Daphnia* spp. 48 h after CPS addition (PERMANOVA results, R^2=0.56, p<0.01; Figure 1 A, SI Table 5). In the control treatment, most *Daphnia* resided in the layer between 3 and 6 m of depth (~68 % of the community; Figure 1 A). In the 1x CPS mesocosms, *Daphnia* were located mainly (42 %) in the layer between 0 and 3 m depth (Figure 1 A), while after addition of 10x CPS the most favored layer was the one between 6 and 9 m (~52 % of the community). Accordingly, a

significantly larger proportion of the *Daphnia* community resided in the bottom part of the mesocosms (6-12 m depth) during daytime (SI Figure 5 A, SI Table 6).

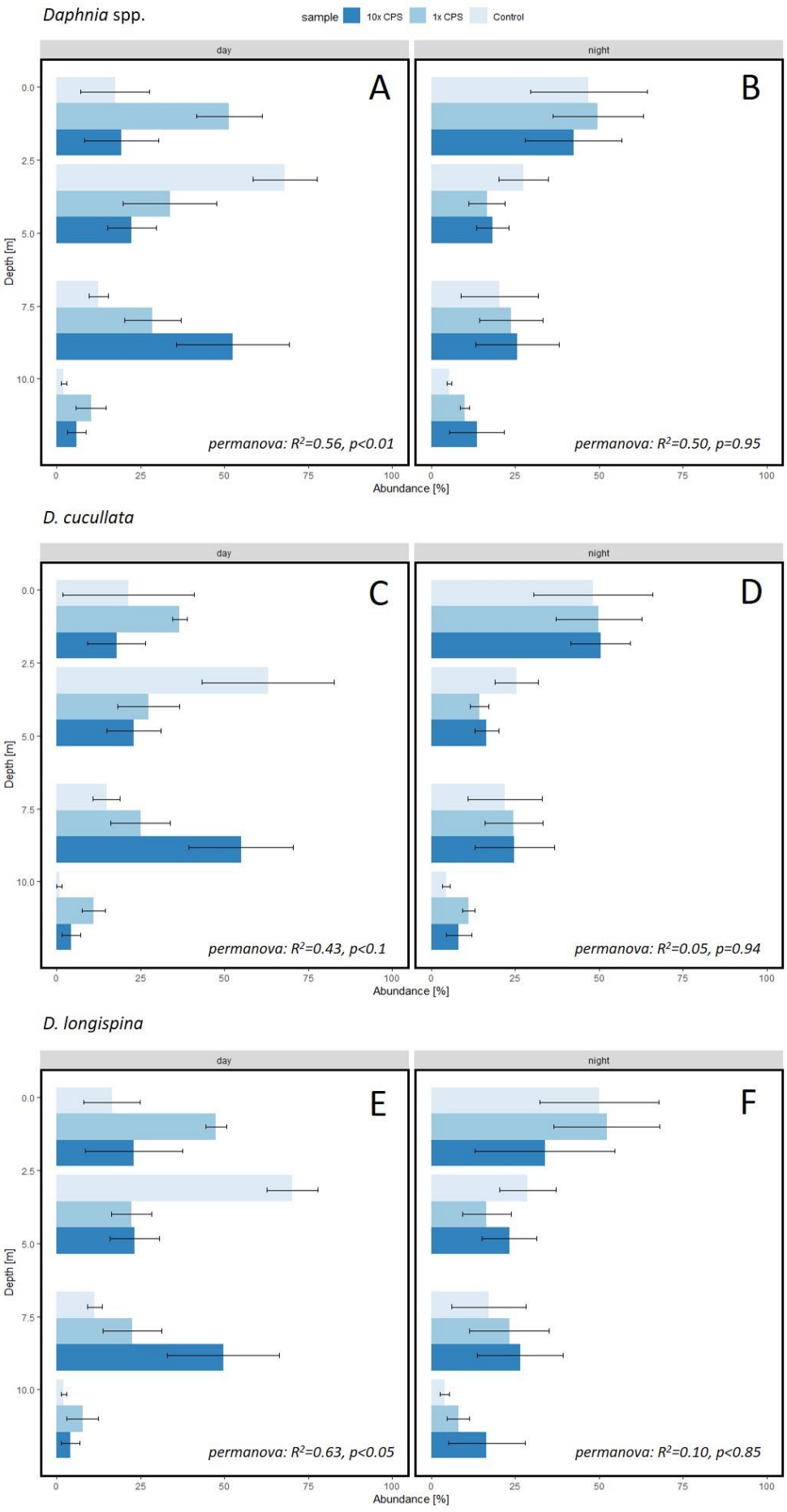

Daphnia spp.
sample 10x CPS 1x CPS Control
day
night
A
B
permanova: R²=0.56, p<0.01
permanova: R²=0.50, p=0.95
D. cucullata
C
D
permanova: R²=0.43, p<0.1
permanova: R²=0.05, p=0.94
D. longispina
E
F
permanova: R²=0.63, p<0.05
permanova: R²=0.10, p<0.85
Depth [m]
0.0
2.5
5.0
7.5
10.0
0
25
50
75
100
Abundance [%]

Figure 1. Vertical distribution of *Daphnia* spp. 48 hours (day) and 60 hours (night) after addition of 5α-cyprinol sulfate (CPS) to mesocosms during 2019. Depicted are the relative distributions of *Daphnia* populations in percent (mean ± SE, n= 3) over the depth ranges '0-3 m', '3-6 m', '6-9 m' and '9-12 m'. Data are depicted for the total *Daphnia* community (A, B), for *D. cucullata* (C, D), and for *D. longispina* (E, F) in response to different CPS concentrations and a control. PERMANOVA results are obtained after 100,000 permutations, testing for the effect of the treatment on distribution patterns.

The same treatment-dependent trends of vertical daytime distribution were observed for individual species, *D. cucullata* and *D. longispina* (SI Figure 5 C, E). The effect of CPS on the vertical daytime distribution was significant for *D. longispina* (PERMANOVA: R^2=0.63, $p<0.05$; Figure 1 E, SI Table 5) but not for *D. cucullata* (PERMANOVA: R^2=0.43, $p<0.1$; Figure 1 C, SI Table 5). As expected for animals that perform DVM, CPS did not affect the vertical distribution of *Daphnia* at night (60 h, Figure 1 B, D, F; SI Table 7, SI Figure 5 B, D, F). As anticipated, in-situ concentrations of CPS in the mesocosms were highest in the 10x CPS treatment and lowest in the control 48 h after its addition. Concentrations were higher in the epilimnion than in the hypolimnion and decreased over time (Tab. 1, SI Figure 6). Seventy-two hours after CPS-addition, there was no effect of CPS on the daytime distribution of *Daphnia* (SI Figure 7): neither in terms of the vertical distribution of individuals nor the share of the population that resided in the lower half of the mesocosms (SI Tables 8, 9).

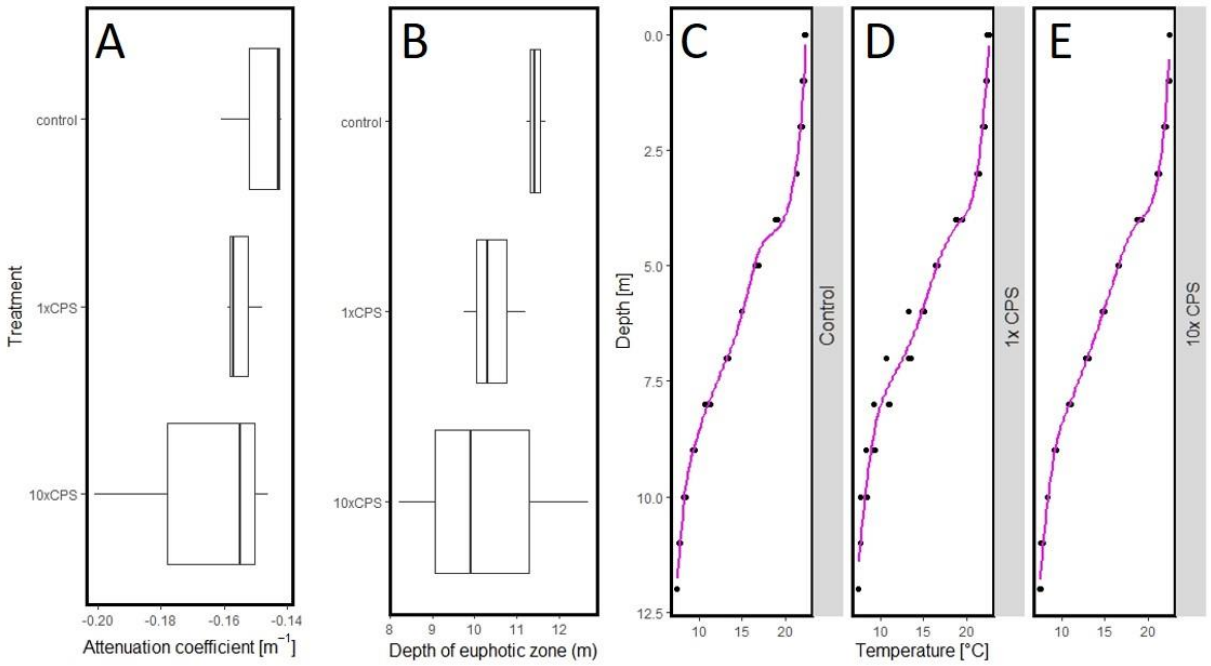


Figure 2. Depth profiles of temperature and attenuation coefficients and depths of euphotic zone in experimental mesocosms 48 hours after addition of 5α-cyprinol sulfate (CPS) during 2019. Boxplots of attenuation coefficients of light (A) and depths of euphotic zones (= 1 % I_0, B) represent three biological replicates per treatments. Depth dependent values of temperature are depicted for three biological replicates of control (C), 1x CPS-treated (D) and 10x CPS-treated (E) mesocosms; the magenta line represents smoothed conditional means of the vertical temperature profiles across all replicates of the respective treatment.

Initial nutrient concentrations in the mesocosms (SI Table 10) did not differ among treatments (SI Table 11); likewise, temperature profiles (Figure 2 C-E) were not distinguishable 48 h after CPS addition (permanova, 1000 permutations, $F_{model,\ 2}$ = 0.743, P = 0.782). Although light intensities seemed to diverge between treatments mainly at the water surface (SI Figure 8), mean coefficients for light attenuation ranged from -0.149 m^{-1} to -0.167 m^{-1} across treatments and were not significantly different among treatments (Figure 2 A; one-way ANOVA, F_2 = 0.802, p = 0.49). Accordingly, the mean depth of the euphotic zone (1 % I_0) ranged from 10.3

m to 11.4 m across treatments and was not significantly different (Figure 2 B; Kruskal-Wallis one-way ANOVA on ranks, $H_2 = 2.489$, $p = 0.339$).

Vertical profiles in Lake Klostersee

During daytime on 17, 18 and 19 August 2022, maximum mean relative abundances of *D. longispina* were observed in the 10-12 m layer of Lake Klostersee, whereas during nighttime the maximum of mean relative abundances occurred at 8-10 m (Figure 3). The overall number of *D. longispina* did not differ between daytime and nighttime samples (daytime: 1052 +/- 147; nighttime 1180 +/- 247 mean +/- SE, n = 3; t-test, t= -0.0477; P = 0.678). In accordance with a pattern of normal DVM, abundance of *D. longispina* differed significantly between daytime and nighttime (Cochran-Mantel-Haenszel test, $M^2(5) = 15.405$, $p < 0.05$). Accordingly, the proportion of *D. longispina* in the upper part (0-8 m) increased significantly from daytime to nighttime (SI Figure 9 A, t-test, F = -2.3594, $p<0.05$). For the lower part of the water column (8-12 m) there was a trend (though almost significant) that relative abundances decreased from daytime to nighttime (SI Figure 9 B, t-test, F = 2.1701, p=0.0697).

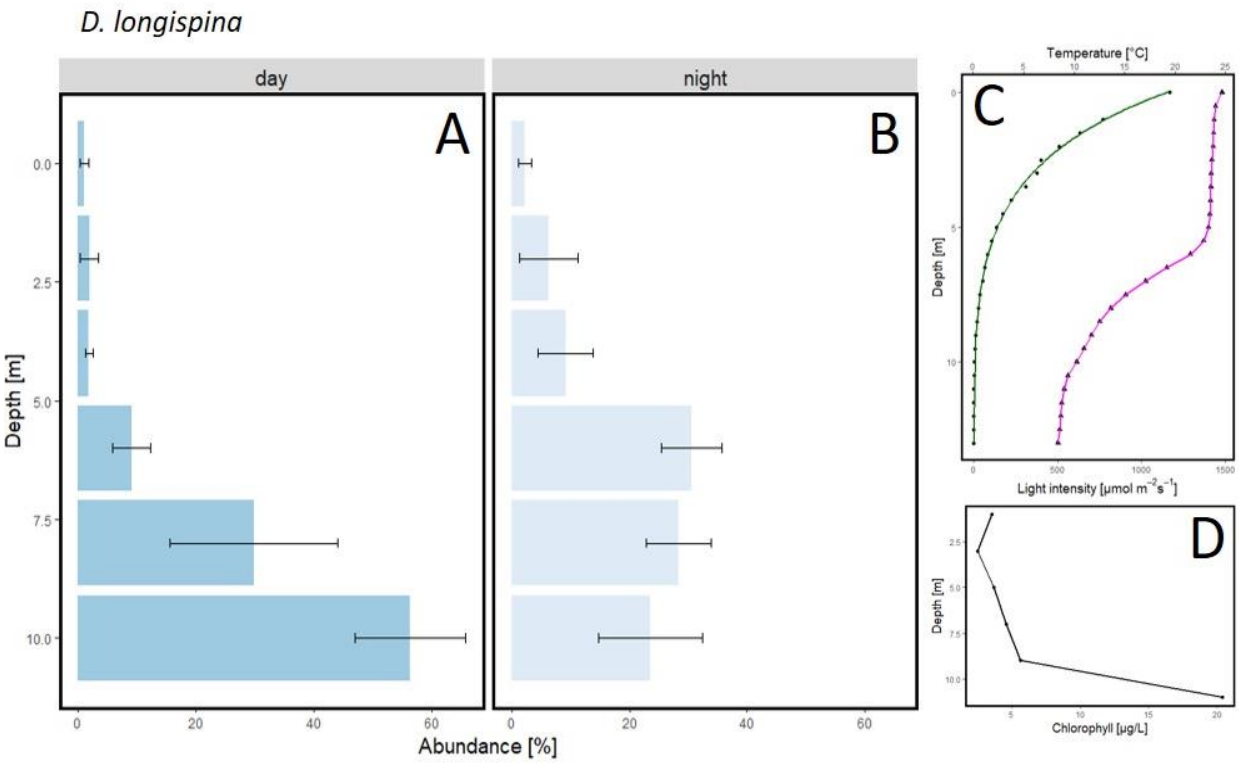


Figure 3. Vertical profiles of Lake Klostersee during 2022. Distribution of *D. longispina* during daytime (A) and nighttime (B). Depicted are relative distributions (mean +/- SE, n = 3) over the depth ranges '0-2 m', '2-4 m', '4-6 m', '6-8 m' and '8-10 m'. Data represent samplings from three consecutive dates. (C) Vertical profile of light intensity and temperature on 1st day of sampling. The green line represents the fit of an exponential model to the vertical profile of light intensity; the magenta line connects the temperature data points. (D) Vertical profile of chlorophyll a on 1st day of sampling; the black line connects the chlorophyll data points.

On 17 August 2022 the coefficient for light attenuation (-0.234 m^{-1}) was within the 95 % C.I. of the respective coefficients in the mesocosms; accordingly, the depth of the euphotic zone (1 % I_0, 9.1 m) fell within the 95 % C.I. of that in the mesocosms. The vertical profile of chlorophyll-a revealed a deep chlorophyll maximum (DCM) of 20.4 µg L^{-1} at 12 m during August 2022 (Figure 3D) and at 11 m during 2023 (SI Figure 10) suggesting that DCMs are typical for this lake.

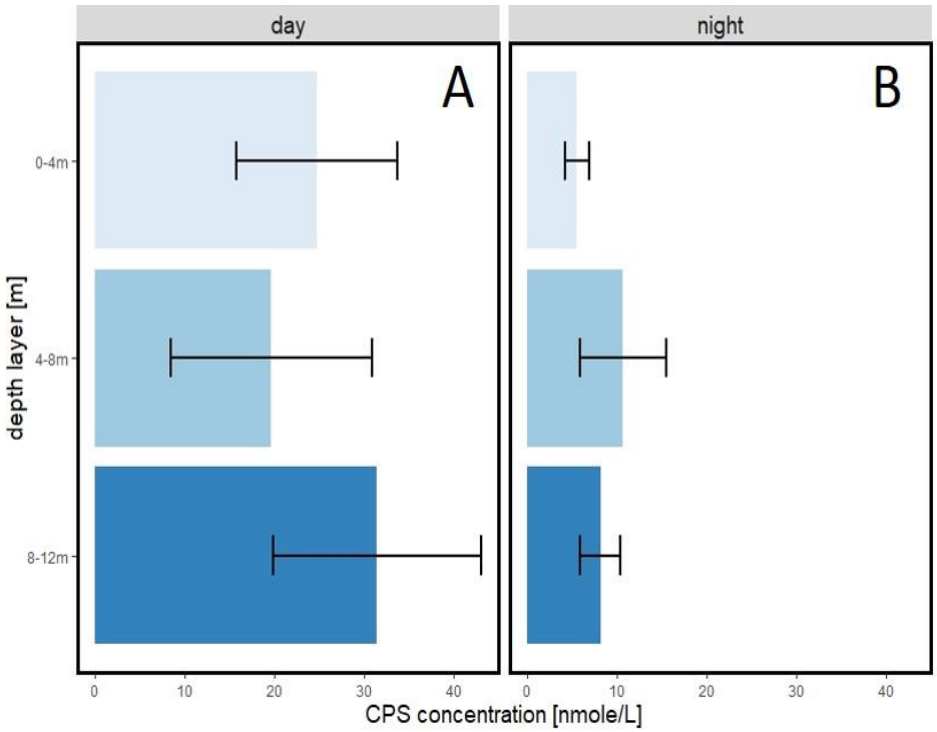


Figure 4. Concentration of 5*α*-cyprinol sulfate (CPS) in Lake Klostersee during 2022. Depicted are mean values (+/- SE, n = 3) for the 0-4 m, 4-8 m and hypolimnion 8-12 m layers that result from three consecutive days.

During 2022 and concomitant with DVM-profiling in the lake (Figure 3; SI Figure 9), mean CPS concentrations in the lake ranged from 19.6 to 31.5 nmol L-1 during daytime and from 5.5 to 10.7 nmol L-1 during nighttime (Figure 4). A two-way ANOVA revealed that concentrations did not differ between the 0-4 m, 4-8 m and 8-12 m layers ($F2 = 0.23$, $P = 0.793$) but were significantly lower during night ($F1 = 7.14$, $P < 0.05$); there was no interaction among depth and day/night sampling ($F2 = 0.44$, $P = 0.648$).

During 2022, at the same time as the DVM profiling, a temperature profile was collected. At each depth, the 2022 temperatures fell within the 95 % C.I. of water temperatures from in total five different years spanning from 2015 – 2022 (SI Figure 11).

1.5 Discussion

In a small-scale bioassay setup, CPS has been shown to induce 'normal' DVM in *D. magna* (Hahn et al. 2019). Hence, we expected similar effects in the field mesocosm experiment during 2019. Under these near-natural conditions, CPS induced a deeper daytime residence in the Daphnia community and in *D. longispina*. Such pronounced DVM-behavior in response to fish has been demonstrated previously for *D. longispina* (King and Miracle 1995; Stich and Lampert 1981; Makino et al. 1996). Similarly, the limited response of *D. cucullata* is also consistent with previous research that fish prefer larger prey over *D. cucullata* (Laforsch and Tollrian 2004), and that the smaller daphnid does not undergo DVM.

In accordance with the normal DVM pattern, the effect of CPS on vertical distribution in the mesocosms during 2019 was absent during nighttime, although there was a trend that animals preferred the upper layer during nighttime. A similar pattern with a more pronounced absence of upward migration at night was also observed for *D. longispina* in Lake Klostersee 3 years later during 2022. This absence of a strong upward migration at night can be explained by several factors. First, food quantity and quality may not have been optimal in the epilimnion of Lake Klostersee, while upward migration of zooplankton during night can increase development due to higher epilimnetic temperatures (Williamson et al. 2011). This factor may not override effects of optimum food conditions. A DCM is commonly present in oligo-mesotrophic lakes in summer (Williamson et al. 2011) like in Lake Klostersee, possibly resulting in elevated food quality of DCMs relative to epilimnetic seston, as seen elsewhere (Rothhaupt 1991; DeMott et al. 2004; Williamson et al. 1996). We hypothesize that food-mediated constraints might have contributed to the absence of a clear upward migration at night in the lake. Pronounced DCMs may result from long stable stratification of mesocosm water

columns similar to the situation in the lake, as suggested by common light and temperature profiles in mesocosms and lake. Second, meteorological conditions may have limited DVM at night: light not only serves as a proximate cue for DVM (Ringelberg 1999), but it also reduces the amplitude of upward migration under full moon conditions (Gliwicz 1986; Dodson 1990). Here, nighttime sampling of zooplankton took place under a clear night sky four days before (mesocosm) and five days after (lake sampling) full moon. We infer that moon light may have dampened the upward migration of Daphnia at night both in mesocosms during 2019 and Lake Klostersee during 2022.

Comparison among treatments of the mesocosm experiment during 2019 helped identify a threshold for CPS effects on Daphnia DVM. Forty-eight hours after CPS addition to mesocosms, there was no effect of CPS on vertical Daphnia distribution in the low concentration trials (0.4 - 2 nmol CPS/L), whereas Daphnia migrated in the high CPS treatment (6.7 - 33 nmol CPS/L). This pattern indicates that more than 2 nmol/L are required for DVM induction in this lake and that the CPS threshold concentration for induction of DVM is reached or even exceeded in the presence of 33 nmol CPS/L in the respective mesocosms. Furthermore, due to high rates of CPS loss from the mesocosms, it is possible that migration may have been triggered by higher CPS concentrations that had been present earlier in the experiment. Interestingly in Lake Klostersee during 2022, the pattern for normal DVM coincided with ≥ 20 nmol CPS/L in the water column, values which lay within the range of CPS concentrations that altered Daphnia distribution in mesocosms. In conclusion, CPS-concentrations in the lake are most likely sufficiently high to cause deeper daytime residence of *D. longispina*.

These evidences that DVM of *D. longispina* in the lake can be explained by in-situ CPS-concentrations were obtained during 2022. The fact that stratification regimes are consistent

from 2015 – 2023 shows that the stratification in 2022 was typical for Lake Klostersee and suggests that the finding that DVM in the lake coincides with sufficiently high CPS concentrations is a representative result.

DVM has been induced in a *D. magna* clone by 100 pmol CPS/L under laboratory conditions (Hahn et al. 2019), whereas 2 nmol CPS/L did not affect daytime position of Daphnia spp. in mesocosms. The higher threshold in the mesocosms may result from (i) insufficient CPS degradation in control mesocosms so that higher CPS concentrations may have been necessary to affect daytime distributions in comparison to controls; (ii) species-specific CPS-thresholds with the smaller sized D. longispina in mesocosms and in Lake Klostersee having higher CPS thresholds than large-bodied *D. magna*.

Interestingly, CPS concentrations in Lake Klostersee were significantly lower in nighttime than in daytime samples in 2022. These diurnal fluctuations of CPS concentrations may result from diurnal activity patterns and habitat changes of fish (Helfman 1986). Furthermore, the pronounced decline of CPS-concentrations over time in the mesocosms suggests that CPS degradation is rapid. Conceptually, kairomones should show rapid turn-over, so that its in-situ concentration can reflect predation risk (von Elert 2012). Although bacterial degradation of the DVM-inducing kairomone has been shown in principle (Loose et al. 1993), and for bile salts in particular (Philipp 2011), it remains to be demonstrated to which degree in-situ bacterial degradation contributes to a turn-over of CPS.

In summary, CPS is able to induce daytime downward migration according to a normal pattern of DVM in a field-derived experimental Daphnia population. Sampling also shows that in-situ

concentrations of CPS in the oligo-mesotrophic study lake ranged from 6 – 32 nmol//L and are high enough for induction of daytime downward migration *D. longispina* in a natural lake.

Further, this study also resulted in the establishment of a new method for the in-situ quantification of CPS that allows for analysis of the spatial and temporal dynamics of the kairomone in natural lakes and ponds and can be used to describe the "landscapes of fear" (Gaynor et al. 2019) in natural aquatic environments which can be linked to zooplankton DVM.

1.6 Author contribution statement

Meike Hahn, Maria Stockenreiter, Herwig Stibor, and Eric von Elert conceived and designed the mesocosms experiment. Meike Hahn and Maria Stockenreiter performed the mesocosm experiment and data acquisition, and Meike Hahn performed analyses of data and CPS-quantification in mesocosms. Johanna Ahlers, Maria Stockenreiter, HS, and Eric von Elert conceived a sampling of the lake. Johanna Ahlers, Maria Stockenreiter, and Eric von Elert performed the sampling. Johanna Ahlers did CPS-quantification and zooplankton data analyses of lake samples. Meike Hahn, Johanna Ahlers, and Eric von Elert wrote the manuscript, and Maria Stockenreiter and Herwig Stibor revised it. All authors reviewed the manuscript.

1.7 Acknowledgements

We thank Cinzia Raviscioni and Jessica Titocci for their assistance in conducting the mesocosm experiment, Jakob Büssemaker for collecting and counting lake zooplankton samples during 2022, Kathrin Otte for help with statistics for analysis of 2022 zooplankton samples, and Susanna Findlay

1.8 References

1. Ahlers, J. and Hahn, M. A.; Stockenreiter, M.; Stibor, H., and von Elert, E. (2024). Mesocosm experiments validate induction of *Daphnia* vertical migration by the fish-derived kairomone 5α-cyprinol sulfate. *Limnol Oceanogr Letters* 9 (3), pp. 307–315.

2. Brierley, A. S. (2014). Diel vertical migration. Current Biology 24: R1074-R1076.

3. DeMott, W. R.; Edington, J. R.; Tessier, A. J. (2004). Testing zooplankton food limitation across gradients of depth and productivity in small stratified lakes. *Limnol Oceanogr* 49: 1408–1416.

4. Dodson, S. (1990). Predicting diel vertical migration of zooplankton. *Limnol. Oceanogr.* 35: 1195–1200.

5. Gaynor, K. M.; Brown, J. S.; Middleton, A. D.; Power, M. E.; Brashares, J. S. (2019). Landscapes of fear: Spatial patterns of risk perception and response. *Trends in Ecology & Evolution* 34: 355–368.

6. Gliwicz, Z. M. (1986). A Lunar Cycle in Zooplankton. *Ecology* 67: 883–897.

7. Hahn, M. A.; von Elert, E.; Bigler, L.; Díaz Hernández, M. D.; Schloerer, N. E. (2018). 5α-Cyprinol sulfate: Complete NMR assignment and revision of earlier published data, including the submission of a computer-readable assignment in NMReDATA format. *Magnetic Resonance in Chemistry* 56: 1201–1207.

8. Hahn, M. A. and von Elert, E. (2022). One Kairomone and multiple effects in *Daphnia* species—5α-Cyprinol Sulfate induces morphological defenses in the invasive species *Daphnia lumholtzi*. *Frontiers in Ecology and Evolution* 10.

9. Hahn, M. A.; Effertz, C.; Bigler, L.; von Elert, E. (2019). 5α-cyprinol sulfate, a bile salt from fish, induces diel vertical migration in *Daphnia*. *eLife* 8: e44791.

10. Hahn, M. A. and von Elert, E. (2020). The impact of diel vertical migration on fatty acid patterns and allocation in *Daphnia magna*. Peerj 8: e8809.

11. Haupt, F.; Stockenreiter, M.; Baumgartner, M.; Boersma, M.; Stibor H. (2009). *Daphnia* diel vertical migration: implications beyond zooplankton. J. *Plankton Res.* 31: 515–524.

12. Haupt, F.; Stockenreiter, M.; Reichwaldt, E. S.; Baumgartner, M.; Lampert, W.; Boersma, M.; Stibor, H. (2010). Upward phosphorus transport by *Daphnia* diel vertical migration. *Limnology and Oceanography* 55: 529–534.

13. Helfman, G. S. (1986). Fish Behaviour by Day, Night and Twilight, p. 366–387. In T. J. Pitcher [ed.], *The Behaviour of Teleost Fishes*. Springer US.

14. Ilić, M.; Cordellier, M.; Fink, P. (2021). Intrapopulation variability in a functional trait: Susceptibility of *Daphnia* to limitation by dietary fatty acids. *Freshw Biol* 66: 130–141.

15. King, C. E. and Miracle, M. R. (1995). Diel vertical migration by *Daphnia longispina* in a Spanish lake: genetic sources of distributional variation. *Limnology and Oceanography* 40: 226–231.

16. Laforsch, C. and Tollrian, R. (2004). Inducible defenses in multipredator environments: cyclomorphosis in *Daphnia cucullata*. *Ecology* 1985: 2302–2311.

17. Lampert, W. (1993). Ultimate causes of diel vertical migration of zooplankton: new evidence for the predator-avoidance hypothesis. *Archiv für Hydrobiologie Beihefte Ergebnisse der Limnologie*: 79–88.

18. Larsson, P. and Dodson, S. I. (1993). Invited review: Chemical communication in planktonic animals. *Archiv für Hydrobiologie* 129: 129–155.

19. Loose, C. J. (1993a). *Daphnia* diel vertical migration behavior: Response to vertebrate predator abundance. *Archiv für Hydrobiologie Beihefte* 39: 29–36.

20. Loose, C. J. (1993b). Lack of endogenous rhythmicity in *Daphnia* diel vertical migration. *Limnology & Oceanography* 38: 1837–1841.

21. Loose, C. J. and Dawidowicz, P. (1994). Trade-offs in diel vertical migration by zooplankton: the costs of predator avoidance. *Ecology* 75: 2255–2263.

22. Loose, C. J.; von Elert, E.; Dawidowicz P. (1993). Chemically-induced diel vertical migration in *Daphnia*: a new bioassay for kairomones exuded by fish. *Archiv für Hydrobiologie*: 329–337.

23. Makino, W.; Haruna, H.; Ban, S. (1996). Diel vertical migration and feeding rhythm of *Daphnia longispina* and Bosmina corexoni in Lake Toya, Hokkaido, Japan. *Hydrobiologia* 337: 133–143.

24. Philipp, B. (2011). Bacterial degradation of bile salts. *Applied Microbiology and Biotechnology* 89: 903–915.

25. Pohnert, G.; Steinke, M.; Tollrian R. (2007). Chemical cues, defence metabolites and the shaping of pelagic interspecific interactions. *Trends in Ecology & Evolution* 22: 198–204.

26. Reichwaldt, E. S. and Stibor, H. (2005). The impact of diel vertical migration of *Daphnia* on phytoplankton dynamics. *Oecologia* 146: 50–56.

27. Ringelberg, J. (1999). The photobehaviour of *Daphnia* spp. as a model to explain diel vertical migration in zooplankton. *Biological Reviews of the Cambridge Philosophical Society* 74: 397–423.

28. Ringelberg, J.; Flik, B. J. G.; Lindenaar, D.; Royackers, K. (1991). Diel vertical migration of *Daphnia hyalina* (sensu latiori) in Lake Maarsseveen: Part 2. Aspects of population dynamics. *Archiv Fur Hydrobiologie* 122: 385–401.

29. Rothhaupt, K. O. (1991). Variations on the zooplankton menu: A reply to the comment by Smith 1. *Limnology Oceanography* 36: 824–827.

30. Schlüter, L.; Behl, S.; Striebel, M.; Stibor, H. (2016). Comparing microscopic counts and pigment analyses in 46 phytoplankton communities from lakes of different trophic state. *Freshwater Biology* 61: 1627–1639.

31. Seitz, A. (1984). Are there allelopathic interactions in zooplankton? Laboratory experiments with *Daphnia*. *Oecologia* 62: 94–96.

32. Stich, H. B. and Lampert, W. (1981). Predator evasion as an explanation of diurnal vertical migration by zooplankton. *Nature* 293: 396–398.

33. Stockenreiter, M.; Isanta Navarro, J.; Buchberger, F.; Stibor, H. (2021). Community shifts from eukaryote to cyanobacteria dominated phytoplankton: The role of mixing depth and light quality. *Freshwater Biology*: 20145–22157.

34. Tilzer, M. M. (1983). The importance of fractional light absorption by photosynthetic pigments for phytoplankton productivity in Lake Constance. *Limnology Oceanography* 28: 833–846.

35. Von Elert, E. (2012). Information conveyed by chemical cues, p. 19–38. In C. Brönmark and L.-A. Hansson [eds.], *Chemical ecology in aquatic systems.*

36. Von Elert, E. and Loose, C. J. (1996). Predator-induced diel vertical migration in *Daphnia*: enrichment and preliminary chemical characterization of a kairomone exuded by fish. *Journal of Chemical Ecology* 22: 885–895.

37. Von Elert, E. and Stibor, H. (2006). Predator-mediated life history shifts in *Daphnia*: enrichment and preliminary chemical characterisation of a kairomone exuded by fish. *Archiv für Hydrobiologie* 167: 21–35.

38. Weiss, L. C.; Albada, B.; Becker, S. M.; Meckelmann, S. W.; Klein, J.; Meyer, M.; Schmitz, O. J. et al. (2018). Identification of Chaoborus kairomone chemicals that induce defences in *Daphnia*. *Nature Chemical Biology*.

39. Williamson, C. E.; Fischer, J. M.; Bollens, S. M.; Overholt, E. P.; Breckenridge, J. K. (2011). Toward a more comprehensive theory of zooplankton diel vertical migration: Integrating ultraviolet radiation and water transparency into the biotic paradigm. *Limnology and Oceanography* 56: 1603–1623.

40. Williamson, C. E.; Sanders, R. W.; Moeller, R. E.; Stutzman, P. L. (1996). Utilization of subsurface food resources for zooplankton reproduction - implications for diel vertical migration theory. *Limnology and Oceanography* 41: 224–233.

1.9 Supporting information

SI 1. Methods

SI 1.1 Lake Klostersee

Lake Klostersee is an oligo-mesotrophic lake (Schlüter et al. 2016) in Germany (47.97296045336554, 12.453592852811333). It is a dimictic hardwater lake (maximum depth 16 m, surface area 47 ha, volume 2,762,000 m^3) with a stable stratification from spring to autumn (www.wwa-ts.bayern.de). The lake has persistent fish populations of Perciformes, Cypriniformes, Esociformes and Salmoniformes (Dr. Bernhard Gum, Bavarian State Institute of Agriculture, pers. comm., 2021).

SI 1.2 Mesocosm experiment during 2019

In May 2019 lake plankton (< 250 µm) was enclosed in nine bottom-sealed polyethylene bags (thickness: 200 µm, diameter 1 m, length 12 m, volume 9400 L, Poly Verpackungen, Germany, SI Figure 1). Their open ends were affixed to floating rubber rings that were attached to anchored rafts, while weights at the sealed bottom parts positioned mesocosms vertically. Thereafter, zooplankton was collected in Lake Klostersee with a plankton net (100 µm; Hydrobios Kiel, Germany) from 12 m to 0 m and inserted into the mesocosms. The experiment was started 33 days after establishment of the fish-free mesocosms. Then, on 11 June 2019, the mesocosms were provided with either CPS (1x or 10x concentrated) or control extract to initiate the experiment. In order to achieve a homogenous vertical distribution, aliquots of 8.7 mL of the respective extracts were dissolved in a 5 L vessel containing surface water of the mesocosms. The vessel was then used to release the CPS or control extract at 10, 7.5, 4.5 and 1.5 m depth (SI Figure 1; for purification of CPS from carp bile see SI 1.3). Samples for

quantification of CPS in the mesocosms were taken at 0-2 m and 9-11 m 48 h, 72 h and 120 h after CPS-addition (SI Figure 1, for details see SI 1.4).

SI 1.3 Purification of 5α-cyprinol sulfate from bile of *Cyprinus carpio*

CPS was purified from carp bile as described in (Hahn et al. 2018). Briefly, a freshly slaughtered *C. carpio* was obtained from a fish farm, and the gall bladder was prepared. Its content was extracted with a syringe and stored at −20°C until further processing. Unlike described in (Hahn et al. 2018), we fractionated the extract by solid phase extraction (SPE) using successive washing and elution steps with different concentrations of organic solvents: The SPE cartridge (Mega Bond Elut, C_{18}.-bonded silica, mass: 75 g, Agilent Technologies) was activated with 100 mL of methanol and equilibrated with 50 mL of 10 % methanol. The digested bile extract was adjusted to 10 % methanol and extracted by the solid phase. After rinsing the cartridge with 50 mL of 10 % methanol and 150 mL of 50 % methanol, the cartridge was eluted with 150 mL of 75 % methanol. The eluate was evaporated to dryness (rotatory evaporator, 37°C), redissolved two times in 15 mL 50 % methanol respectively with the aid of sonication and evaporated to dryness in a vacuum centrifuge at 37°C. The residue was re-dissolved in 50 % methanol and is referred to as 10x CPS extract in the following. It was diluted 1:10 in 50 % methanol to yield the 1x CPS extract. The control extract was prepared the same way as the 10x CPS extract, but ultrapure water was used initially instead of carp bile. For control of the purity of CPS see SI 1.9. The purity of CPS was confirmed by extracted ion chromatograms (SI Figure 3) and isotope patterns (SI Figure 4, SI Table 4))

SI 1.4 Quantification of 5α-cyprinol sulfate in mesocosms during 2019

For analysis of water samples of the control mesocosms and the 1x CPS mesocosms, 50 ng of the bile salt sodium glycocholic acid (GCA, CAS: 1192657-83-2, Sigma Aldrich) dissolved in

methanol was added as internal standard added per L, while for the 10x CPS mesocosms 500 ng GCA were added except for the samples from 16 June 2019 (addition of 500 ng GCA solution irrespective of the treatment). Samples were stored at 4 °C until filtration (Ø=47 mm, glass fiber filter (GF/A) and cellulose acetate 0.45 µm). 1 L of the filtered sample was adjusted to 10 % methanol, subjected to SPE (Mega Bond Elut, C_{18}-bonded silica, mass: 75 g, Agilent Technologies) and eluted with 100 mL methanol. The eluate was evaporated to dryness and re-dissolved twice in 15 mL 50 % methanol. The pooled solution was stored at -80 °C and freeze dried afterwards. Finally, the dried sample was re-dissolved in 100 µL of 50 % methanol. Liquid chromatography-mass spectrometry

Processed water samples were analyzed by HPLC-MS to track the CPS concentrations within the mesocosms over time. 10 µL of sample were subjected to a reversed-phase HPLC (C_{18} EC 125/2 Nucleosil 100-3 C_{18} column, 720150.20) and separated by liquid chromatography (300 µL/min, solvent A: ultrapure water, solvent B: acetonitrile/isopropanol (7:3, v:v) with both solvents containing 10 mM ammonium acetate. The following gradient was applied: 0 min: 60 % A, 1 min: 60 % A, 4 min: 25 % A, 5 min: 0 %, solvent A, 7 min: 0 % A, 8 min: 60 % A and 9 min: 60 % A. Following negative electrospray ionization, ions in the range of 230 to 2000 m/z were detected by an Exactive Orbitrap mass spectrometer (Thermo Scientific, USA). The ESI source parameters were set as follows: sheath gas flow rate at 35 arbitrary units, aux gas flow rate at 5 arbitrary units, spray voltage at 4.3 KV, capillary temperature at 325°C, capillary voltage at -60 V, tube lens voltage at -200 V, skimmer voltage at -20 V. Peak areas of CPS, GCA and sodium cholesteryl sulfate (calibration curve) were integrated from the extracted ion chromatograms (m/z of $[M– H]^-$ for GCA = 464.3012, CPS = 531.2992, cholesteryl sulfate = 465.3039). Calibration curves for the quantification of CPS were established using

sodium cholesteryl sulfate as an equivalent for CPS (Hahn et al. 2019) since CPS is not commercially available. Ratios of increasing sodium cholesteryl sulfate concentrations and the internal standard GCA were correlated to the respective ratios of the detected signals in the mass spectrometer, which allowed quantification (SI Figure 2). For validation of the water sample processing method for CPS quantification, artificial water samples (tap water) were set up by addition of either 0.05 or 0.5 µg/L CPS and GCA and were processed and quantified by HPLC-MS exactly as the experimental water samples. The obtained peak area ratios of CPS and GCA were compared to those in non-processed controls by two-way ANOVA in order to check for unequal losses of CPS and the internal standard (GCA) during processing and for influences of the initial analyte concentration on the detection (SI Tables 1, 2, 3).

SI 1.5 Data analysis of zooplankton data in mesocosms during 2019

Data analysis was performed with the software R (version 2023.06.1). To detect treatment effects on the vertical *Daphnia* distribution, densities (individuals/L) of *D. cucullata* and *D. longispina* were calculated and compared between treatments by permutational MANOVA (PERMANOVA) based on Euclidian distance matrices (100,000 permutations; RVAideMemoire package version 0.9-77). Prior to PERMANOVA calculation, data were checked for homogeneity of multivariate group dispersion using the package vegan (version 2.56). Betadispersions of the treatments were compared by ANOVA. *Daphnia* abundances within the two lowest layers (6 to 12 m), were summed up and their share on the *Daphnia* community (0 to 12 m depth) was calculated and compared between treatments by one-way ANOVA and Tukey's post hoc test. Individuals of *Daphnia hyalina, D. curvirostris* and *D. galeata* could not be found in all experimental mesocosms, and hence statistical analysis of their depth distribution was not possible on species level, but only in the course of the pooled

community samples. Repeated measures ANOVA or Friedman repeated measures analysis and follow-up Tukey's test were used to test for effects of time on *Daphnia* density. Initial concentrations of POC, PON, chlorophyll a and TP were compared between treatments by one-way ANOVA. The vertical light and temperature profiles were compared between treatments by PERMANOVA.

SI 1.6 Total phosphorus and particulate carbon and nitrogen in mesocosms during 2019

After CPS (or control extract) addition to mesocosms, surface water samples (0-40 cm) were collected and concentrations of total phosphorous and particulate carbon and nitrogen were analyzed. Total phosphorus concentrations were measured using established standard methods (Stockenreiter et al. 2021). For quantification of particulate carbon and nitrogen, 100 mL of the water sample were filtered onto a pre-combusted (four hours at 500°C), acid washed (8 % hydrochloric acid) GF/F filter (Whatman; pore diameter: 0.7 µm). The filters were incubated with 0.5 M phosphoric acid in order to remove calcium carbonate and were thereafter dried for 24 hours at 60°C. Amounts of particulate organic carbon (POC) and particulate organic nitrogen (PON) were determined using an elemental analyzer (vario Micro cube, Elementar, Germany). 12 mL of each water sample was used for the spectrophotometrical quantification of total phosphorous (Shimadzu UV-1700, Shimadzu Cooperation, Germany) using the molybdenum blue method.

SI 1.7 Vertical profiles of chlorophyll a, light and temperate in mesocosms during 2019.

The chlorophyll a concentration was estimated spectrofluorometrically using an Algae Lab Analyzer (bbe Moldaenke, Schwentinental, Germany): a 25 mL water sample was excited by LED lamps emitting light of different wave lengths in order to allow an in vivo quantification

of chlorophyll a. Furthermore, vertical profiles (at 1 m intervals) of light intensity and temperature were acquired using a LI-250A light meter (LI-COR Biosciences, USA) and a YSI Professional Plus multiparameter probe (Xylem Inc., USA). In all mesocosms light intensities at 1 m and 2 m depth were decreased due to shading from the floating rubber rings to which the mesocosm bags were affixed. Those values were excluded from the calculation of the attenuation coefficient. R-package ggplot2 was used to fit an exponential model to the vertical profiles of light intensity and to fit a model to smoothed conditional means of temperature.

SI 1.8 Quantification of 5α-cyprinol sulfate in the lake during 2022

Samples for the determination of in-situ concentrations of CPS in lake Klostersee were collected between 17 and 19 August 2022. Samples were collected at each date at 11 am and at 10 pm from the 0-2m, 2-4m, 4-6m, 6-8m, 8-10m, and 10-12m layer with the help of a Ruttner sampler. Each sample was filtered through a gauze (pore size: 250 µm) to exclude macro and meso zooplankton. Then, 500 ng of sodium-cholesteryl-sulfate (CS, CAS: 2864-50-8, Sigma Aldrich) were added as internal standard to each of two 1L samples of lake water (technical replicates). Samples were immediately filtered (Ø=47 mm, glass fiber filter (GF/A) and cellulose acetate 0.45 µm), adjusted to 1 % methanol, subjected to SPE (Mega Bond Elut, C18-bonded silica, mass: 250 mg, Agilent Technologies) and eluted with 10 mL methanol. The eluate was evaporated to dryness, re-dissolved and stored in 200 µl of methanol.

5 µL of sample were subjected to a C18 100/3 Hydrosphere 120-3 column and separated by liquid chromatography (300 µL/min, solvent A: ultrapure water, solvent B: acetonitrile/methanol (7:3, v:v) with both solvents containing 10 mM ammonium acetate and 0.015 % formic acid. The following gradient was applied: 0 min: 80 % A, 28 min: 0% A, 32.00 min: 0 % A,33.00 min: 80 %, solvent A, 35 min: 80 % A. Following negative

electrospray ionization, ions in the range of 230 to 1050 m/z were detected by a Q-Exactive Orbitrap mass spectrometer (Thermo Scientific, USA). (UHPLC CECAD). CPS was quantified as depicted above (SI 1.4), and the values from the two technical replicates were averaged. A two-way ANOVA was run to test for differences among in-situ concentrations of CPS.

SI 1.9 Purity of the isolated 5α-cyprinol sulfate

From the total ion chromatogram (TIC) and the mass spectra of the purified 5-alpha cyprinol sulfate (CPS; before inoculation of the mesocosm), one can clearly identify the presence of CPS (m/z = 531.2992, retention time 2.66 min, SI Figure 3A). Additionally, several peaks, which are not corresponding to CPS (SI Figure 3 A & B) were found, which theoretically might indicate impurities. Their m/z ratios are 675.19 and 677.19 (retention time 6.22 min). Since they can be found in the control sample with even higher peak areas (SI Table 3), these analytes might be artefacts that are only present during LCMS measurements, or impurities. If the analytes were impurities, they would not contradict our finding that CPS causes DVM in the experiment, since these compounds are present in the control and the CPS treatments and thus cannot explain differential residential depths between treatments. Two more ions (m/z ratios of 1063.60 and 1080.63) were coeluting with CPS (SI Figure 3 A). This coelution suggests that they are formed during electro spray ionization from CPS and CPS and ammonia, the latter being derived from the solvent used for UPLC. The isotope pattern of m/z=1063.60 (SI Figure 4 B) perfectly matches that of a CPS dimer (SI Table 4), carrying a single negative charge, and the isotope pattern of m/z=1080.63 (SI Figure 4 C) perfectly matches the theoretical pattern of an ammonium adduct of the CPS dimer (SI Table 4), carrying a single negative charge. In conclusion, two ions result from adduct formation of CPS during measurement, and two others

indicate impurities that are present in controls and CPS treatments, so that the observed effects on depth distribution of zooplankton can clearly be attributed to CPS.

SI Table 1. Influence of analyte concentration and sample processing by SPE on area ratios of 5α-cyprinol sulfate (CPS) and the internal standard sodium glycocholic acid (GCA) after quantification via LC-MS.

Sample processing (SPE)	GCA and CPS concentration	Area ratio [CPS/GCA]
No	0.5 µg/mL	2.1164
No	5 µg/mL	2.8556
Yes	0.5 µg/mL	3.7786
Yes	0.5 µg/mL	3.2268
Yes	0.5 µg/mL	3.2077
Yes	5 µg/mL	2.31
Yes	5 µg/mL	3.1355
Yes	5 µg/mL	2.8478

SI Table 2. Influence of analyte concentration and sample processing by SPE on area ratios of 5α-cyprinol sulfate (CPS) and glycocholic acid (GCA). The influence of both factors and their interaction was tested by two-way ANOVA.

	Sum of squares	Df	F	p-value
Analyte concentration	0.17423	1	1.2414	0.32764
Sample processing	0.53712	1	3.827	0.12208
Analyte concentration:Sample processing	0.71325	1	5.0819	0.08723
Residuals	0.56141	4		

SI Table 3. Relative comparison of quantities of unknown analytes in 'Control' and '10x CPS'. The peak areas detected for the unknown analytes with the m/z ratios 675.19 and 677.19 are given for the Control and the 10x CPS sample after negative ionization and detection of ions, whose m/z lies between 230 and 2000.

m/z	Peak area 'Control'	Peak area '10xCPS'
675.19	26,475,381	19,152,787
677.19	27,375,134	20,415,758

SI Table 4. Theoretical isotope patterns of 5α-cyprinol sulfate (CPS) and suggested sum formulas for coeluting analytes. Isotope patterns calculated by enviPat Web 2.4 are depicted for (A) CPS: C27H48O8S, (B), a CPS-dimer: C54H96O16S2 and (C), an ammonium adduct of CPS: C54H99O16S2N.

A		**B**		**C**	
m/z	**Abundance [%]**	**m/z**	**Abundance [%]**	**m/z**	**Abundance [%]**
531.3	100	1063.61	100	1080.63	100
532.3	29.2	1064.61	58.4	1081.64	58.4
533.3	4.47	1065.61	16.74	1082.64	16.74
533.31	4.11	1065.6	8.95	1082.63	8.95
533.3	1.64	1066.61	5.23	1083.63	5.23
534.3	1.31	1065.61	3.29	1082.64	3.29
532.3	0.79	1066.62	3.14	1083.64	3.14
532.31	0.54	1066.61	1.92	1083.64	1.92
534.31	0.48	1064.61	1.58	1081.63	1.58
534.31	0.37	1067.61	1.5	1084.64	1.5

SI Table 5. Comparison of vertical *Daphnia* distribution between experimental mesocosms of different treatments (5*α*-cyprinol sulfate [CPS] concentrations) at daytime (48 h after CPS addition) and at nighttime (60 h after CPS addition) during 2019. Results of permanova (100,000 permutations) are presented.

***Daphnia* spp.**

Day	Df	SumOfSqs	R^2	F	Pr(>F)
Treatment	2	7750.90	0.61	4.70	0.0070
Residual	6	4942.70	0.39		
Total	8	12693.60	1.00		
Night	Df	SumOfSqs	R^2	F	Pr(>F)
Treatment	2	432.99	0.05	0.17	0.9544
Residual	6	7482.26	0.95		
Total	8	7915.26	1.00		

D. cucullata

Day	Df	SumOfSqs	R^2	F	Pr(>F)
Treatment	2	6269.25	0.43	2.31	0.0966
Residual	6	8144.45	0.57		
Total	8	14413.70	1.00		
Night	Df	SumOfSqs	R^2	F	Pr(>F)
Treatment	2	298.39	0.05	0.15	0.9400
Residual	6	5876.99	0.95		
Total	8	6175.37	1.00		

D. longispina

Day	Df	SumOfSqs	R^2	F	Pr(>F)
Treatment	2	8497.42	0.63	5.12	0.0108
Residual	6	4978.25	0.37		
Total	8	13475.67	1.00		
Night	Df	SumOfSqs	R^2	F	Pr(>F)
Treatment	2	1215.40	0.10	0.35	0.8457
Residual	6	10553.10	0.90		
Total	8	11768.50	1.00		

SI Table 6. One-way ANOVA results on testing the effect of 5*α*-cyprinol sulfate (CPS) on the percentual part of *Daphnia* populations residing in the lower half of experimental mesocosms 48 hours after CPS addition at night during 2019.

***Daphnia* spp.**	**Df**	**Sums of squares**	**Mean squares**	**F**	**p-value**
Treatment	2	2906	1453	5.75	0.04
Residuals	6	1516	253		
Daphnia cucullata	**Df**	**Sums of squares**	**Mean squares**	**F**	**p-value**
Treatment	2	2870	1435	5	0.053
Residuals	6	1721	287		
Daphnia longispina	**Df**	**Sums of squares**	**Mean squares**	**F**	**p-value**
Treatment	2	2471	1236	4.14	0.074
Residuals	6	1790	298		

SI Table 7. One-way ANOVA results on testing the effect of 5*α*-cyprinol sulfate (CPS) on the percentual part of *Daphnia* populations residing in the lower half of experimental mesocosms 60 hours after CPS addition at night during 2019.

***Daphnia* spp.**	**Df**	**Sums of squares**	**Mean squares**	**F**	**p-value**
Treatment	2	543.9	271.9	0.635	0.562
Residuals	6	2571.1	428.5		
Daphnia cucullata	**Df**	**Sums of squares**	**Mean squares**	**F**	**p-value**
Treatment	2	140	70	0.207	0.818
Residuals	6	2026	337.7		
Daphnia longispina	**Df**	**Sums of squares**	**Mean squares**	**F**	**p-value**
Treatment	2	715.5	357.7	1.011	0.419
Residuals	6	2124.1	354		

SI Table 8. Comparison of vertical daytime *Daphnia* distribution between experimental mesocosms of different treatments (CPS concentrations) 72 hours after CPS addition during 2019. Results of permanova (100,000 permutations) are presented.

	Df	Sums of squares	Mean squares	F model	R^2	p-value	
Treatment	2	3054.5	1527.25	1.5428	0.3396	0.202	*Daphnia* spp.
Residuals	6	5939.7	989.95		0.66039		
Total	8	8994.2			1		
Treatment	2	5112.6	2556.3	1.877	0.38487	0.1493	*Daphnia cucullata*
Residuals	6	8171.4	1361.9		0.61513		
		13284			1		
Treatment	2	3031.7	1515.9	1.4768	0.32988	0.2107	*Daphnia longispina*
Residuals	6	6158.6	1026.4		0.67012		
Total	8	9190.4			1		

SI Table 9. One-way ANOVA results on testing the effect of 5α-cyprinol sulfate (CPS) on the percentual part of *Daphnia* populations residing in the lower half of experimental mesocosms 72 hours after CPS addition at daytime during 2019.

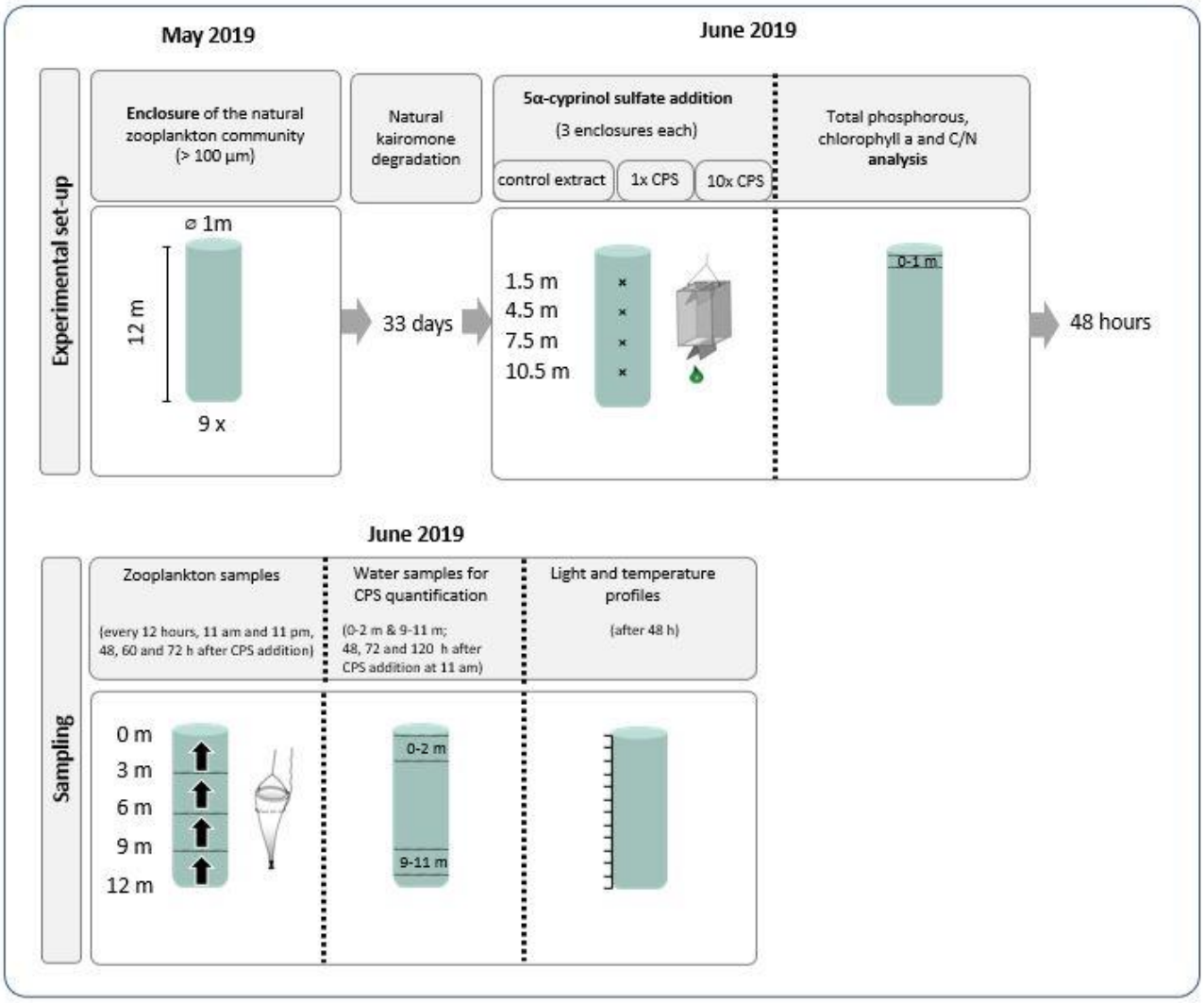
	Df	Sums of squares	Mean squares	F	p value	
Treatment	2	199.9	99.9	0.269	0.773	
Residuals	6	2228.3	371.4			*Daphnia* spp.
Treatment	2	565	282.5	0.415	0.678	
Residuals	6	4084	680.7			*D. cucullata*
Treatment	2	176.5	88.2	0.249	0.788	
Residuals	6	2130.2	355			*D. longispina*

SI Table 10. Initial (0 h after CPS addition) concentrations of carbon, nitrogen, chlorophyll a and phosphorous in the experimental mesocosms during 2019. Mean values ± SD of the initial particulate carbon concentration [mg/L], chlorophyll a concentration [µg/L] and the total phosphorous concentration [µg/L] are depicted for the respective treatments.

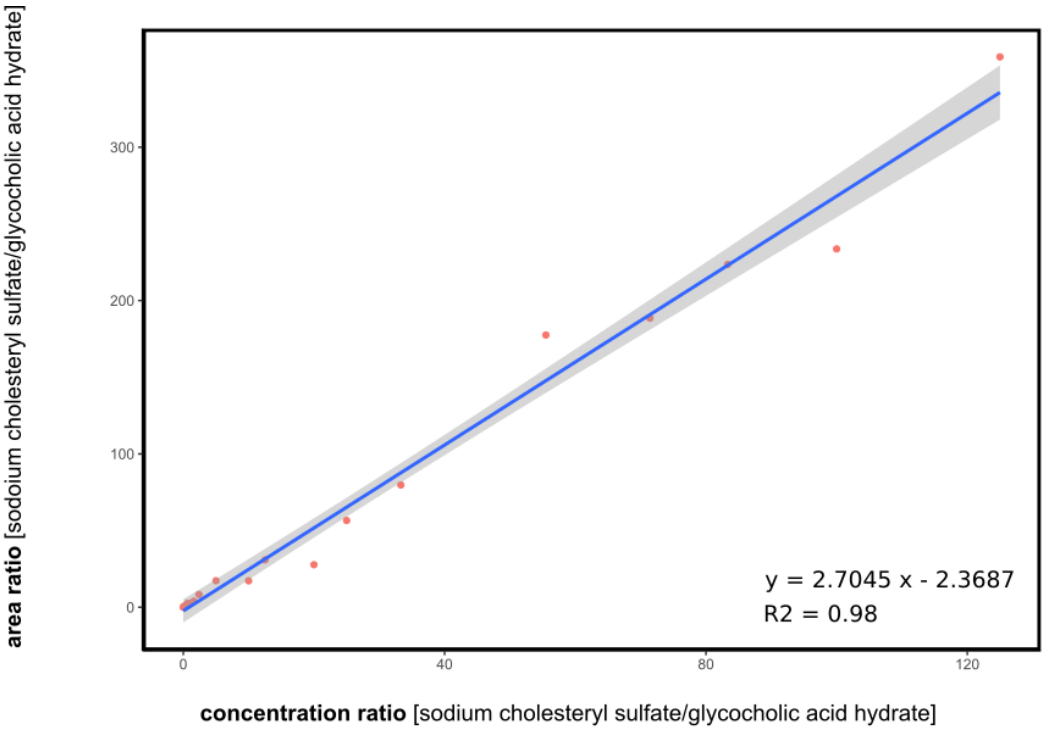
Treatment	Particulate carbon [mg/L]	Particulate nitrogen [mg/L]	Chlorophyll a [µg/L]	Total phosphorous [µg/L]
Control	1.04 ± 0.41	0.20 ± 0.05	1.27 ± 0.05	12.64 ± 8.21
1x CPS	0.93 ± 0.32	0.22 ± 0.04	3.31 ± 1.70	10.87 ± 3.19
10x CPS	0.75 ± 0.09	0.19 ± 0.03	1.81 ± 0.26	10.93 ± 3

SI Table 11. Comparison of initial (0 h after CPS addition) concentrations of particulate carbon and nitrogen, chlorophyll a and total phosphorous concentrations of experimental mesocosms during 2019. Results of one-way ANOVAs showed no effect of the different experimental treatments on particulate carbon, nitrogen, chlorophyll a and total phosphorous concentrations before addition of CPS.

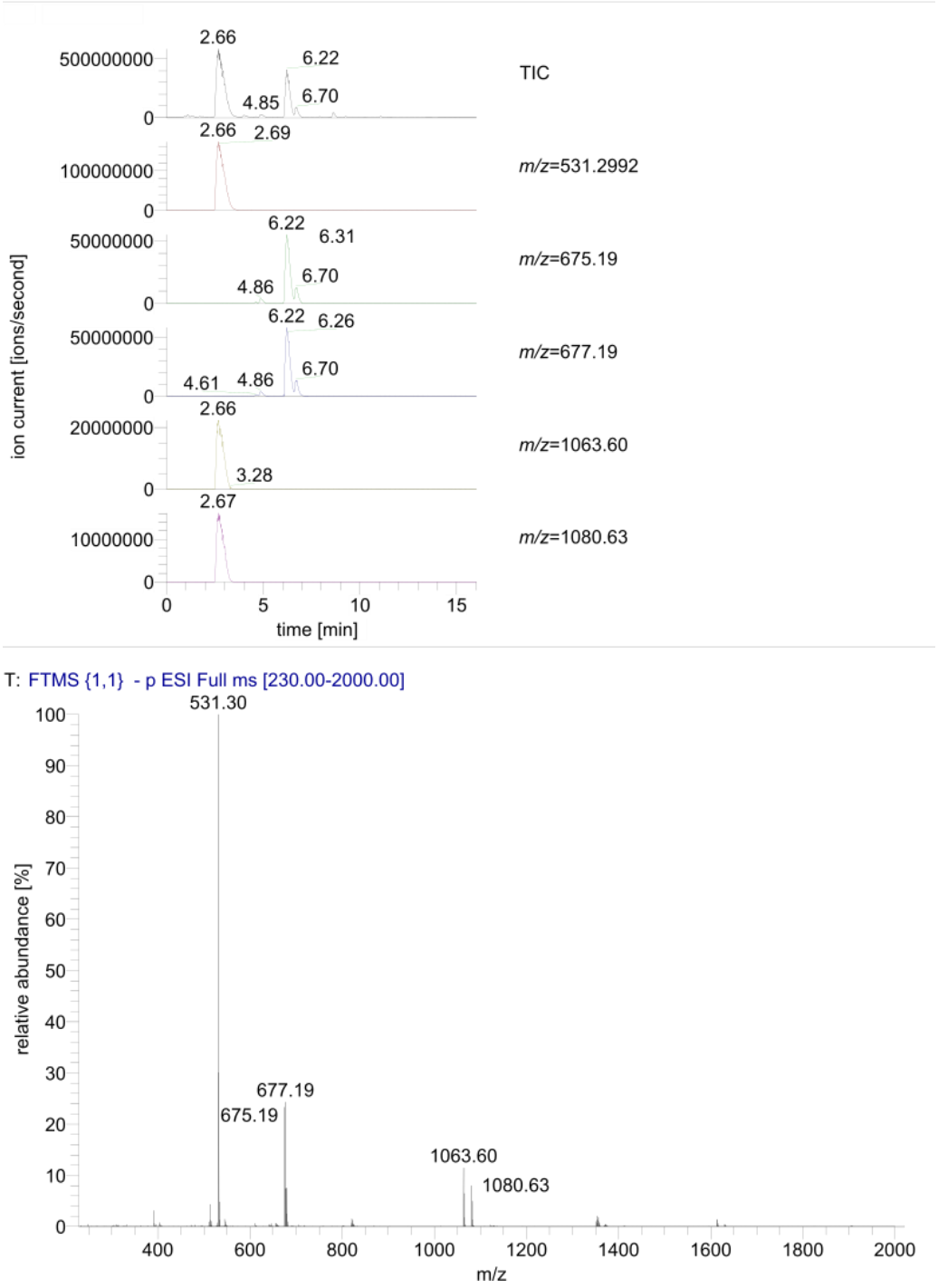
Particulate carbon	**Df**	**Sums of squares**	**mean squares**	**F-value**	**p-value**
Treatment	2	0.1255	0.06274	0.668	0.547
Residuals	6	0.5632	0.09387		
Particulate nitrogen					
Treatment	2	0.001327	0.0006636	0.44	0.663
Residuals	6	0.009049	0.0015082		
Chlorophyll a					
Treatment	2	6.727	3.363	3.395	0.103
Residuals	6	5.944	0.991		
Total phosphorous					
Treatment	2	6.07	3.033	0.105	0.902
Residuals	6	173.58	28.93		



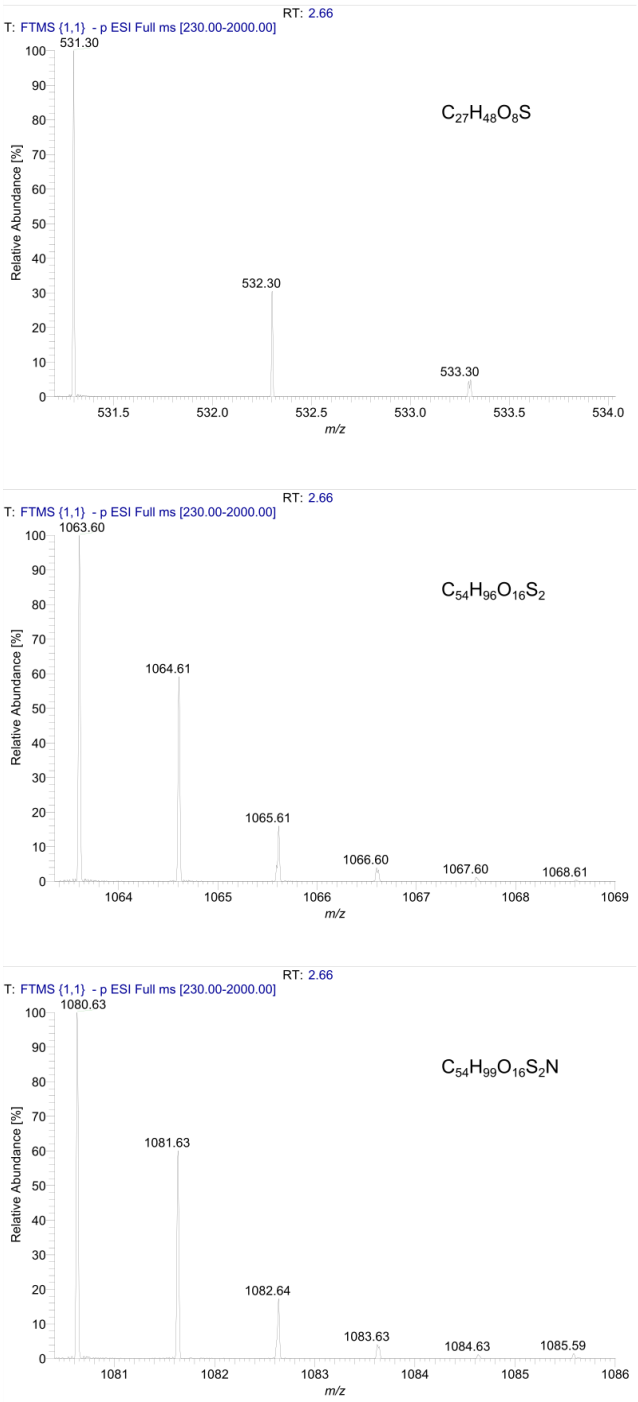
SI Figure 1. Experimental set-up and time schedule of the mesocosm experiment during 2019.



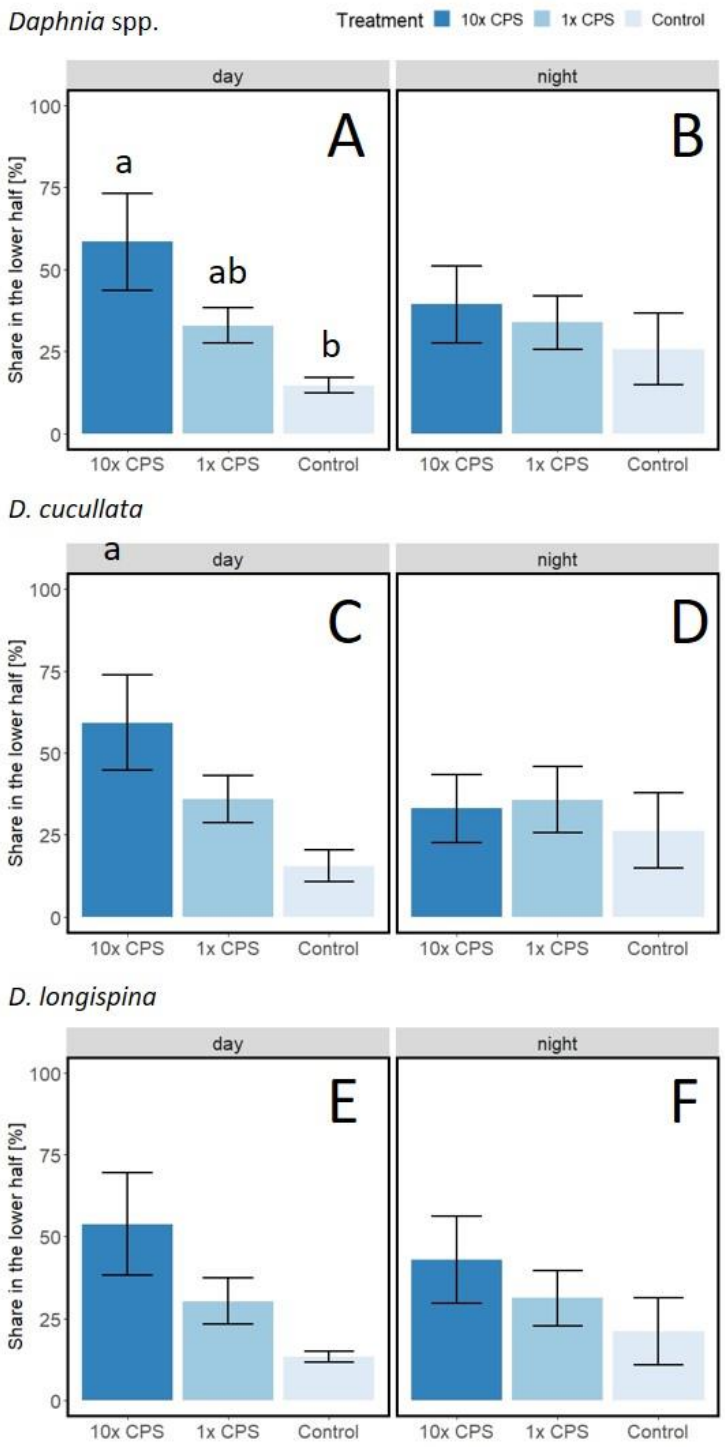
SI Figure 2. Calibration curve for LC-MS analysis of 5α-cyprinol sulfate (CPS). CPS is quantified as equivalents of sodium cholesteryl sulfate, using the internal standard glycocholic acid hydrate. The 95% confidence interval is depicted in light blue.



SI Figure 3. LCMS analysis of applied 5α-cyprinol sulfate (CPS). (A) Total ion chromatograms (TIC) and the extracted ion chromatograms (EIC) of the most prominent m/z ratios and (B) the mass spectra averaged over time (0-16 min) after negative electro spray ionization and detection of m/z ratios ranging from 230 to 2000.

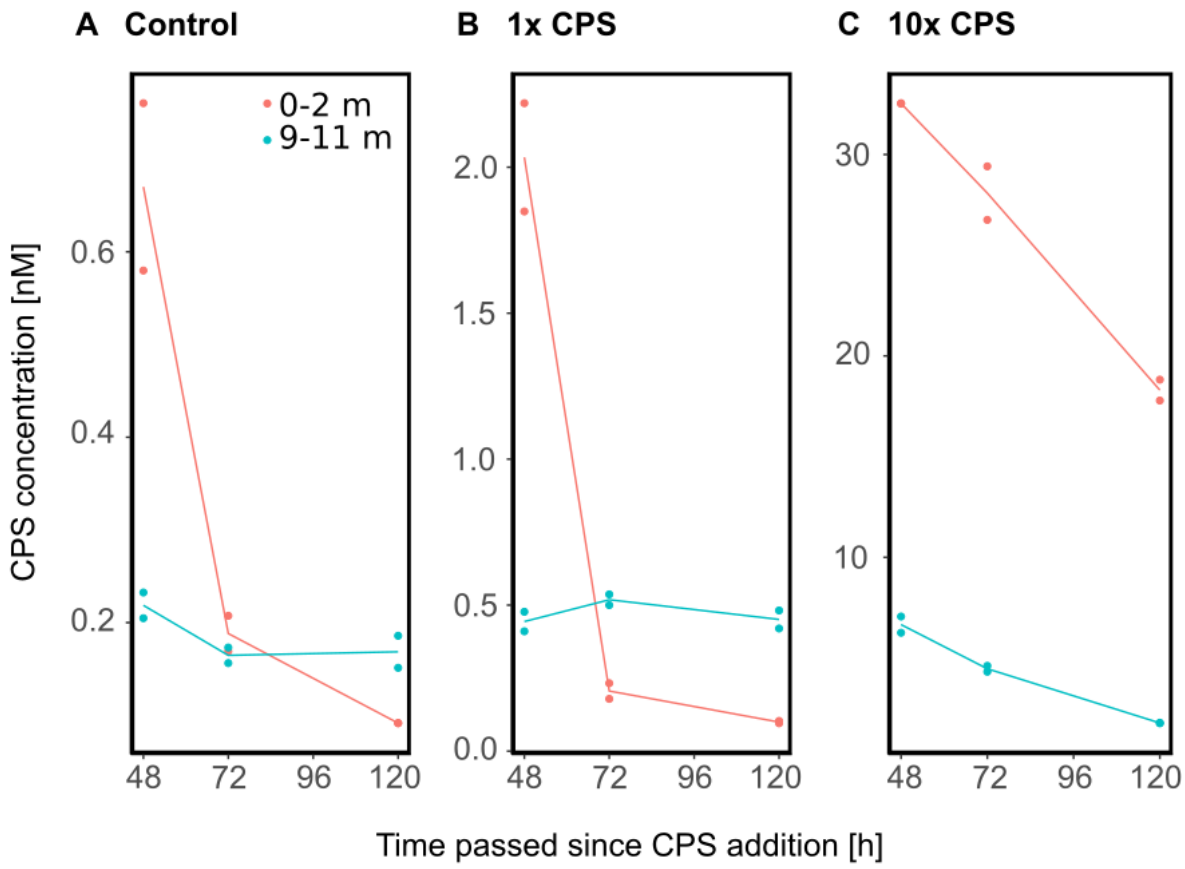


SI Figure 4. Isotope patterns of 5*α*-cyprinol sulfate (CPS) and coeluting analytes. The isotope patterns of m/z= (A) 531.30, (B) 1063.61 and (C) 1080.63 after separation by liquid chromatography and detection in the negative ionization mode are presented at the retention time 2.66 min. Suggested sum formulas for the detected molecules are depicted.

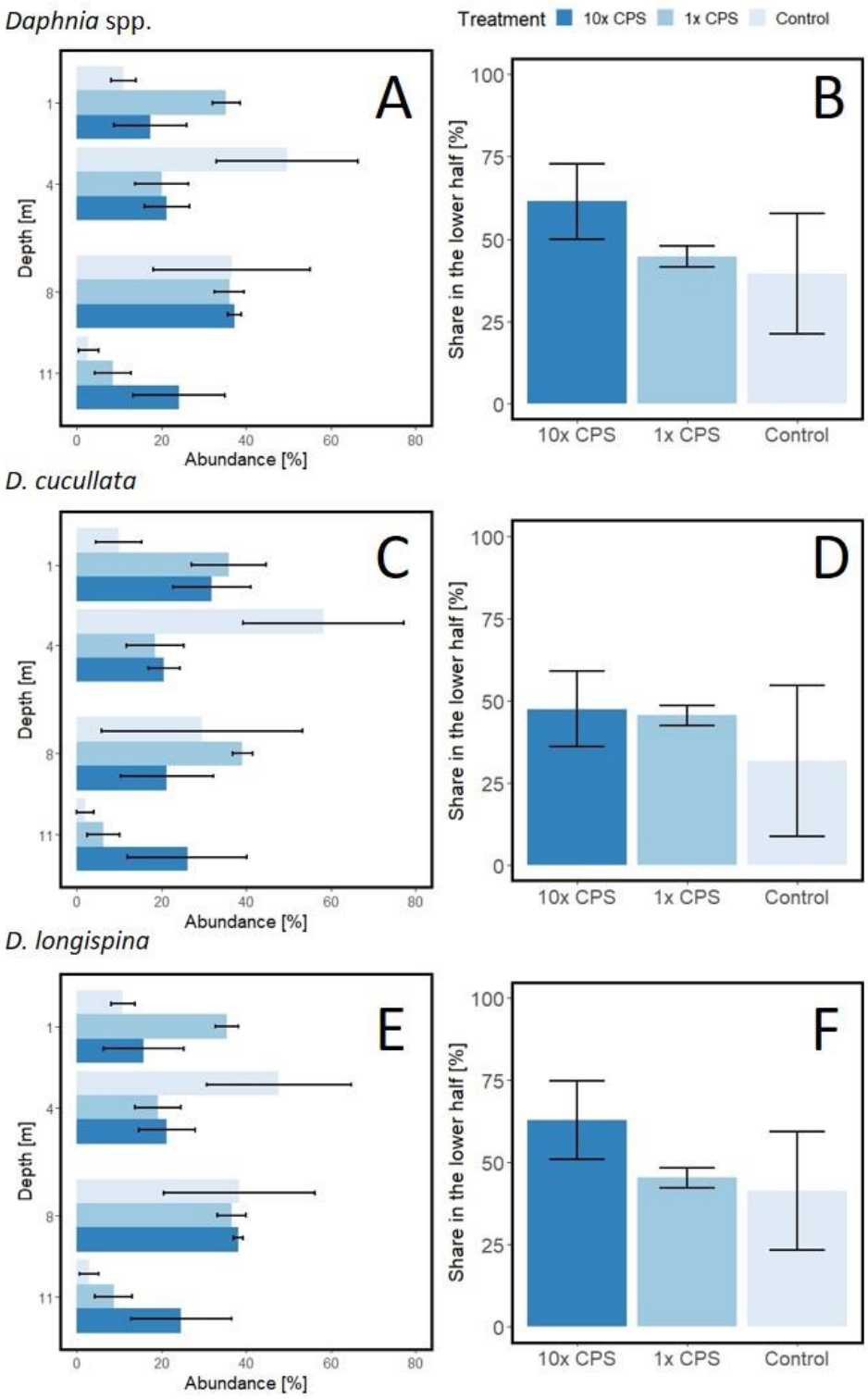


SI Figure 5. **Vertical distribution of *Daphnia* 48 h (day) and 60 h (night) after addition of 5α-cyprinol sulfate (CPS) to experimental mesocosms during 2019.** The relative parts of the

populations in percent (mean ± SE, n=3) residing within the lower half of the mesocosms (6-12 m) are depicted for the total *Daphnia* population (A, B), *D. cucullata* (C, D) and *D. longispina* (E, F) in response to different CPS concentrations and a control. Significant differences among treatments are indicated by different letters and were revealed by Tukey's post-hoc test after significant one-way ANOVA.

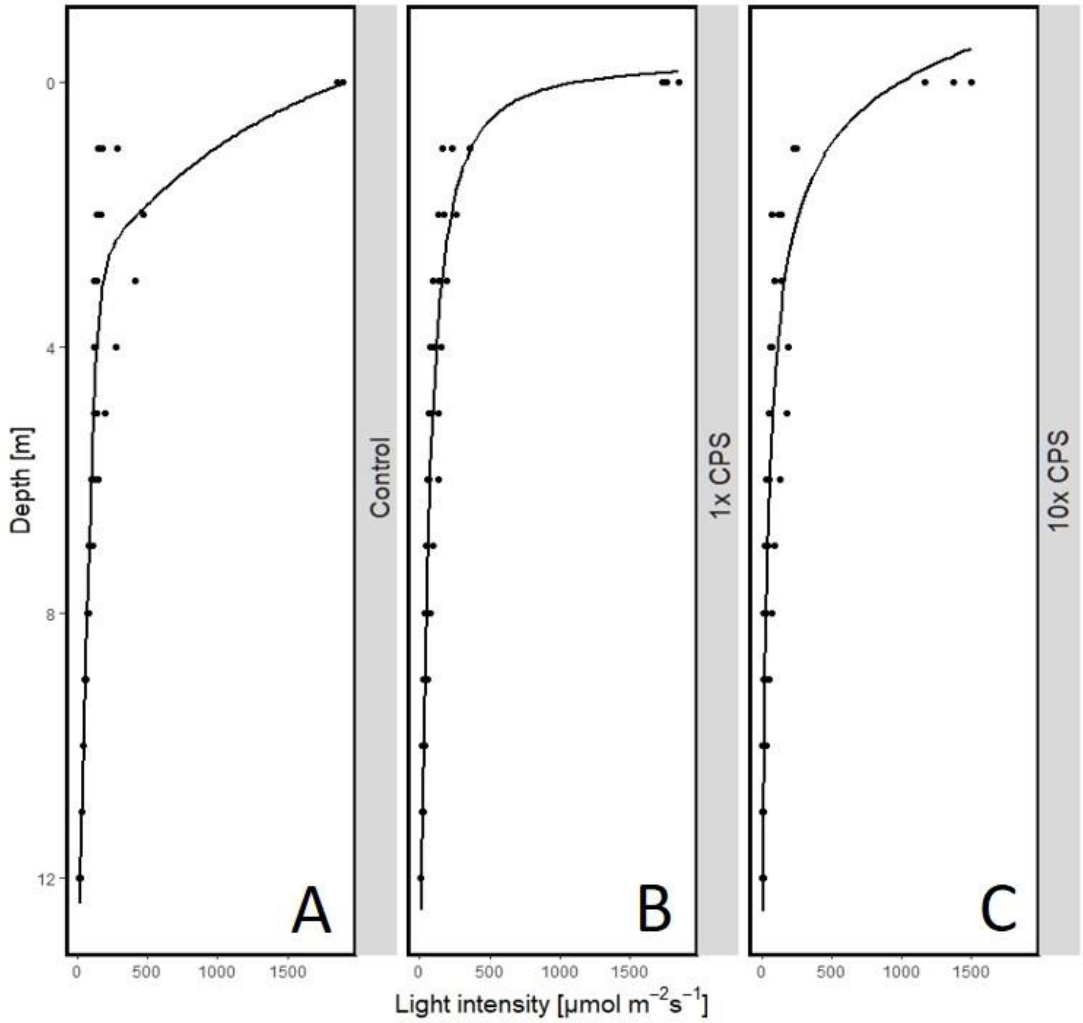


SI Figure 6. **5α-cyprinol sulfate (α-CPS) concentrations over time in experimental mesocosms during 2019.** Technical replicates of HPLC-MS quantification of in-situ α-CPS concentrations in (A) control, (B) 1x α-CPS treated and (C) 10x CPS treated mesocosms are depicted as well as the average values, connected by an orange (0-2 m) or a blue (9-11 m) line. Note different scales of the y-axes.

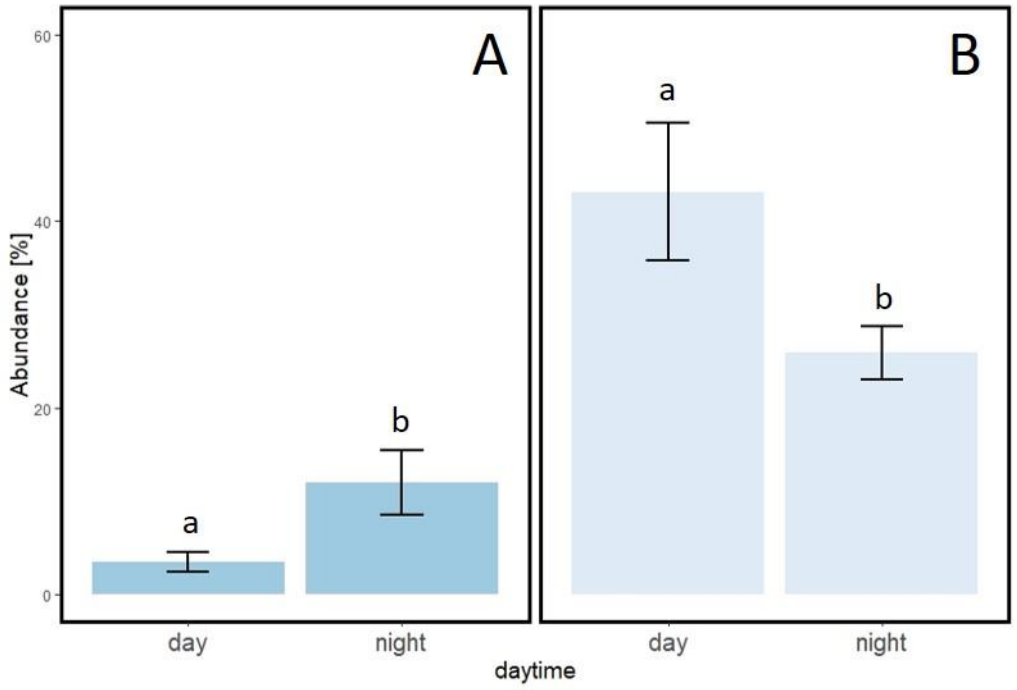


SI Figure 7. Day time vertical distribution of *Daphnia* 72 h after addition of 5α-cyprinol sulfate (CPS) to experimental mesocosms during 2019. Distribution of *Daphnia* populations over the depth ranges '0-3 m', '3-6 m', '6-9 m' and '9 bis 12 m' and the part of the populations

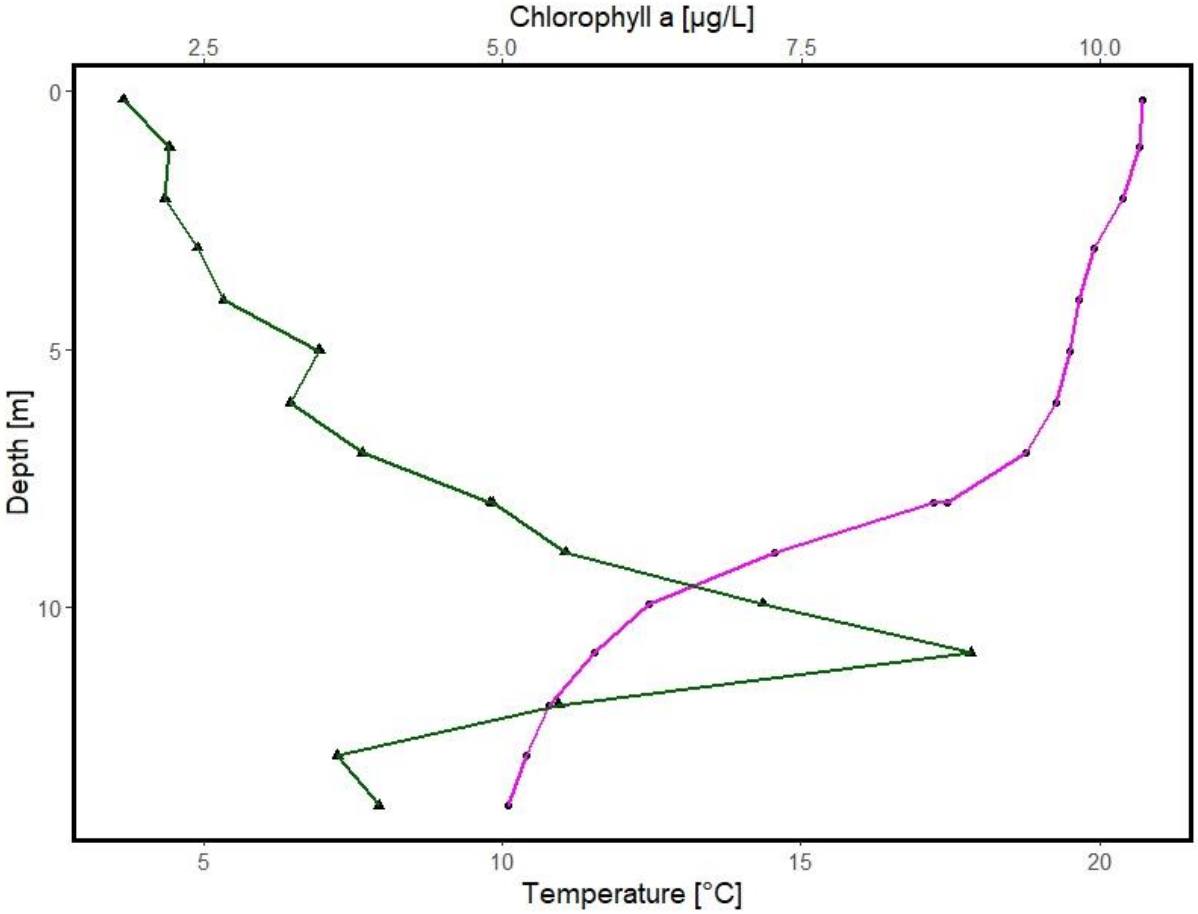
residing within the lower part of the enclosures (6-12 m) are depicted for the total *Daphnia* population (A, B), *D. cucullata* (C, D), and *D. longispina* (E, F) in response to different α-CPS concentrations and a control. Depicted are mean values +/- SE, n = 3).



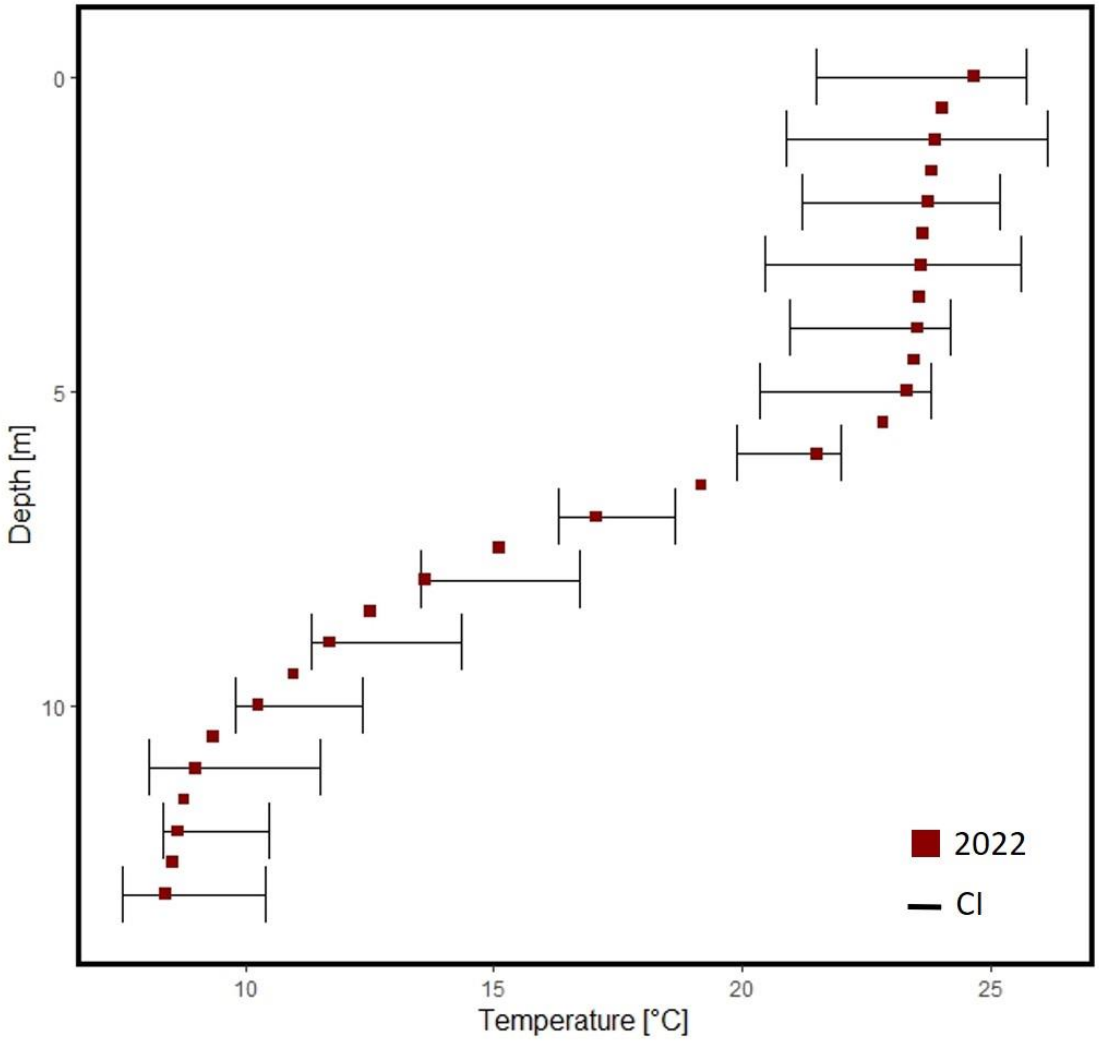
SI Figure 8 Vertical profiles of light intensity in mesocosms 48 hours after addition of 5α-cyprinol sulfate (CPS) during 2019. Depth dependent values of light intensity are depicted for three biological replicates of control (A), 1x CPS-treated (B) and 10x CPS-treated (C) mesocosms. The line represents the fit of an exponential model to the vertical profiles of light intensity across all replicates of the respective treatment.



SI Figure 9. Vertical distribution of *D. longispina* in Lake Klostersee at day and night in the upper and lower part of the water column during 2022. Depicted are mean (± SE, n=3) relative parts of the populations in percent (mean ± SE, n=3) that result from three consecutive dates. (A) relative parts residing in the upper part (0-8 m), and (B) residing in the lower part (8-12 m) of the water column during daytime and nighttime. Significant differences among daytime and nighttime within each layer are indicated by different letters (t-test).



SI Figure 10. Vertical profiles of temperature and chlorophyll a in Lake Klostersee during 2023. The green line connects the chlorophyll data points that were measured with a fluorescence probe; the magenta line connects the temperature data points.



SI Figure 11. Vertical profile of temperature in Lake Klostersee. Horizontal lines indicate 95 % C. I. of temperatures based on measurements in late summer of 2015, 2016, 2019, 2022 and 2023. The 2022 temperatures are displayed as red symbols.

Chapter 2: "Landscape of fear" in diel vertical migration: 5-alpha-cyprinol sulfate shapes the temporal and spatial dynamics of the perceived risk of predation in *Daphnia*

2.1 Abstract

In freshwater ecosystems, chemical cues play a critical role in shaping predator-prey interactions, offering a unique lens to explore the "landscape of fear" concept. 5α-cyprinol sulfate (CPS), a fish-borne chemical cue, induces diel vertical migration (DVM), a predator-avoidance behavior in *Daphnia*. This study examines 5α-CPS as a quantifiable fear metric in Lake Klostersee, where 5α-CPS concentrations reveal predation risk from fish perceived by *Daphnia* prey. "By mapping 5α-CPS levels across depths and time, we captured both diel and seasonal fluctuations. Laboratory bioassays demonstrated that *D. longispina* clones isolated from the same lake exhibited distinct 5α-CPS thresholds for the DVM induction, highlighting genotypic diversity in their response to predation risk. These findings underscore 5α-CPS's role in driving predator-prey dynamics, where chemical signals guide prey movement and ecosystem interactions, providing a robust model for the "landscape of fear" in aquatic environments, advancing our understanding of how chemical signaling shapes freshwater ecological networks.

2.2 Introduction

In ecological systems, the risk of predation plays a profound role in shaping prey behavior, influencing population dynamics, community interactions and entire ecosystem functions (Werner and Peacor 2003; LaManna and Martin 2016). The concept of the "landscape of fear" has become a valuable framework for understanding how prey species respond to spatial and temporal variations in predation risk (Laundré et al. 2001; Palmer et al. 2017; Gaynor et al. 2019b; Gallagher et al. 2017). Here, 'fear' refers to the risk of predation perceived by the prey, rather than actual predation. As prey adjust their behavior to the changing risk, they create heterogeneous patterns of distribution, which in turn shape interactions across trophic levels and influence ecosystem processes (Zelnik et al. 2021; Blubaugh et al. 2017; Zelnik et al. 2024). The landscape of fear offers a lens through which the non-consumptive effects of predators can be studied. Such non-consumptive effects of predators alter prey habitat use and movement patterns, even in the absence of direct predation. These changes in prey behavior can have far-reaching consequences, influencing resource distribution, prey population dynamics, and triggering trophic cascades, where the indirect effects of predators exceed the direct impacts of predation (Preisser et al. 2005; Turner et al. 2000). When applying the landscape of fear concept to real-world environment, a key challenge is to properly quantify the predation risk perceived by prey. The inherent difficulties in measuring risk perception have resulted in a variety of operational definitions and approaches in which prey behavior or habitat use are used as proxies for perceived risk of predation. In both terrestrial and marine ecosystems, the risk of predation perceived by prey is often assessed through direct observations of predator-prey interactions or inferred from prey distributions across high- and low-risk habitats (Laundré et al. 2001; Altendorf et al. 2001; Nicholson et al. 2014; Hammerschlag et al. 2015). However, prey behavior and distribution patterns reflect not only the perceived risk of predation but also the

trade-offs associated with changes in behavior or habitat use. These trade-offs may vary in time and space, and the same level of perceived risk of predation may therefore result in different patterns of habitat use in prey e.g. due to differences in preys' nutritional status (Gaynor et al. 2019a; Bleicher 2017). Moreover, recent findings show that human presence can substantially alter the perceived landscape of fear, influencing prey foraging behavior and habitat selection, particularly in semi-urban environments (Ortiz-Jimenez et al. 2025). In such environments, human activity may create a 'human shield' effect, reducing predator pressure and altering prey risk perception in ways not previously considered. These findings emphasize the need to account for varying ecological settings and external influences when evaluating the landscape of fear across different ecosystems. Thus, developing novel methodologies to accurately measure predation risk perceived by prey is crucial to refining our understanding of the landscape of fear and its ecological implications.

In freshwater ecosystems, such as lakes and ponds, predation imposes both direct and indirect effects on prey populations. For example, planktivorous fish strongly impact zooplankton prey through consumption, but already fish presence alone can induce profound behavioral changes in prey, such as altered movement patterns and reduced foraging activity (Brönmark et al. 2013). These non-consumptive effects are recognized as dominant forces that may shape community structure and ecosystem function (Schmitz et al. 2010). In freshwater systems, predator-prey interactions are often mediated by infochemicals - chemical cues that prey use to detect predators in their environment (Brönmark and Hansson 2012). These cues provide essential information that allow prey to adjust their behavior and habitat use based on the perceived risk of predation (von Elert 2012). One of the most well-known predator-induced behaviors in freshwater lakes and ponds is diel vertical migration (DVM), commonly observed in zooplankton species like *Daphnia* - a small herbivorous crustaceans playing an important

role in nutrient cycling and energy transfer through trophic levels (Miner et al. 2012). DVM involves *Daphnia* ascending toward the surface at dusk to feed on phytoplankton and descending to deeper, darker waters at dawn to avoid visually hunting fish (Stich and Lampert 1981). This adaptive behavior is a classic example of an inducible defense, triggered by chemical cues released by predators (von Elert and Pohnert 2000). Recent studies have identified the chemical cue responsible for inducing DVM in *Daphnia* as 5α-cyprinol sulfate (CPS), a bile salt released by cyprinid fish (Hahn et al. 2019). The identification of the inducing chemical cue opens up a unique opportunity to study the landscape of fear in aquatic environments by directly measuring CPS concentrations as the fear factor in the water. In aquatic systems, visual detection of predators is often limited, making chemical signals like CPS essential for prey species to perceive and evaluate predation risk (Brönmark and Hansson 2012). By measuring CPS concentrations in situ, we can directly map the landscape of fear in real time instead of using proxies to deduce the spatial and temporal dynamics within this landscape. This approach offers a precise method to link perceived risk of predation risk with prey behavior, allowing for a more accurate assessment of fear-driven interactions in aquatic ecosystems, a dimension that has largely been neglected in landscape of fear studies to date.

In this study, we present the first detailed spatio-temporal analysis of CPS concentrations in a natural lake environment during the stratification period. By measuring CPS levels at various depths at intervals ranging from months to days, we generate a high-resolution map of the chemical landscape of fear experienced by *Daphnia*. This allows us to track how CPS concentrations fluctuate in space and time and how these fluctuations are affected by environmental conditions.

Additionally, we explore the variability in *Daphnia's* response to CPS by examining the CPS threshold concentrations required to induce DVM in different *Daphnia longispina* genotypes originating from this very lake. Our results reveal significant variation in CPS sensitivity, with thresholds spanning three orders of magnitude across genotypes. This genetic diversity within the *Daphnia* population suggests that different clones, though experiencing the same landscape of fear, respond to predation risk in distinct ways, which may lead to differences in DVM patterns. Our study advances the understanding of how chemical signals like CPS mediate predator-prey interactions in freshwater ecosystems in space and time. By examining the spatial and temporal distribution of CPS alongside short-term observations of *Daphnia* behavior, we provide insights into chemically mediated landscapes of fear in aquatic environments. As climate change and other human impacts intensify, understanding how chemical signals indirectly influence predator-prey dynamics will be crucial for managing and preserving aquatic ecosystems.

2.3 Methods

Field Sampling

Field sampling was conducted in August 2022 and throughout the year in the prealpine mesotrophic lake "Klostersee" in Bavaria, Germany (47.97296045336554, 12.453592852811333). Klostersee is a dimictic hardwater lake with a maximum depth of 16 m, a surface area of 47 ha, and a volume of 2,762,000 m^3, characterized by stable stratification from spring to autumn (www.wwa-ts.bayern.de). Monthly sampling was conducted from April to October, covering various water layers (0-2 m, 2-4 m, 4-6 m, 6-8 m, 8-10 m, 10-12 m), with the exception of September, when no samples were collected. Sampling at deeper layers was avoided due to the presence of muddy sediments. Water samples from each layer were collected

using a tube sampler (integrated water sample, KC Denmark), and to remove larger particles, they were filtered through a 250 µm plankton net. Additionally, day and night sampling at the same water layers took place on three consecutive days from August 17th to August 19th. For interpreting the diel and seasonal CPS concentration patterns, it is essential to consider the potential influence of sample processing methods. The samples collected to assess seasonal patterns were immediately frozen post-sampling and extracted right after thawing, preserving CPS concentrations by minimizing microbial activity. In contrast, the samples collected over the three consecutive days for examining diel patterns were stored in the refrigerator overnight prior to solid-phase extraction. This difference in handling may have allowed for bacterial degradation, potentially reducing the overall CPS concentrations in the short-term, day-night samples. Consequently, while we can confidently report temporal patterns, the absolute CPS concentrations in diel samples may be slightly underestimated. This assumption should be considered when comparing CPS levels across different timescales.

Solid phase extraction

The C_{18}-SPE cartridges (Agilent Bond Elute C18, 500 mg, 3 ml) were activated with 10 mL of 100% methanol (MeOH) and conditioned to 1% MeOH. Each sample was made up to MeOH and passed through the cartridge, which was subsequently eluted with 10 mL of MeOH and collected in a glass tube. Each sample was applied to a new cartridge to avoid cross contamination. Technical replicates were applied to the same cartridges. The collected samples were dried overnight in a vacuum centrifuge at 30 °C and 1500 rpm. Once dried, samples were re-dissolved in 200 µL of MeOH and transferred into glass vials for further analysis.

Mass spectrometry and quantification

Mass analysis was conducted by applying 5 µL of each sample to a Vanquish™ Horizon UHPLC system coupled with a Q-Exactive HF mass spectrometer (Thermo Fisher Scientific, Dreieich, Germany). Metabolite separation was achieved on an EC 125/2 Nucleosil 100-3 C18 column (Macherey-Nagel, Düren, Germany) maintained at 30 °C and a constant flow rate of 300 µL/min. The mobile phase comprised solvent A (0.01% ammonium acetate and 10 mM formic acid in water) and solvent B (0.01% ammonium acetate and 10 mM formic acid in a 6:9 [v/v] mixture of acetonitrile and methanol). Three solvent gradient programs were applied: Gradient A (20% B, 0–28 min gradient to 100% B; 28–32 min at 100% B; 32–33 min gradient to 20% B; 33–35 min at 20% B), Gradient B (30% B, 0–8 min gradient to 100% B; 8–10 min at 100% B; 10–11 min gradient to 30% B; 11–12 min at 30% B), and Gradient C (30% B, 0–12 min gradient to 100% B; 12–14 min at 100% B; 14–15 min gradient to 30% B; 15–16 min at 30% B). We used different gradient programs for the analysis. Gradient A was applied to a subset of lake water samples to allow for the detection of additional seasonal patterns of other kairomones in future analyses. Gradient B was used to quantify the remaining subset of lake water samples. For the Day and Night samples, an optimized gradient was developed to achieve the highest resolution of the CPS peak. Negative ionization was performed for each gradient, with a spray voltage of 3.0–3.53 kV and a capillary temperature set to 360 °C. To ensure accurate CPS quantification, a calibration curve for the internal standard cholesteryl sulfate was included in each sample sequence (Figure SI 5).

Diel vertical migration bioassays

We used a plankton organ (Dawidowicz and Loose 1992) to assess the vertical daytime distribution of *Daphnia longispina* clones, following the setup described by (Brzeziński and von Elert 2015). This standardized experimental design reliably indicates kairomone effects, as the daytime depth on day 3 correlates with kairomone concentrations (von Elert and Pohnert 2000). Briefly, Plexiglas tubes (1 m long, 200 mL volume, stoppered at the bottom) were placed vertically in a thermally stratified water bath and illuminated from the top (photoperiod 16L:8D). A thermal gradient in the organ simulated a thermally stratified lake in summer. Tubes were filled with either control water (negative and positive controls) or treatments with various volumes of C_{18}-solid-phase extract of incubation water of fish (*Rutilus rutilus*), which resulted in different concentrations of CPS (5684.91 ng/L, 568.29 ng/L, 56.85 ng/L, 5.31 ng/L, 0.53 ng/L). Each treatment and control had four replicates, resulting in a total of 28 tubes. Cohorts of 10-day-old *D. longispina*, which originated from the third or fourth clutch, were used. Four to five individuals were transferred to each tube and fed with the green alga *C. klinobasis* to a concentration of 2 mg C/L. After two days, a 1:1 mixture of *C. klinobasis* and *Acutodesmus* sp. was provided to maintain the carbon concentration. The vertical position of the *Daphnia* was recorded at 9 a.m. and 3 p.m. for three consecutive days with 5 cm accuracy.

Statistical analyses

Data collected from field sampling, laboratory analyses and weather data from the Climate Data Center (CDC) of the Deutscher Wetterdienst (DWD) were compiled and preprocessed using R software (version 3.6.2). Descriptive statistics, including means, medians, standard errors, and ranges, were calculated for CPS concentrations, *Daphnia* abundance, and other relevant parameters. Shapiro-Wilk tests were conducted to evaluate the normality of CPS concentration

data and *Daphnia* abundance data. To compare CPS concentrations between day and night, both above and below the thermocline, Welch's Two-Sample t-tests were applied, as the data violated normality assumptions. A Welch's Two-Sample t-test was used to test for differences in CPS concentrations between nighttime samples collected above and below the thermocline. Statistical significance was determined at a threshold of $p < 0.1$. The distribution *of Daphnia longispina* individuals was also compared between day and night for depths above and below the thermocline. Mann-Whitney U tests were performed due to non-normal distributions of abundance data. Statistical significance was determined at a threshold of $p < 0.05$. Data visualization was performed using the ggplot2. Error bars in the figures represent the standard error of the mean, and letters above the bars in boxplots indicate significant differences based on Tukey's test. Statistical analyses and graphical representations were conducted in R software.

2.4 Results

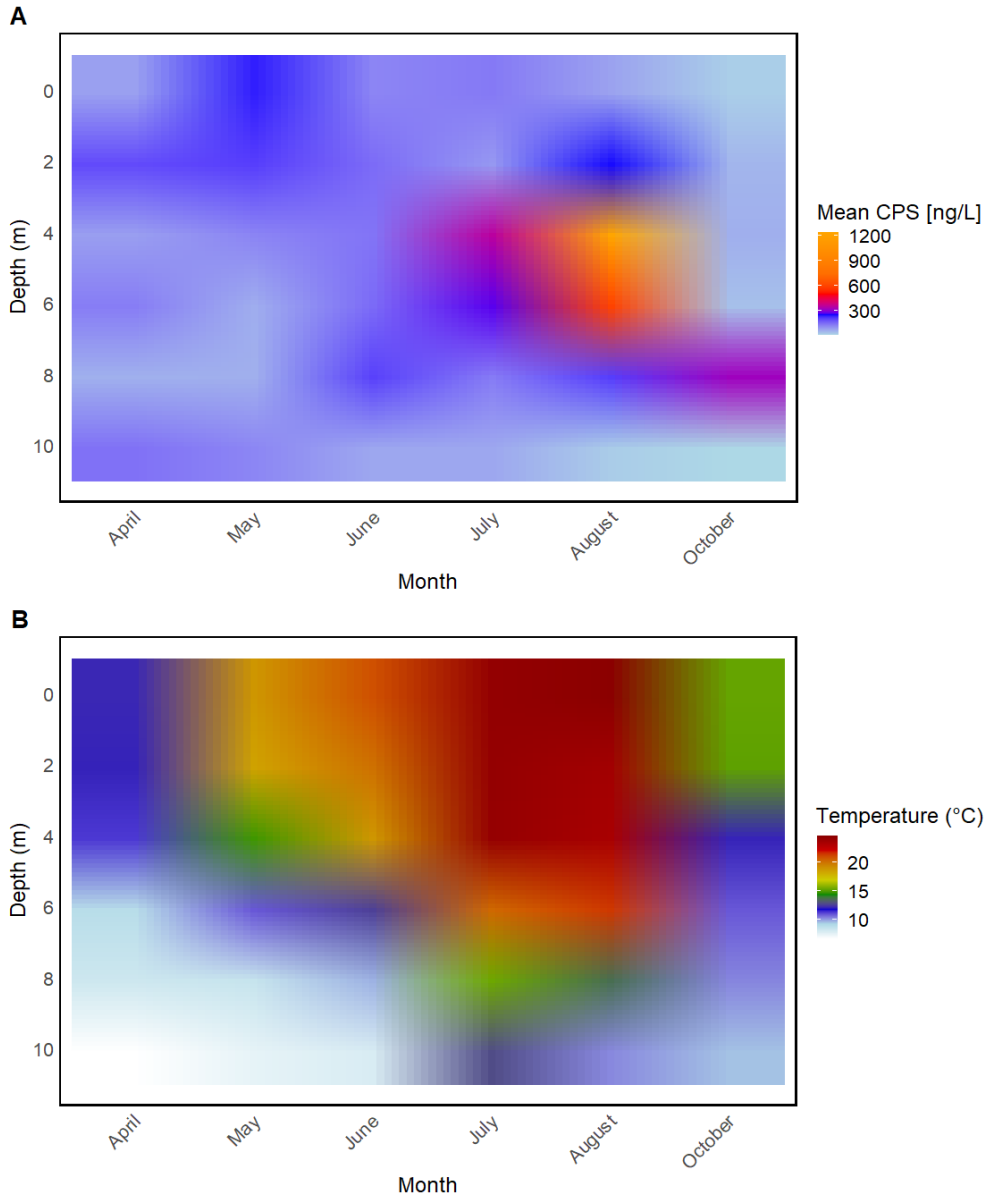


Figure 1: Depth profiles of 5α-cyprinol sulfate (CPS) concentration and temperature over time in Lake Klostersee, 2022. Panel A shows a heatmap illustrating the CPS concentrations (ng/L) across depths (0–10 meters) and months (April to October). The color gradient represents CPS concentrations, from low (blue) to high (red). **Panel B** shows the temperature profile (°C) for the same time period. The color scale indicates water temperatures with cooler temperatures in blue and warmer temperatures in red, showing the vertical thermal stratification of the lake.

Seasonal variability of CPS concentrations and temperature profiles

5α-cyprinol sulfate (CPS) concentrations and temperature profiles in Lake Klostersee exhibited pronounced seasonal and depth-dependent variability (Figure 1). The temperature profile (Figure 1B) shows a pronounced seasonal stratification of the water column, with surface layers warming up from June to August, creating a distinct thermocline around 6 meters at 23°C. Although thermal stratification of the lake started from April on, CPS levels remained consistently low across all depths (<300 ng/L) until June. However, between July and August, CPS concentrations increased markedly, reaching up to four times higher levels in the metalimnion (6 to 8 meters) whereas they remained almost unchanged in the epilimnion (0 to 4 meters) By October, CPS levels decreased alongside a general cooling trend. During the warmest months, CPS levels peak in the metalimnion (6–8 meters), aligning with the thermocline where temperature gradients are steepest. This pattern likely reflects temperature-driven biological or chemical processes. Figure 6 further supports the relationship, illustrating a positive correlation between CPS concentration and temperature, with higher CPS levels at warmer temperatures (linear regression model, $p < 0.001$).

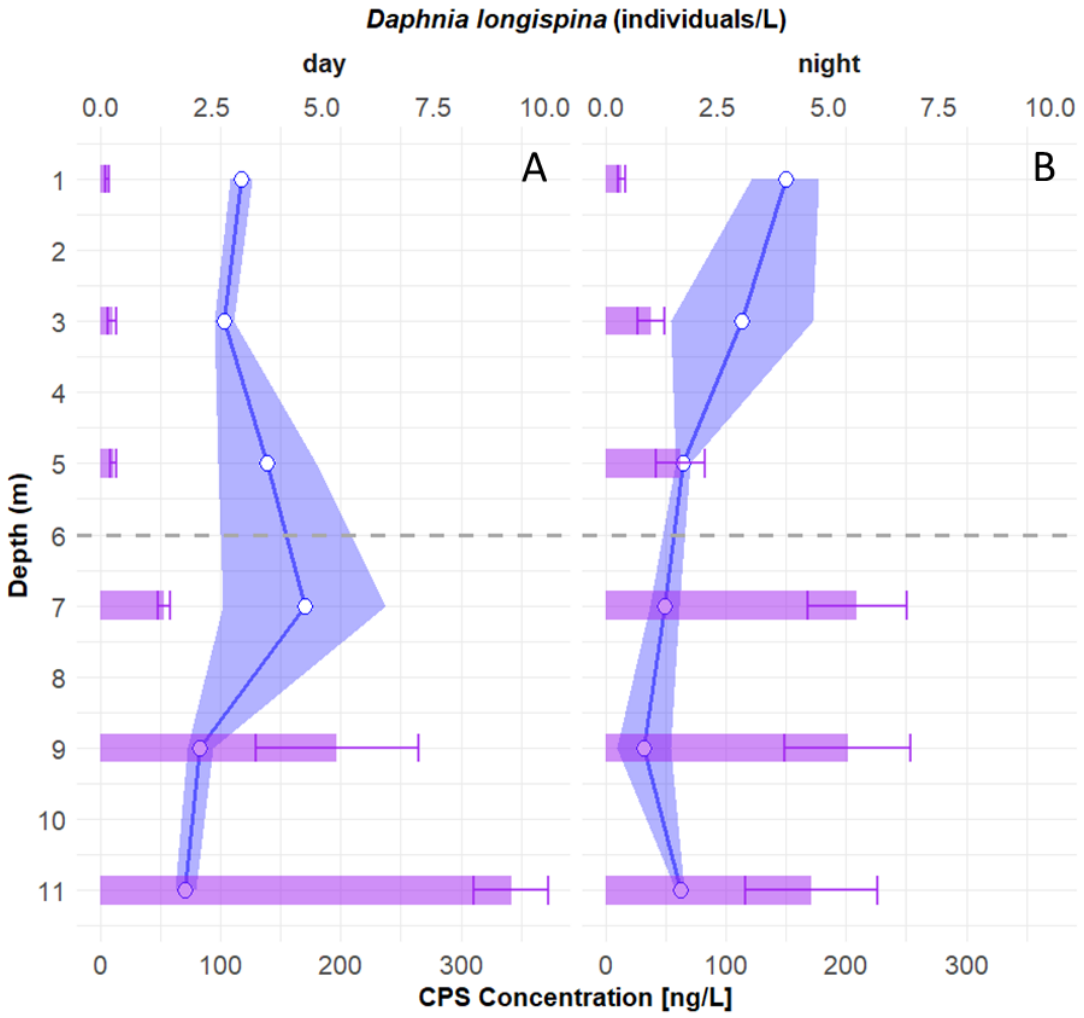


Figure 2: Depth profiles of 5α-cyprinol sulfate (CPS) concentrations and *Daphnia longispina* abundances during day and night conditions. The CPS concentration (ng/L) is represented by a blue shaded area and white-filled points that indicate the mean CPS concentrations with a darker blue shaded area reflecting the standard error. Purple horizontal bars (mean +/- SE, n = 3) show abundances of *Daphnia longispina* (individuals/L). **Panel A** depicting daytime and **Panel B** depicting nighttime vertical distributions. The dashed horizontal line marks the thermocline at 6 m depth.

Short-term depth profiles of CPS concentration and *Daphnia longispina* DVM

The short-term depth profiles of CPS concentration and *Daphnia longispina* abundance, collected simultaneously, reveal distinct day-night distribution patterns (Figure 2). During the daytime, CPS concentrations were relatively balanced between the epilimnion (above the thermocline, mean concentration over 3 days: 119 ng/L) and the hypolimnion (below the thermocline, 107.8 ng/L). At night (Fig Sl 2), however, CPS concentrations shifted notably, with a greater proportion found above the thermocline (mean concentration over 3 days: 109 ng/L) compared to below (47.6 ng/L). For samples collected above the thermocline, the mean CPS concentration was significantly higher at night compared to the day (Welch Two-Sample t-Test, $p < 0.1$). In contrast, below the thermocline, CPS concentrations were significantly higher during the day compared to nighttime samples (Welch Two-Sample t-Test, $p < 0.05$; Figure 5). These findings indicate that the time of day has a significant impact on CPS concentrations below the thermocline, whereas concentrations above the thermocline show a notable nighttime increase. This vertical distribution of CPS coincides with DVM patterns *of D. longispina*, which demonstrate increased abundance at deeper water layers during nighttime compared to daytime (Figure 2). There are significantly more individuals above the thermocline at night than during the day (daytime median above thermocline: 0.207 ind./L, nighttime median above thermocline: 0.716 ind./L, Wilcoxon rank-sum test, $p = 0.001976$). Below the thermocline there is no significant difference between day and nighttime abundance of the *D. longispina* individuals (Wilcoxon rank-sum test, $p=1$).

Impact of a storm event on CPS concentrations

During the three-day observation period (17–19 August), CPS concentrations above the thermocline were generally similar during the day and night (Figure S1). However, a distinct diel pattern emerged, with CPS concentrations increasing above the thermocline at night, particularly on the first two nights (17th and 18th of August; Figure S1D, E). This nighttime increase coincided with a higher abundance of *Daphnia longispina* individuals migrating upwards towards the thermocline during nighttime. In contrast, during the final night of the observation period (19th of August), a notable reduction in CPS concentrations was observed across all depths (Figure S1F). This change coincided with a storm event (Figure Sl 4), characterized by substantial precipitation (66.73 mm/day) and increased wind speeds (up to 5.6 m/s). However, the vertical distribution of *Daphnia longispina* during the final night remained similar to the patterns observed on the previous nights.

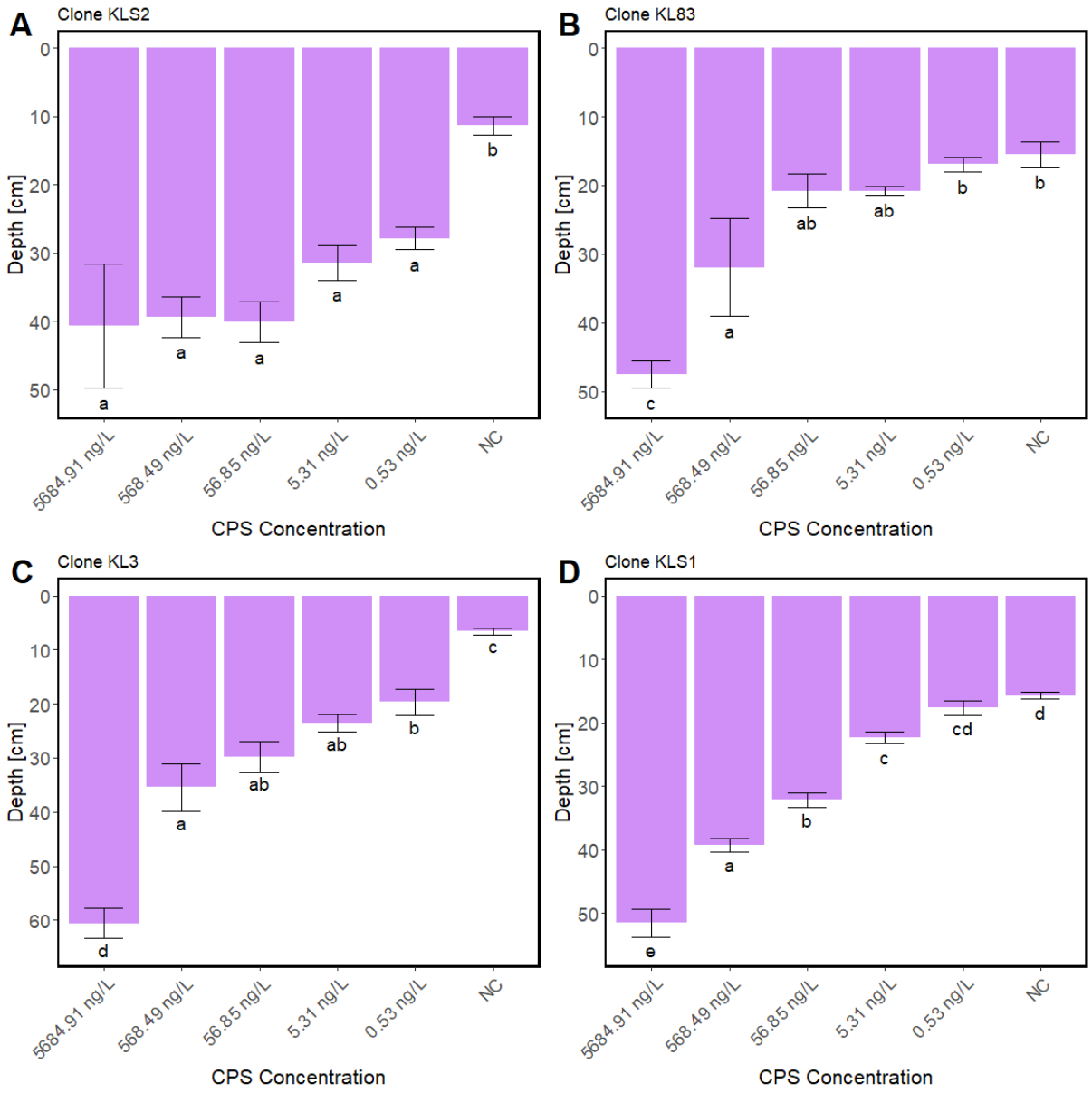


Figure 3: Depth daytime distribution of *Daphnia longispina* clones in response to 5α-cyprinol sulfate (CPS) concentrations in an indoor bioassay. Panel A-D: Mean (+/- SE, n = 4) daytime depth distribution (cm) across various *D. longispina* clones for different concentrations (ng/L) of CPS. Each plot represents a different *D. longispina* clone (**A:** clone KLS2, **B:** clone KL83, **C:** clone KL3, **D:** clone KLS1). Different letters indicate statistical differences at $p < 0.05$ level, analyzed by ANOVA followed by HSD Tukey post-hoc test. Error bars indicate standard error, NC: negative control.

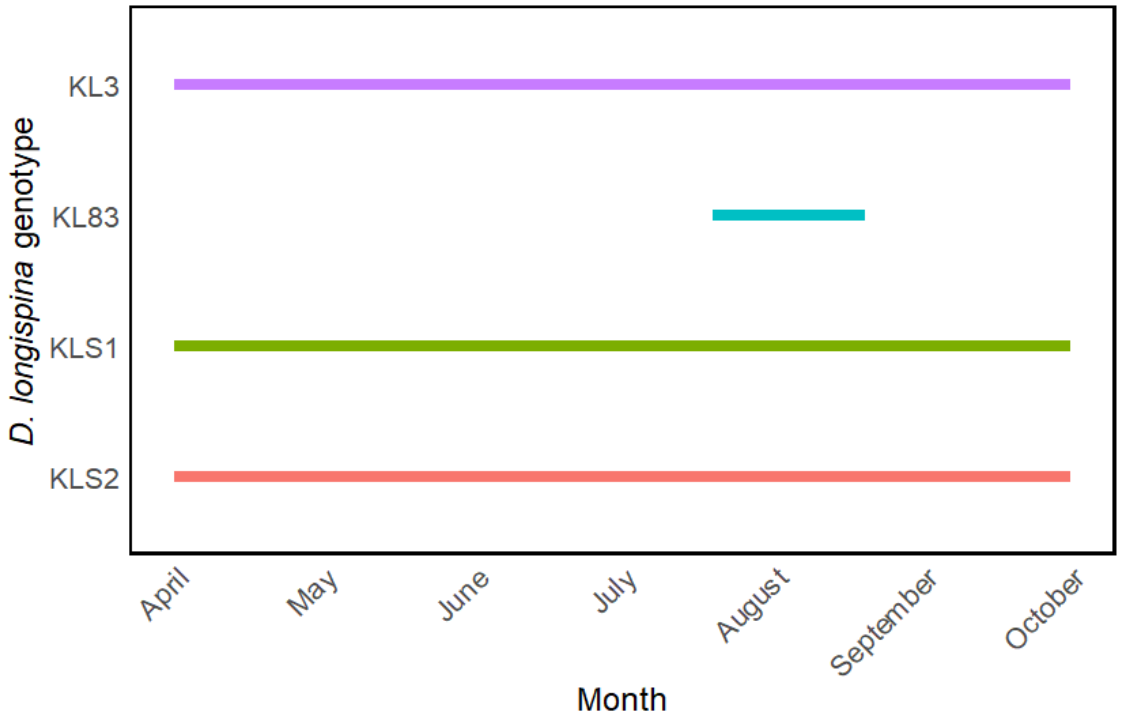


Figure 4: Predicted periods during which four *Daphnia longispina* clones (KLS2, KLS1, KL83, and KL3) are expected to exhibit diel vertical migration (DVM) in lake Klostersee. Predictions are based on in-situ concentrations of 5α-cyprinol sulfate (CPS) throughout the year and clone-specific CPS threshold concentrations required to induce DVM. The x-axis represents the months (April to October), while the y-axis shows the *D. longispina* genotypes. Horizontal colored bars indicate the time windows during which CPS concentrations are sufficient to trigger DVM for each clone.

Bioassays on CPS thresholds for DVM in *Daphnia longispina* clones

In the laboratory, bioassays indicated that each *Daphnia longispina* clone isolated from lake Klostersee exhibited a distinct threshold CPS concentration that triggered diel vertical migration (DVM). In Clone KLS2 (Figure 3A), DVM behavior is initiated at a CPS concentration of 0.53 ng/L, as evidenced by a significantly deeper daytime residence in the water columns compared to the control. Clone KL83 (Figure 3B) required a higher CPS concentration threshold of 558.49 ng/L to induce significant vertical migration. Clone KL3 (Figure 3C) and clone KLS1 (Figure 3D) both showed a response to CPS concentrations of 5.35 ng/L, migrating to deeper water in comparison to lower CPS levels and the control. These findings indicated variability in CPS sensitivity among *D. longispina* clones, with CPS concentration thresholds for DVM ranging from 0.53 ng/L to 568.49 ng/L. This diversity in threshold concentrations points to differences in responsiveness to fish in terms of induction of DVM across genotypes, which for the first time allow to predict when during the season these genotypes will perform DVM (Figure 4).

2.5 Discussion

Our study provides the first detailed exploration of the landscape of fear in aquatic environments by using 5α-cyprinol sulfate (CPS) concentrations as a quantitative measure of perceived fish predation risk, offering a real-time assessment of seasonal and diel variations. This empirical approach goes far beyond traditional models (Schmidtand Kuijper 2015), extending theoretical insights from terrestrial studies on spatial and temporal risk perception and prey response (Bleicher 2017; Laundré et al. 2010; Laundré et al. 2014; Gaynor et al. 2019b). In parallel with terrestrial studies (Hopcraft et al. 2014; Kohl et al. 2018), our findings reveal that the landscape of fear in aquatic environments is dynamic and fluctuates on a seasonal

and daily time scale. *Daphnia* migration patterns in response to CPS concentrations further emphasize the dynamic nature of predator-prey interactions in aquatic ecosystems, reinforcing the cross-system relevance of the landscape of fear concept.

Seasonal fluctuations in CPS landscape of fear

In Lake Klostersee, Bavaria, Germany, cyprinids are highly abundant, particularly in the lower littoral and benthic areas, with species like roach (*Rutilus rutilus*), rudd (*Scardinius erythrophthalmus*), and bream (*Abramis brama*) dominating the fish population in these habitats. In the benthic areas, older bream and tench (*Tinca tinca*) are most prevalent, further emphasizing cyprinid dominance (Dr. Bernhard Gum and Dr. Leonhard Egg, Fachberatung für Fischerei, Bezirk Oberbayern, pers. comm.). Seasonal mapping of the cyprinid kairomone CPS across the lake profile reveals distinct patterns in perceived predation risk, with an up to a fourfold increase in CPS concentrations, peaking in July and August. These seasonally fluctuating CPS concentrations align with increased fish predation activity on zooplankton during summer, particularly in July and August (van Densen 1985; Persson 1983a; Vijverberg et al. 2005). Warmer water temperatures, reaching up to 23°C in the epilimnion and extending to the 6-meter thermocline in August 2022, likely amplify fish metabolism, driving higher kairomone release rates. Studies have shown that elevated temperatures accelerate digestion rates in fish, increasing the production of metabolic byproducts such as CPS, which in turn elevates predation risk for zooplankton (Bohl 1979; Lassand Spaak 2003). Furthermore, summer feeding intensities are known to peak under these conditions, with cyprinids exploiting the abundant zooplankton populations to meet their energy demands (Chapman et al. 2013; Brodersen et al. 2011; Persson 1983a). Interestingly, CPS concentrations during July and August were not uniformly distributed throughout the epilimnion but peaked around the

thermocline, at depths of 4–8 meters. This thermocline boundary presents distinct temperature and oxygen gradients that strongly influence fish distribution, as it provides optimal conditions for balancing feeding and safety. At these depths, fish likely aggregate to capitalize on higher prey densities while reducing their own risk of predation by larger piscivores (Levy 1990; Vašek et al. 2009; Mehner 2012). In contrast, the reduced CPS concentrations in colder months are likely tied to lower metabolic demands and feeding rates in fish, as supported by observations of reduced gut fullness during winter (Chapman et al. 2013). Seasonal horizontal migrations of fish to refuge areas, such as streams, during colder months may further reduce kairomone release into the water column (Brodersen et al. 2011).The interplay between temperature, predation dynamics, and kairomone release underscores the importance of seasonal factors in shaping the chemical landscape of fear in Lake Klostersee.

Diel fluctuations in CPS landscape of fear

During the day, fish typically avoid the surface, likely due to increased predation risk and metabolic costs associated with warmer, well-lit waters. Instead, they remain near the thermocline—a "safe zone", where light levels support foraging but are low enough to reduce predation risk (Mehner 2012). By overlaying CPS concentration patterns with those of *Daphnia* migration, we observe that *Daphnia* migrate deeper during the day, nearly reaching the lake bottom. This behavior likely reflects a response to increased predation risk in mid-depth layers, which may be reflected by elevated CPS concentrations in the metalimnion during the day, near the thermocline. This supports the idea that fish balance their foraging needs with the risk of predation at these depths, creating a localized landscape of fear for *Daphnia*.

At night, significantly higher CPS concentrations in the upper water layer strongly suggest that cyprinid fish migrate back towards the surface, a behavior previously observed in other fish

taxa, such as juvenile sockeye salmon and coregonids (Scheuerell and Schindler 2003; Hrabik et al. 2006). This nocturnal upward movement of cyprinids aligns with the general pattern of diel vertical migration (DVM) seen in many freshwater systems, where *Daphnia* ascend towards the surface at night to feed while avoiding visually hunting predators during the day (Loose and Dawidowicz 1994; Stich and Lampert 1981). However, in the studied lake, *Daphnia* tend to remain just below the thermocline at nighttime, a behavior likely influenced by the presence of a deep chlorophyll maximum (DCM), which provides both a nutrient-rich habitat and partial refuge from fish predators (Ahlers and Hahn et al. 2024). As noted by Rinke & Petzoldt (2008), *Daphnia* dynamically adjust their migration patterns in response to vertical gradients of food and temperature, optimizing their position to balance energy intake and predation risk. Their study highlights that the DCM serves as a strong attractor, prompting *Daphnia* to modify their migration amplitude accordingly. Furthermore, DVM behavior of fish may contribute to a dynamic environment in which *Daphnia* strategically occupy depths just below the thermocline, thereby minimizing predation risk. By inhabiting this intermediate layer, *Daphnia* can balance their need for essential food resources with reduced exposure to visual predators during the night.

This pattern supports the hypothesis that *Daphnia* use CPS as a chemical risk indicator to adjust their migration depth and minimize predation risk while maximizing fitness. Interestingly, during diel patterns observed over three consecutive days (17-19 August 2022), we noted a decline in nighttime CPS concentrations above the thermocline on the 19th of August. This reduction coincided with a storm event characterized by strong winds and heavy rainfall after the daytime sampling, which likely enhanced vertical mixing, disrupting the thermal stratification and leading to a redistribution or dilution of CPS concentrations throughout the water column, thus temporarily altering the landscape of fear for *Daphnia* on a short-term scale.

Despite the reduced CPS concentrations on the final night, the *Daphnia* DVM behavior persisted. This suggests that *Daphnia* may possess a longer memory of perceived predation risk or respond to threshold CPS concentrations that indicate predation pressure, independent of the spatial distribution of the chemical cue. Overall, the observed diel and seasonal patterns of CPS concentrations, along with the increased metabolism and feeding rates of zooplanktivorous fish in warmer waters, suggest that feeding intensity and digestion efficiency of fish significantly shape CPS release. This, in turn, influences the vertical profile of CPS concentrations and the associated landscape of fear, driving predator-prey dynamics. These findings mirror patterns observed in terrestrial ecosystems, where predator activity peaks seasonally or daily, prompting prey to adjust their behavior to mitigate risk (Kohl et al. 2018; Palmer et al. 2017).

Genotypic variation in *Daphnia*'s CPS sensitivity thresholds

A notable finding in our study is the variability among *Daphnia longispina* clones in their sensitivity to CPS concentrations. Clone KL83, with the highest threshold of 569 ng/L, is predicted to initiate DVM only in August when CPS concentrations in the 4 to 6-meter layer exceed this threshold. This observation aligns with the findings of (de Meester et al. 1995), who demonstrated that coexisting *Daphnia* clones exhibit distinct vertical distributions in response to the fish kairomone. Their study highlighted how genetic polymorphism drives variability in antipredator strategies, enabling clones to respond differently to predation cues. Building on this, our study provides the first direct evidence of differing CPS thresholds among coexisting clones within a single population, illustrating how genotypic variability allows clones to exploit temporal niches throughout the season. This genotype-specific variability demonstrates that while all clones experience the same landscape of fear, their DVM initiation depends on individual thresholds for risk tolerance. DVM describes the diurnal changes in vertical

distribution among zooplankton individuals within a population, which in the case of *Daphnia*, exhibits substantial genetic and trait variation (Tams et al. 2018; Chaturvedi et al. 2021). As a consequence, DVM patterns reflect the mean response of a population composed of genotypes with different sensitivities. By combining in-situ CPS concentrations with CPS thresholds for DVM onset in various *D. longispina* genotypes from the same lake, we can, for the first time, predict which genotype will perform DVM at specific times during the season. This supports the hypothesis by (Stich and Lampert 1981) that seasonally changing DVM amplitudes in *Daphnia* arise from shifts in the composition of genotypes that differ in their responsiveness to predation cues. The genotypic differences observed in *Daphnia* profoundly influence nutrient cycling and energy flow within lake ecosystems. As *Daphnia* migrate in response to CPS concentrations, they reduce predation by fish and redistribute nutrients vertically in the water column, affecting resource availability for primary producers and modifying nutrient flow across trophic levels (Haupt et al. 2010). During summer, higher predation risk could drive increased DVM among predation-tolerant clones, influencing nutrient redistribution and energy transfer across trophic levels. This underscores the role of genetic variation in prey populations in shaping ecosystem dynamics in response to seasonal shifts in predation pressure.

Broader ecological implications and future directions

Here we include chemical ecology in the consideration of predator-prey dynamics, and by doing so we expand the landscape of fear framework to include non-visual communication between predators and prey. The genotypic variation observed in *D. longispina* with respect to CPS-thresholds for the onset of DVM highlights the complexity of anti-predator strategies shaped by chemical cues within prey populations. While in-situ measurements of CPS provide, for the first time, a true landscape of fear for prey, this will not necessarily predict the patterns of DVM.

It is well known that DVM comes with the benefit of reducing predator-mediated mortality and accordingly increases with predator abundance (Loose et al. 1993b) and CPS-concentration (Hahn et al. 2019). DVM comes with trade-offs resulting in strong demographic costs (Stich and Lampert 1981), which are caused by low temperature and food scarcity during daytime residence in lower water layers (Dawidowicz and Loose 1992; Loose and Dawidowicz 1994). As a result, for a given risk of predation, the amplitude of DVM is affected by environmental conditions like food availability (Johnsen and Jakobsen 1987) and the temperature difference between epi- and hypolimnion (Dawidowicz et al. 2023). These complex factors suggest that CPS alone may not capture the full range of influences driving prey fear behavior. Future research should incorporate more variables to expand and strengthen this landscape of fear model, which we believe is an ideal framework for understanding predator-prey dynamics in aquatic ecosystems.

2.6 Author contribution statement

Johanna Ahlers conceptualized the study, performed CPS-quantification, compiled data, fitted statistical models, analyzed and visualized modeling outputs, interpreted results, and wrote the first draft of the manuscript. Jonas Lange performed indoor bioassays, and Maria Stockenreiter conducted monthly water sampling from Lake Klostersee. Eric von Elert conceptualized the study, supervised the work and revised the manuscript, and all authors provided feedback and approved the final version.

2.7 Acknowledgements

We thank Jakob Büssemaker for collecting and analyzing lake zooplankton samples during 2022 and Dr. Bernhard Gum and Dr. Leonhard Egg from the Fachberatung für Fischerei (Bezirk Oberbayern) for providing unpublished data on fish populations in Lake Klostersee, which contributed substantially to the ecological context of our study. This research was supported by the German Science Foundation (DFG) through a grant awarded to EVE (EL 179/16-1). Open Access funding was partly provided by the University of Cologne and organized through Projekt DEAL.

2.8 References

1. Ahlers, J. and Hahn, M. A.; Stockenreiter, M.; Stibor, H.; von Elert, E (2024). Mesocosm experiments validate induction of *Daphnia* vertical migration by the fish-derived kairomone 5α-cyprinol sulfate. *Limnology & Oceanography Letters*, 9(3), 307–315.

2. Altendorf, K. B.; Laundré, J. W.; López González, C. A.; Brown, J. S. (2001). Assessing effects of predation risk on foraging behavior of mule deer. *Journal of Mammalogy*, 82(2), 430–439.

3. Bleicher, S. S. (2017). The landscape of fear conceptual framework: Definition and review of current applications and misuses. *PeerJ*, 5, e3772.

4. Blubaugh, C. K.; Widick, I. V.; Kaplan, I. (2017). Does fear beget fear? Risk-mediated habitat selection triggers predator avoidance at lower trophic levels. *Oecologia*, 185(1), 1–11.

5. Bohl, E. (1979). Diel pattern of pelagic distribution and feeding in planktivorous fish. *Oecologia*, 44(3), 368–375.

6. Brodersen, J.; Nicolle, A.; Nilsson, P. A.; Skov, C.; Brönmark, C.; Hansson, L.-A. (2011). Interplay between temperature, fish partial migration, and trophic dynamics. *Oikos*, 120(12), 1838–1846.

7. Brönmark, C.; Hulthén, K.; Nilsson, P. A.; Skov, C.; Hansson, L.-A.; Brodersen, J.; et al. (2013). There and back again: Migration in freshwater fishes. *Canadian Journal of Zoology*, 92(6), 467–479.

8. Brönmark, C. and Hansson, L.-A. (2012). Chemical Ecology in Aquatic Systems. OUP Oxford.

9. Brzeziński, T. and von Elert, E. (2015). Predator evasion in zooplankton is suppressed by polyunsaturated fatty acid limitation. *Oecologia*, 179(3), 687–697.

10. Chapman, B. B.; Eriksen, A.; Baktoft, H.; Brodersen, J.; Nilsson, P. A.; Hulthen, K. et al. (2013). A foraging cost of migration for a partially migratory cyprinid fish. *PLoS ONE*, 8(5), e61223.

11. Chaturvedi, A.; Zhou, J.; Raeymaekers, J. A. M.; Czypionka, T.; Orsini, L.; Jackson, C. E. et al. (2021). Extensive standing genetic variation from a small number of founders enables rapid adaptation in *Daphnia*. *Nature Communications*, 12(1), 4306.

12. Dawidowicz, P.; Barzycka, K.; Pijanowska, J. (2023). Costs of *Daphnia* diel vertical migrations under forecasted increase of lake temperature. *Hydrobiologia,* 850(21), 4831–4837.

13. Dawidowicz, P. and Loose, C. J. (1992). Metabolic costs during predator-induced diel vertical migration of *Daphnia*. *Limnology & Oceanography*, 37(8), 1589–1595.

14. De Meester, L.; Weider, L. J.; Tollrian, R. (1995). Alternative antipredator defences and genetic polymorphism in a pelagic predator–prey system. *Nature, 378*(6556), 483–485.

15. Gallagher, A. J.; Creel, S.; Wilson, R. P.; Cooke, S. J. (2017). Energy landscapes and the landscape of fear. *Trends in Ecology & Evolution*, 32(2), 88–96.

16. Gaynor, K. M.; Brown, J. S.; Middleton, A. D.; Power, M. E.; Brashares, J. S. (2019). Landscapes of fear: Spatial patterns of risk perception and response. Trends in Ecology & Evolution, 34(4), 355–368.

17. Hahn, M. A.; Effertz, C.; Bigler, L.; von Elert, E. (2019). 5α-cyprinol sulfate, a bile salt from fish, induces diel vertical migration in *Daphnia*. *eLife*, 8, e44791.

18. Hammerschlag, N.; Broderick, A. C.; Coker, J. W.; Coyne, M. S.; Dodd, M.; Frick, M. G. et al. (2015). Evaluating the landscape of fear between apex predatory sharks and mobile sea turtles across a large dynamic seascape. *Ecology*, 96(8), 2117–2126.

19. Haupt, F.; Stockenreiter, M.; Reichwaldt, E. S.; Baumgartner, M.; Lampert, W.; Boersma, M.; Stibor, H. (2010). Upward phosphorus transport by *Daphnia* diel vertical migration. *Limnology & Oceanography*, 55(2), 529–534.

20. Hopcraft, J. G. C.; Morales, J. M.; Beyer, H. L.; Borner, M.; Mwangomo, E.; Sinclair, A. R. E. et al. (2014). Competition, predation, and migration: Individual choice patterns of Serengeti migrants captured by hierarchical models. *Ecological Monographs, 84*(3), 355–372.

21. Hrabik, T. R.; Jensen, O. P.; Martell, S.J.D.; Walters, C.J.; Kitchell, J.F. (2006): Diel vertical migration in the Lake Superior pelagic community. I. Changes in vertical migration of coregonids in response to varying predation risk. *Can. J. Fish. Aquat. Sci.* 63 (10), 2286–2295.

22. Johnsen, G. H. and Jakobsen, P. J. (1987). The effect of food limitation on vertical migration in *Daphnia longispina*. *Limnology & Oceanography, 32*(4), 873–880.

23. Kohl, M. T.; Stahler, D. R.; Metz, M. C.; Forester, J. D.; Kauffman, M. J.; Varley, N. et al. (2018). Diel predator activity drives a dynamic landscape of fear. *Ecological Monographs, 88*(4), 638–652.

24. LaManna, J. A. and Martin, T. E. (2016). Costs of fear: Behavioural and life-history responses to risk and their demographic consequences vary across species. *Ecology Letters, 19*(4), 403–413.

25. Lass, S. and Spaak, P. (2003). Temperature effects on chemical signalling in a predator–prey system. *Freshwater Biology, 48*(4), 669–677.

26. Laundré, J. W.; Hernández, L.; Ripple, W. J. (2010). The landscape of fear: Ecological implications of being afraid. *The Open Ecology Journal, 3*(1), 1–7.

27. Laundré, J. W.; Hernández, L.; Altendorf, K. B. (2001). Wolves, elk, and bison: Reestablishing the "landscape of fear" in Yellowstone National Park, U.S.A. *Canadian Journal of Zoology, 79*(8), 1401–1409.

28. Laundré, J. W.; Hernández, L.; López Medina, P.; Campanella, A.; López-Portillo, J.; González-Romero, A. et al. (2014). The landscape of fear: The missing link to understand top-down and bottom-up controls of prey abundance? *Ecology, 95*(5), 1141–1152.

29. Levy, D. A. (1990). Reciprocal diel vertical migration behavior in planktivores and zooplankton in British Columbia lakes. *Canadian Journal of Fisheries and Aquatic Sciences, 47*(9), 1755–1764.

30. Loose, C. J. and Dawidowicz, P. (1994). Trade-offs in diel vertical migration by zooplankton: The costs of predator avoidance. *Ecology, 75*(8), 2255–2263.

31. Loose, C. J.; von Elert, E.; Dawidowicz, P. (1993). Chemically-induced diel vertical migration in *Daphnia*: A new bioassay for kairomones exuded by fish. *Archiv für Hydrobiologie, 126*(3), 329–337.

32. Mehner, T. (2012). Diel vertical migration of freshwater fishes – Proximate triggers, ultimate causes, and research perspectives. *Freshwater Biology, 57*(7), 1342–1359.

33. Miner, B. E.; de Meester, L.; Pfrender, M. E.; Lampert, W.; Hairston, N. G. (2012). Linking genes to communities and ecosystems: *Daphnia* as an ecogenomic model. *Proceedings of the Royal Society B: Biological Sciences, 279*(1735), 1873–1882.

34. Nicholson, K. L.; Milleret, C.; Månsson, J.; Sand, H. (2014). Testing the risk of predation hypothesis: The influence of recolonizing wolves on habitat use by moose. *Oecologia, 176*(1), 69–80.

35. Ortiz-Jimenez, C. A.; Conroy, S. Z.; Person, E. S.; DeCuir, J.; Gall, G. E. C.; Sih, A. et al. (2025): Human presence shifts the landscape of fear for a free-living mammal. *Ecology* 106 (1), e4499.

36. Palmer, M. S.; Fieberg, J.; Swanson, A.; Kosmala, M.; Packer, C. (2017). A ‘dynamic’ landscape of fear: Prey responses to spatiotemporal variations in predation risk across the lunar cycle. *Ecology Letters, 20*(11), 1364–1373.

37. Persson, L. (1983). Food consumption and the significance of detritus and algae to intraspecific competition in roach *Rutilus rutilus* in a shallow eutrophic lake. *Oikos, 41*(1), 118.

38. Preisser, E. L.; Bolnick, D. I.; Benard, M. F. (2005). Scared to death? The effects of intimidation and consumption in predator–prey interactions. *Ecology, 86*(2), 501–509.

39. Rinke, K.; Petzoldt, T. (2008): Individual-based simulation of diel vertical migration of Daphnia: A synthesis of proximate and ultimate factors. *Limnologica* 38 (3-4), pp. 269–285.

40. Scheuerell, M. D.; Schindler, D. E. (2003): Diel vertical migration by juvenile sockeye salmon: empirical evidence for the antipredation window. *Ecology* 84 (7), 1713–1720.

41. Schmidt, K. and Kuijper, D. P. J. (2015). A "death trap" in the landscape of fear. *Mammalian Research, 60*(4), 275–284.

42. Schmitz, O. J.; Hawlena, D.; Trussell, G. C. (2010). Predator control of ecosystem nutrient dynamics. *Ecology Letters, 13*(10), 1199–1209.

43. Stich, H.-B. and Lampert, W. (1981). Predator evasion as an explanation of diurnal vertical migration by zooplankton. *Nature, 293*(5831), 396–398.

44. Tams, V.; Lüneburg, J.; Seddar, L.; Detampel, J.-P.; Cordellier, M. (2018). Intraspecific phenotypic variation in life history traits of *Daphnia galeata* populations in response to fish kairomones. *PeerJ, 6*, e5746.

45. Turner, A. M.; Bernot, R. J.; Boes, C. M. (2000). Chemical cues modify species interactions: The ecological consequences of predator avoidance by freshwater snails. *Oikos, 88*(1), 148–158.

46. Van Densen, W. L. T. (1985). Feeding behaviour of major 0+ fish species in a shallow, eutrophic lake (*Tjeukemeer*, The Netherlands). *Journal of Applied Ichthyology, 1*(2), 49–70.

47. Vašek, M.; Kubečka, J.; Čech, M.; Draštík, V.; Matěna, J.; Mrkvička, T. et al. (2009). Diel variation in gillnet catches and vertical distribution of pelagic fishes in a stratified European reservoir. *Fisheries Research, 96*(1), 64–69.

48. Vijverberg, J.; Koelewijn, H. P.; van Densen, W. L. T. (2005). Effects of predation and food on the population dynamics of the raptorial cladoceran *Leptodora kindtii*. *Limnology & Oceanography, 50*(2), 455–464.

49. Von Elert, E. and Pohnert, G. (2000). Predator specificity of kairomones in diel vertical migration of Daphnia: A chemical approach. *Oikos*, 88(1), 119–128.

50. Von Elert, E. 2012. Information conveyed by chemical cues, In Chemical ecology in aquatic systems. [eds.] C. Brönmark and L.-A. Hansson, Oxford Univ. Press. p. 19–38.

51. Werner, E. E. and Peacor, S. D. (2003). A review of trait-mediated indirect interactions in ecological communities. *Ecology, 84*(5), 1083–1100.

52. Zelnik, Y. R.; Barbier, M.; Shanafelt, D. W.; Loreau, M.; Germain, R. M. (2024). Linking intrinsic scales of ecological processes to characteristic scales of biodiversity and functioning patterns. *Oikos, 2024*(3), e10514.

2.9 Supporting information

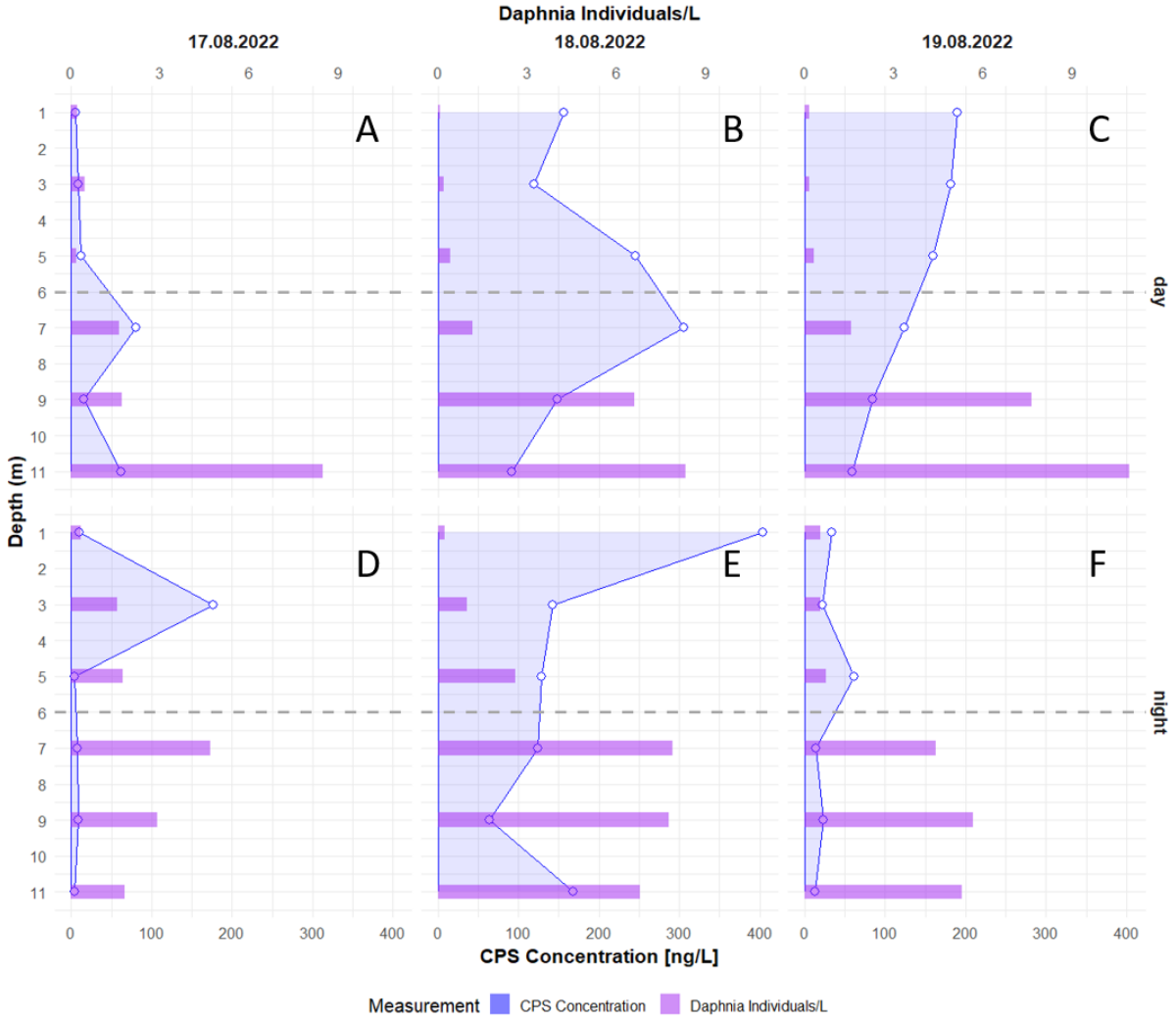


Figure SI 1: Depth profiles of 5α-cyprinol sulfate (CPS) concentrations and *Daphnia longispina* abundances (individuals/L) at different times of day and night over three consecutive days (17–19 August 2022). The panels illustrate vertical profiles of CPS concentrations (ng/L) and *Daphnia longispina* abundances across depths from 1–11 m during the daytime (**A–C**) and nighttime (**D–F**). Each panel corresponds to a specific date, as indicated at the top of the figure: 17th August (**A, D**), 18th August (**B, E**), and 19th August (**C, F**). CPS concentrations are represented by blue shaded areas with points showing mean values at each

depth, while *Daphnia* abundances are displayed as purple horizontal bars. The dashed horizontal line marks the thermocline at 6 m depth.

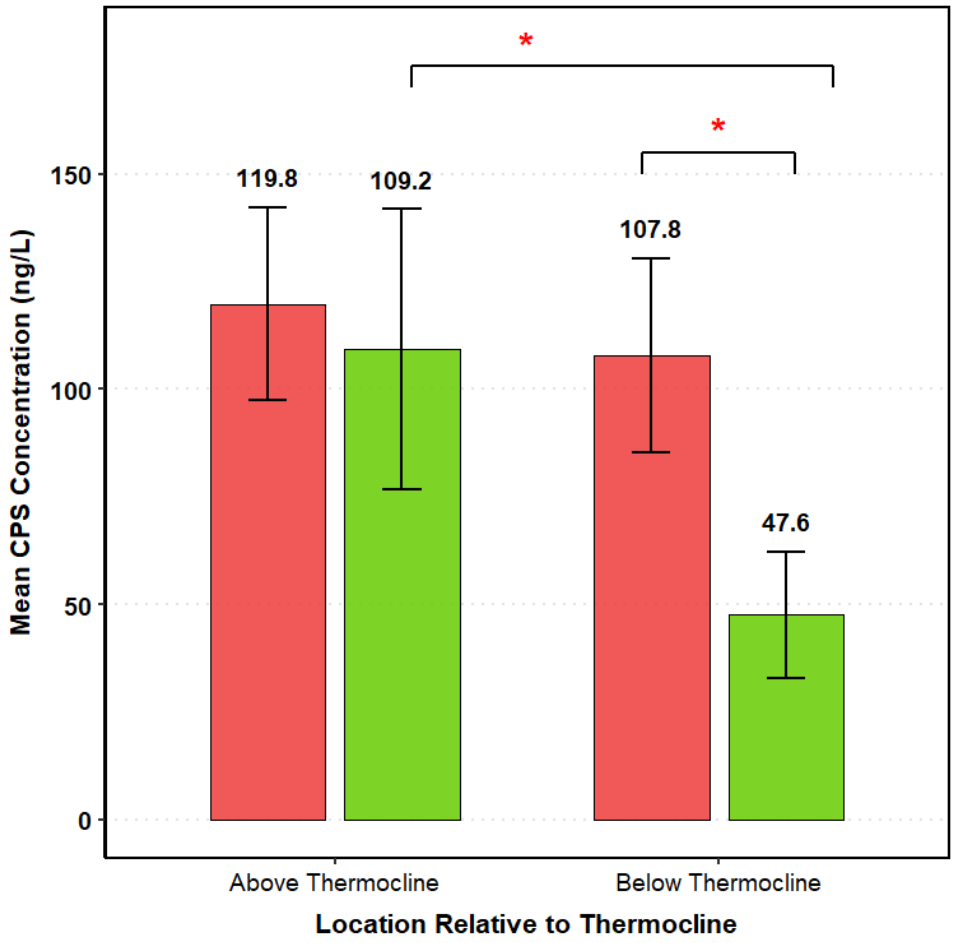


Figure Sl 2: Mean concentrations of 5α-cyprinol sulfate (CPS) above and below the thermocline (6 m depth) during day (red) and night (green) in Klostersee observed over three consecutive days (17–19 August 2022). Error bars represent the standard error (SE) of the mean. Significant differences, identified by Welch's two-sample t-test, are marked with an asterisk, indicating a significant difference between day and night below the thermocline ($p < 0.05$) and between nighttime concentrations above and below the thermocline ($p < 0.1$).

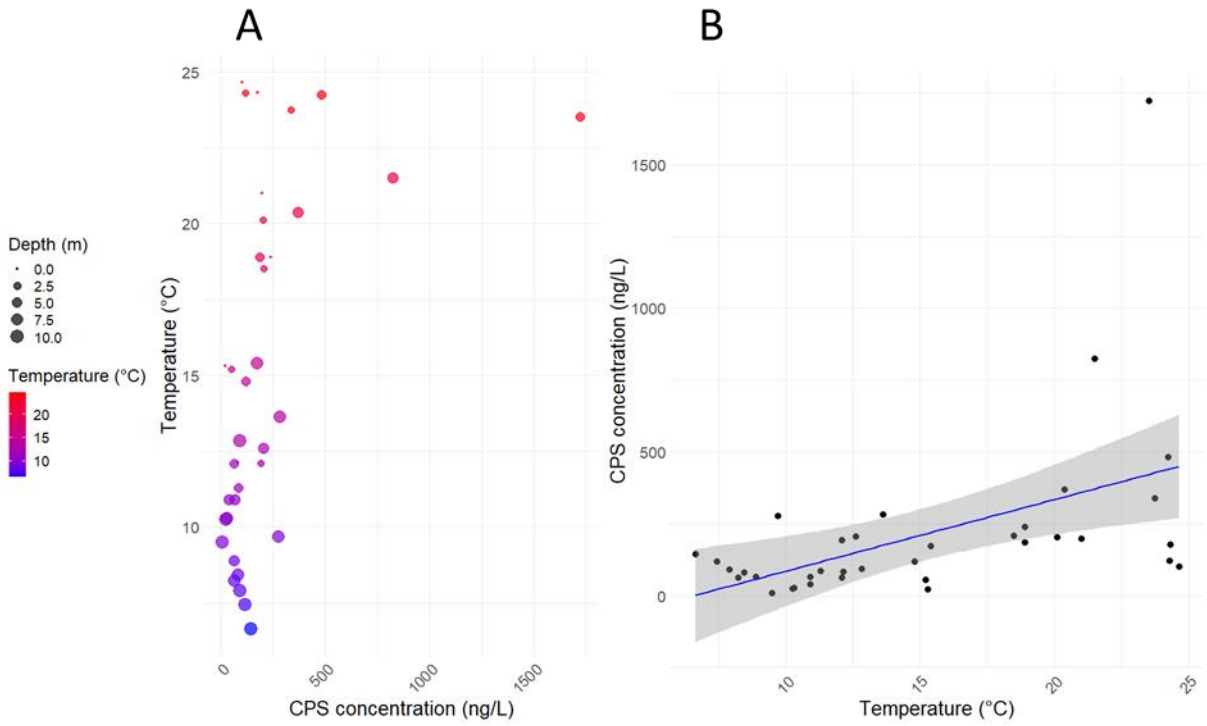


Figure SI 3: Relationship between 5α-cyprinol sulfate (CPS) concentrations, temperature, and depth. Panel A shows the relationship between CPS concentration (ng/L), temperature (°C), and depth (m) in the water column. Each point represents a sample, with CPS concentration on the x-axis and temperature on the y-axis. The color gradient (from blue to red) indicates temperature, with blue representing cooler temperatures (10°C) and red representing warmer temperatures (25°C). The size of the points corresponds to the sampling depth, where larger points represent deeper water (up to 10 m). **Panel B** illustrates the results of a multiple regression analysis, showing a significant ($p < 0.001$) positive relationship between temperature (x-axis) and CPS concentration (y-axis), with the blue regression line indicating the trend and the shaded area representing the 95 % confidence interval.

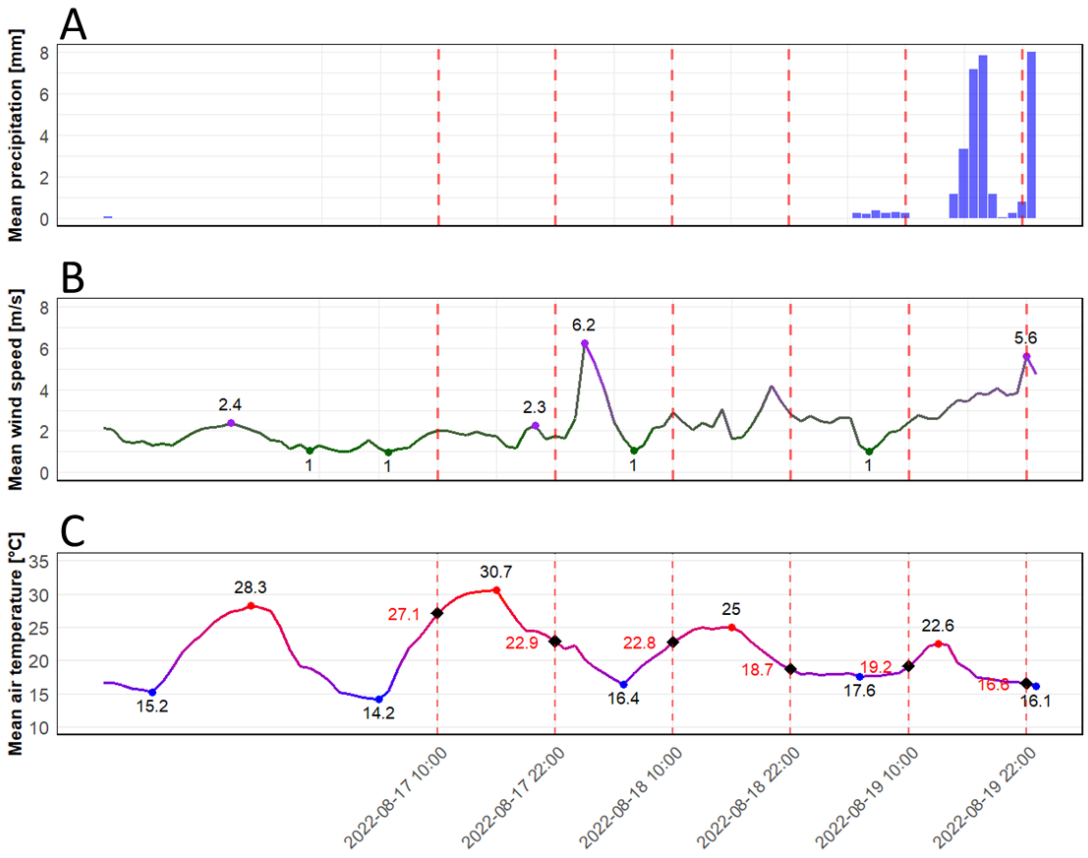


Figure SI 4: Weather conditions over three consecutive days and nights (17-19 August 2022): Precipitation, wind speed and air temperature. Panel A: Mean precipitation (mm) over time. Precipitation data derived and averaged from the nearby stations Trostberg, Chieming, Amerang-Pfaffing. **Panel B:** Mean wind speed (m/s) over time. Wind speed data derived and averaged from the nearby stations Chieming, Vogtareuth, Waging am See, Frasdorf-Geimelberg. Daily maxima (purple dots) and daily minima (green dots) are displayed within the plot. **Panel C:** Mean air temperature (°C) over time. Daily maxima (red dots), daily minima (blue dots) and the temperatures during the sampling event (black diamonds) are displayed within the plot. Data derived and averaged from the nearby stations Trostberg, Chieming, Amerang-Pfaffing. Red vertical dotted lines indicate the sampling events from August 17th to August 19th.

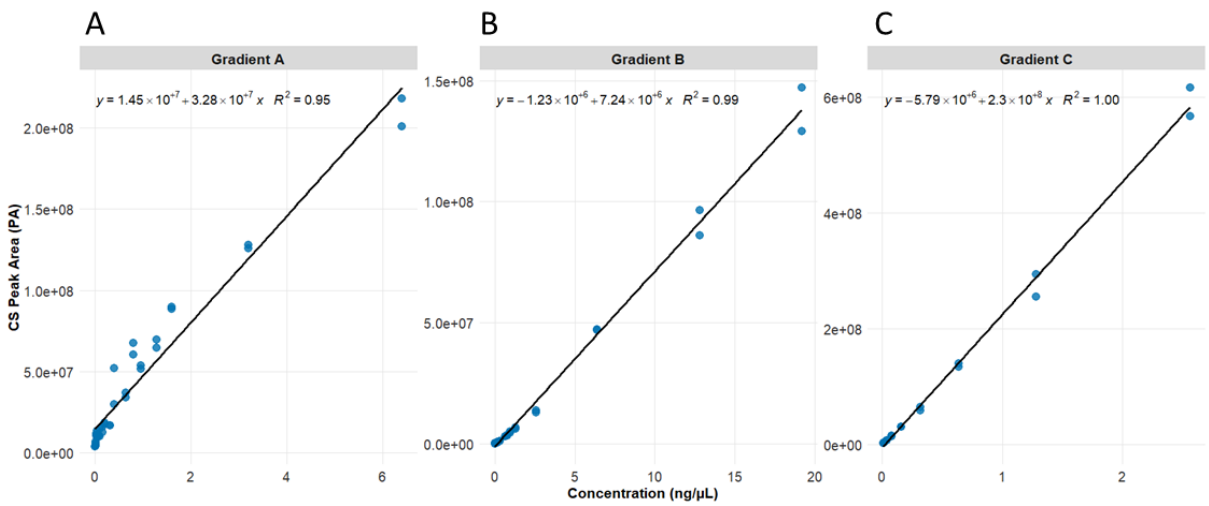


Figure SI 5: Calibration curves for cholesteryl sulfate (CS) in different gradient conditions for the mass spectrometry analysis (Gradient A, Gradient B, Gradient C). Each panel **(A, B, C)** corresponds to one gradient with the CS peak area (PA) on the y-axis and concentration (ng/µL) on the x-axis. The regression line is fitted to each data set, with the corresponding equation and R^2 value displayed within each plot.

Chapter 3: "Signals in flux: Investigating the seasonal turnover of the cyprinid kairomone 5α-cyprinol sulfate"

3.1 Abstract

5α-cyprinol sulfate (CPS) is a chemical signal released by cyprinid fish that plays a crucial role in predator-prey interactions by inducing diel vertical migration (DVM) in *Daphnia*, a key process driving freshwater ecosystem dynamics. While CPS-mediated DVM has long been considered a stable and predictable response to predator abundance, this study challenges previous assumptions by demonstrating that CPS undergoes rapid turnover in aquatic systems. We show that CPS exudation is tightly linked to fish feeding intensity, independent of fish size, while microbial degradation emerges as the dominant removal process, with degradation rates reaching up to 85.7% per day in lake water. Seasonal field data from a mesotrophic lake reveal that CPS concentrations range from 40 to 900 ng/L over a season, peaking in late summer, putatively indicating increased fish feeding and shifts in prey availability. Using an integrated approach combining laboratory feeding trials, field sampling, and predictive modeling, we present a temperature-dependent framework that captures the interplay between CPS exudation and degradation. Our findings highlight a fundamental reconsideration of CPS as an environmental cue: rather than reflecting predator abundance, CPS concentrations primarily track predator feeding activity, dynamically modulating the strength of DVM and its cascading effects on freshwater food webs. This study provides the first in-situ quantification of CPS turnover, offering new insights into the temporal variability of chemical signaling and its ecosystem-wide consequences in fluctuating aquatic environments.

3.2 Introduction

Chemical signaling is a fundamental mechanism driving ecological interactions in aquatic systems, shaping community structures and sustaining ecosystem functions (von Elert, 2012). Among the diverse organisms responding to such signals, *Daphnia*, a genus of freshwater planktonic crustaceans, plays a crucial role in aquatic food webs as a primary grazer and a key prey species for fish (Miner et al. 2012). To cope with predation, *Daphnia* exhibit a variety of inducible defenses, including behavioral shifts (e.g., diel vertical migration (DVM)), morphological changes, and life-history modifications. These adaptive responses enhance predator avoidance and improve survival chances. Among the signals triggering these defenses, 5α-cyprinol sulfate (CPS) has recently emerged as a key kairomone released by cyprinid fish, inducing defensive traits in *Daphnia* (Hahn et al. 2019; Hahn and von Elert 2022; Ahlers and Hahn et al. 2024) Thus, CPS plays a pivotal role in predator-prey interactions and broader ecological dynamics in aquatic environments.

From a chemical and environmental perspective, the bile salt CPS possesses properties that influence its behavior in natural systems. As a low-molecular-weight (<500 Da), non-volatile, anionic compound of medium polarity, CPS exhibits remarkable chemical stability across extreme pH levels (0.8–14.0) and temperatures (−20°C to +120°C) (Loose et al. 1993a; von Elert and Loose 1996). This high stability is believed to have evolutionary significance, making bile compounds in general and CPS in particular well-suited to function as infochemicals (Buchinger et al. 2014), as it is reasonable to assume that this resilience enables bile compounds to persist and remain effective under diverse and challenging environmental conditions. Additionally, CPS's amphiphilic nature theoretically allows it to form micelles, which could

enhance its dispersal and chemical stability in aquatic environments (von Elert and Pohnert 2000; Goto et al. 2003).

However, potential degradation of CPS in natural water bodies remains largely unexplored, but insights from other low molecular weight organic compounds suggest that microbial and photochemical processes may play an important role (Sterr and Sommaruga 2008; Ghuneim et al. 2021). Based on studies of other kairomones, CPS degradation by microbes can been suggested. (Loose et al. 1993a) demonstrated removal of DVM-inducing activity upon incubation with bacteria and hypothesized that similar processes may occur in natural water bodies, limiting the persistence of kairomones in aquatic systems. This idea was supported by Beklioglu et al. (2006), who demonstrated the rapid disappearance of DVM of *Daphnia* in response to cyprinid fish water in laboratory conditions. While these studies highlight plausible microbial degradation, no direct evidence currently exists to confirm whether CPS undergoes microbial breakdown under environmentally relevant conditions. Importantly, for a kairomone to serve as a reliable indicator of current predation risk, it must degrade in a timely manner once the threat subsides. If such signals were too persistent, prey organisms might continue investing in costly defensive traits even when they are no longer necessary, leading to reduced fitness. Therefore, the degradation of CPS is not only ecologically relevant but also essential for the adaptive value of predator-induced responses.

Temperature is a critical factor influencing many biological and chemical processes in aquatic ecosystems, including fish exudation and microbial degradation. Studies show that temperature-dependent excretion rates in fish are linked to metabolic activity and food intake (Persson 1982; Hölker 2003; Hölker 2006). However, whether CPS exudation of fish follows similar temperature-related patterns remains untested. Similarly, microbial activity accelerates

the degradation of organic compounds, including bioactive substances (Simon and Wünsch 1998; Vrede 2005), but the impact of temperature on CPS degradation by microbial communities remains unknown. The dynamic interplay between CPS exudation and degradation likely determines its persistence and signaling efficacy in natural systems. Warmer temperatures may enhance both exudation and degradation, potentially stabilizing CPS concentrations if the processes counterbalance. Alternatively, if degradation outpaces exudation under conditions of high microbial activity and low fish density or reduced feeding intensity, CPS levels might decline. Conversely, high exudation rates during periods of intensive feeding and elevated metabolic activity of fish (e.g., during zooplankton blooms in summer) could sustain CPS levels despite increased degradation. This highlights the critical role of temperature in modulating CPS turnover, yet the extent of these effects remains poorly understood.

To address these knowledge gaps, this study investigates whether CPS turnover is temperature-dependent by examining both exudation and degradation processes through an integrated approach of laboratory experiments, field observations, and mathematical modeling. Specifically, we aim to (i) determine how fish size, food intake, and temperature influence CPS release; (ii) investigate the role of temperature on microbial CPS breakdown and (iii) examine temporal fluctuations of in-situ CPS concentrations and their relationship with environmental factors. By integrating experimental data and modeling, we aim to elucidate the biotic (fish exudation, microbial degradation) and abiotic (temperature) drivers shaping CPS dynamics. This study offers new insights into the ecological significance of CPS in predator-prey interactions and ecosystem stability under changing environmental conditions.

3.3 Methods

In situ assessment of CPS degradation in lake water

To investigate the in-situ degradation rates of 5-α-cyprinol sulfate (CPS), we collected water samples in June 2024 from the epilimnion (1–2 m depth) of two lakes: Reeser Meer Nord Erweiterung (RMNE) (51°45'3" N 6°27'59" E) and Fühlinger See (FS) (51°1'23" N 6°55'27" E). RMNE covers an area of 0.618 km², with a maximum depth of 10.5 m and was originally formed by gravel excavation and has undergone extensive restoration efforts. Populations of the cyprinid species *Leucaspius delineatus* were first recorded in RMNE in 2019 (Jost Borcherding, pers. comm.). The phosphorus concentration in the lake water, measured as total phosphorus (TP), indicated that RMNE is mesotrophic (mean TP value of 13 µg P/L across the water column). This measurement was conducted using a segmented flow analyzer (SKALAR, Breda, The Netherlands) and a wavelength of 880 nm (DIN EN ISO 15681 Part 2-D46). FS spans an area of 1 km² and reaches a maximum depth of 14 m (www.fuehlinger-see-koeln.de). Parts of the lake are designated for recreational use. The cyprinid species present in FS include Bream (*Abramis brama*), Tench (*Tinca tinca*), Common Roach (*Rutilus rutilus*), Rudd (*Scardinius erythrophthalmus*), and Common Carp (*Cyprinus carpio*) (www.asg-ford.com). The phosphorus analysis for FS also indicated a mesotrophic status (mean TP value of 14 µg P/L across the water column).

Using a Ruttner water sampler, water was collected from FS on June 4, 2024, and from RMNE on June 12, 2024. The samples were then filtered through a 250 µm plankton net to remove large organisms. Filtered water was stored in 1 L glass bottles, with four liters subsequently being autoclaved to eliminate microbial activity (Control) and four untreated (NA treatment). The bottles were incubated at 18°C, matching in-situ temperatures at the time of the sampling.

After 20 hours, aliquots of 200 mL were removed under sterile conditions from each of the bottles. Then, each aliquot was filtered through a glass microfiber filter (Whatman Grade GF/A: 1.6 μm) to remove particles. To each filtered sample, we added an internal standard (100 ng of cholesteryl sulfate) to account for variability during sample processing. Additionally, 2 mL of 100% methanol was added to each sample to prepare them for solid-phase extraction (SPE). The samples were then subjected to C18-SPE cartridges (as detailed below). To determine the degradation rate of CPS, this procedure was repeated daily for four consecutive days. Daily CPS concentrations from each of the replicate bottles resulted in scatter plots of CPS concentration over time for Control and NA treatment for both lakes. An exponential decay curve was then fitted to these data points to estimate the degradation rate constant (k) (as detailed below).

Assessment of CPS exudation rates in fish

To assess the exudation rates of CPS, individual roach fish (*Rutilus rutilus*) were kept at 18 °C in separate, darkened aquaria filled with 20 L tap water. Fish were categorized as small and large, and showed a significant difference in body mass (Welch's *t*-test, $p < 0.001$). Small fish weighed 18.2 ± 6.7 g (range = 12–29 g, n = 13), whereas large fish weighed 89.9 ± 13.5 g (range = 77–110 g, n = 14). Prior to the experiment, fish were acclimated without food in their respective aquaria for three days to standardize conditions and ensure empty digestive tracts. At the start of the experiment, individual fish were fed varying amounts of food based on their body weight. Fish were fed frozen chironomid larvae (www.nature2aqua.de, Article no. 624010). To simulate a natural feeding regime and avoid overfeeding during the short feeding period, fish received only 1/6 of their daily ration, corresponding to 4 hours of the feeding cycle. This ration, when scaled to a 24-hour period, would constitute 0.5–5% of the fish's body weight.

All of the provided food was fully consumed by the fish within the 4-hour feeding period. Following the feeding period, fish were transferred into 20 L of fresh tap water for a 20-hour incubation. Then, two 1 L water samples were taken from each aquarium to serve as technical replicates. Water samples were filtered through glass microfiber filter (Whatman Grade GF/A: 1.6 μm) to remove particles. To each 1 L sample, 500 ng of cholesteryl sulfate was added as an internal standard. Subsequently, 10 mL of 100% methanol was added to each sample, which then was subjected to C18-SPE (as detailed below). To determine total CPS exudation per fish, CPS exudation was totaled over four consecutive days following feeding.

Seasonal CPS concentrations in lake Reeser Meer Nord Erweiterung (RMNE)

To assess seasonal changes of in-situ CPS concentrations in RMNE, surface water samples were collected using a bucket. Samples were collected monthly during the first or second week of each month from March to September 2023. The water samples were immediately transported to the laboratory and then filtered through glass microfiber filters (Whatman Grade GF/A: 1.6 μm). Four 1 L subsamples (technical replicates) were taken from the filtered water, and 500 ng of cholesteryl sulfate was added as an internal standard to each replicate for normalization during quantification. The samples were stored overnight at 7–10°C to maintain stability and minimize degradation processes, because immediate extraction was logistically infeasible. The other day, 10 mL of 100% methanol was added to each sample to prepare them for C18- SPE (detailed below).

Solid phase extraction

The C18-SPE cartridges (Agilent Bond Elute C18, 500 mg, 3 ml) were activated with 10 mL of 100% methanol (MeOH) and subsequently conditioned with 1% MeOH dilution. Each

sample was drawn into the cartridge at a controlled flow rate of approximately 50 µL/s using silicone tubing, ensuring a stable flow and minimizing disturbances during the extraction process. The samples were then washed with 10 mL 1% MeOH and finally eluted with 10 mL of 100% MeOH, collected in a glass tube. Each sample was applied to a new cartridge to avoid cross-contamination. Technical replicates were applied to the same cartridges. The collected samples were dried overnight in a vacuum centrifuge at 30 °C and 1500 rpm. Once dried, samples were re-dissolved in 200 µL of 100% MeOH and transferred into glass vials for further analysis.

Mass spectrometry and quantification of CPS

Mass analysis was conducted by applying 5 µL of each sample to a Vanquish™ Horizon UHPLC system coupled with a Q-Exactive HF mass spectrometer (Thermo Fisher Scientific, Dreieich, Germany). Metabolite separation was achieved on an EC 125/2 Nucleosil 100-3 C18 column (Macherey-Nagel, Düren, Germany) maintained at 30 °C and a constant flow rate of 300 µL/min. The mobile phase comprised solvent A (13 mM ammonium acetate and 10 mM formic acid in water) and solvent B (0.01 % ammonium acetate and 10 mM formic acid in a 9:6 [v/v] mixture of acetonitrile and methanol). The following gradient programs were applied: Gradient A (20% B, 0.0–28 min gradient to 100% B; 28–32 min at 100% B; 32–33 min gradient to 20% B; 33–35 min at 20% B) and Gradient B (30% B, 0.0–12 min gradient to 100% B; 12–14 min at 100% B; 14–15 min gradient to 30% B; 15–17 min at 30% B). We used two different gradient programs because a longer gradient (Gradient A) was chosen for the seasonal lake water samples from RMNE to potentially detect additional seasonal patterns for other kairomones in future analyses. Negative and positive ionization was performed for each run simultaneously, with a spray voltage of 3.0–3.53 kV and a capillary temperature set to 360 °C.

To ensure accurate CPS quantification, a calibration curve for the internal standard cholesteryl sulfate was included in each sample sequence.

Modeling the temperature-dependent release of CPS

From the perspective of an individual cyprinid fish, the net release of CPS normalized to the food ration is the difference between the rate of exudation from the individual fish and the rate of microbial degradation. Since the exudation from the individual fish proved to scale linearly with food ration (see Results), we here model the net release of CPS normalized to the food ration. To model the net release of CPS into the aquatic environment, we developed a temperature-dependent approach that integrates CPS exudation rates and degradation rates. The model assumes a dynamic balance between the exudation of CPS by fish and its removal by microbial activity (degradation). The temperature-dependent exudation rate (*E*) and degradation rate (*D*) are calculated using Q10 scaling, which accounts for the respective exponential effect of temperature on these biological processes. Specifically, the exudation rate is adjusted from a reference rate (E_{ref}) measured at a reference temperature (T_{ref}) for a given food ration using the equation

$$E = E_{ref} \times Q10_{exudation}^{\frac{temperature - T_{ref}}{10}} \times food.$$

Similarly, the degradation rate is adjusted from a reference rate (D_{ref}) using

$$D = D_{ref} \times Q10_{degradation}^{\frac{temperature - T_{ref}}{10}}.$$

The ratio of the rate of exudation E and the rate of degradation D gives the net release of CPS in ng/fish

$$CPS_{net\ release} = \frac{E}{D}.$$

This model enabled us to simulate the net CPS release across a range of temperatures, providing insights into the interplay between fish-mediated exudation and microbial degradation under different temperatures. The parameter values for the reference rates (E_{ref} = 63.68 ng/h x gram of food per fish and D_{ref} ~ 0.0778 1/h) were derived from experimental data. Q10 factors were calculated based on the standard metabolic rate of roach (*Rutilus rutilus*), yielding a value of 2.4 (Hölker 2006), and bacterial cell multiplication, yielding a value of ~2 (Simon and Wünsch 1998). This model is an equilibrium-based simplification and assumes that the system is in a dynamic steady state—where inputs and outputs are ongoing but remain balanced. The model focuses on the long-term average CPS concentration in the water under stable conditions of temperature, exudation, and degradation, rather than capturing transient fluctuations or short-term changes. To demonstrate how this model can be applied, we incorporated predicted daily in-situ feeding rations of cyprinids based on Persson (1983). This example illustrates how the model can help predict CPS dynamics in other aquatic ecosystems and serves as a framework to obtain information about the potential ecological impacts of CPS-mediated signaling.

Exudation Rate (E): The reference exudation rate (E_{ref}) is defined as the amount of CPS exuded per hour per gram of food consumed per fish, expressed in ng/h/fish. This rate represents the amount of CPS exuded into the water under reference conditions (18°C). The temperature dependence of exudation is modeled using a Q10-factor, which scales E with temperature. The experimental results determined a reference exudation rate (E_{ref}) of 64.5 ng/h x gram of food per fish. This rate was determined using a linear regression model analyzing the relationship between final CPS concentration in the water and food amount consumed. Fish size was omitted from the model, as it was found to have no significant effect on the CPS concentration released by the fish.

Degradation Rate (D): The degradation rate (D) is defined as the rate at which a compound degrades. It is determined using the degradation constant k derived from an exponential decay model. In this model, the degradation follows first-order kinetics, meaning the rate of degradation is proportional to the concentration of the compound. The rate constant k is influenced by temperature, with higher temperatures generally accelerating degradation. This temperature dependence is incorporated using a Q10-factor, which scales k with temperature changes. For the purpose of this model, we focus on a degradation rate of approximately 7,78% per hour, corresponding to a reference degradation rate (D_{ref}) of 0.0778 per hour under

Zooplankton sampling

Zooplankton samples in RMNE were collected once per month from March to September 2023 at two time points per day: midday (10 am–3 pm) and night (9 pm–11 pm). At each time point, five samples were taken from both the epilimnion (~2 m) and hypolimnion (~9 m) using a Schindler-Patalas trap (10 L capacity and a 200 μm mesh size). This resulted in a total of 20

samples per month. Samples were preserved in a sucrose-ethanol solution (285 mL distilled water, 714 mL ethanol (C_2H_6O) (96–98%), 40 g sucrose ($C_{12}H_{22}O_{11}$), and 40 mL glycerol ($C_3H_8O_3$)) and were analyzed using a HydroptiC ZooScan system (Vogelmann et al. 2022) and Plankton Identifier (PkID) software (Gorsky et al. 2010). Classification was conducted semi-automatically based on a validated learning set, and *Daphnia* abundance was calculated as the sum of all samples across both depths and both time points (Jost Borcherding, pers. comm.).

Statistical analysis

All statistical analyses were conducted in R (version 4.2.0; R Core Team, 2022) within the RStudio environment (Posit Team, 2023) to explore CPS degradation, exudation dynamics, and model predictions. For degradation experiments, a linear mixed-effects model (lme) was applied to analyze log-transformed CPS concentrations over time. This approach linearized the exponential decay relationship and allowed for the inclusion of replicates as random factors, accounting for variability between experimental replicates. The lme model facilitated the estimation of degradation rate constants (k) and initial CPS concentrations (C_0) for different treatments, while also testing for statistically significant differences between lakes and treatments. Temperature-dependent degradation rates at 15°C and 25°C were predicted using the Q10 scaling factor, derived from the estimated rate constants at 18°C. For exudation experiments, linear regression models were applied to assess the relationships between CPS exudation rates, food intake, and fish size, highlighting the critical influence of feeding activity on exudation dynamics. Furthermore, predictive modeling incorporated Q10 scaling to integrate the temperature-sensitive processes of exudation and degradation, enabling robust estimates of steady-state CPS under varying thermal conditions. Statistical results were visualized using ggplot2.

3.4 Results

The degradation of 5-α-cyprinol sulfate (CPS) was investigated in a four-day experiment using autoclaved (Control) and non-autoclaved (NA) water treatments from two lakes: lake Fühlinger See (FS) and lake Reeser Meer Nord Erweiterung (RMNE). In the Control treatments (Figure 1A), CPS concentrations showed no significant changes over time in either lake (FS: k=−0.0002, p=0.9286; RMNE: k=0.0025, p=0.4826, SI Table 1.). In the NA treatment (Figure 1B), exponential models were fitted to assess CPS degradation rates. For Lake FS, the degradation constant (k) was 0.043 h^{-1} ($p< 0.01$, indicating significant CPS degradation, SI Table 2.), corresponding to a 4.21% decay per hour (daily decay rate: 64.4 %, half-life: 16.1 h, Figure 2). In contrast, Lake RMNE exhibited a higher degradation (constant of 0.081 h^{-1} ($p=0.0021$, indicating significant CPS degradation, SI Table 2), corresponding to a 7.78% decay per hour (daily decay rate: 85.7 %, half-life: 8.6 h) (Figure 2).

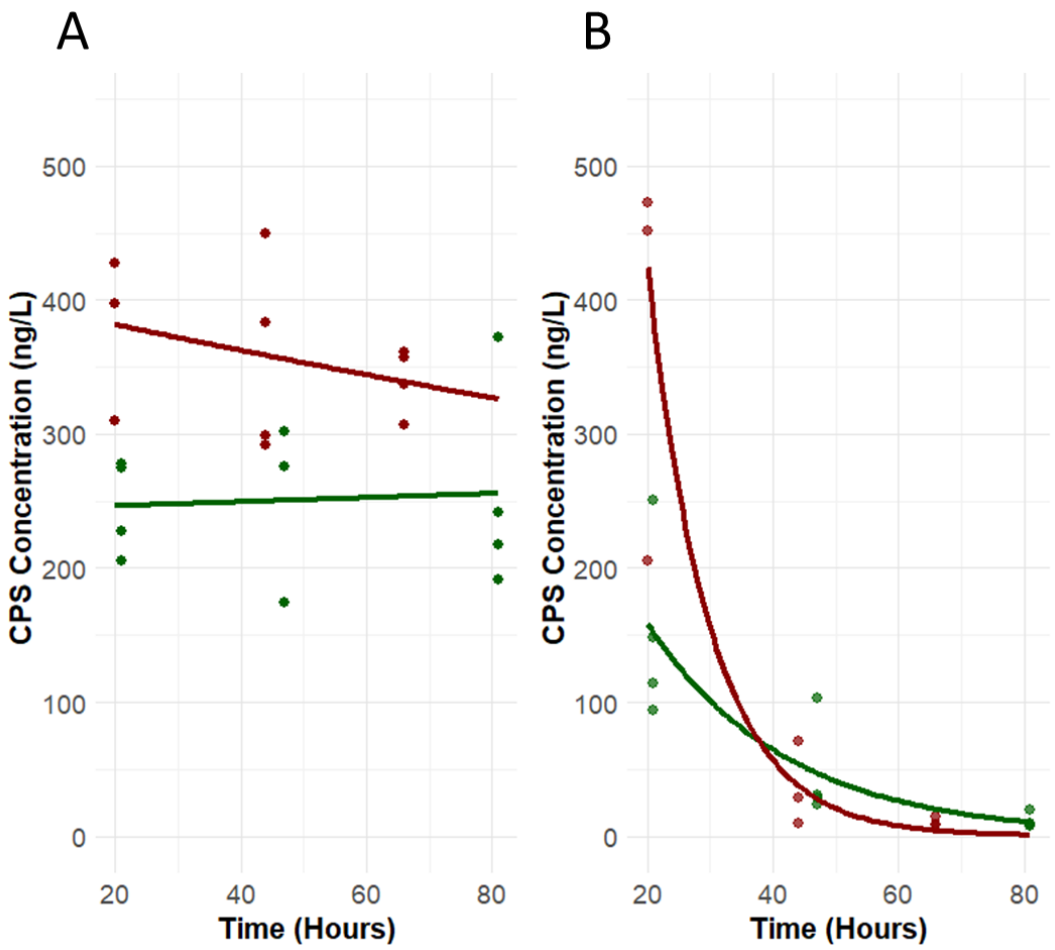


Figure 1: 5α-cyprinol sulfate (CPS) concentration (ng/L) over time (hours) in lake water that was incubated indoors with and without initial autoclaving. Water samples originated from two lakes, FS (dark green) and RMNE (dark red), sampled in June 2024. **(A)** CPS concentration in autoclaved lake water (Control) with observed data points and fitted exponential decay models overlaid, showing no degradation over time in either FS (k = −0.0002, p = 0.9286) or RMNE (k = 0.0025, p = 0.4826) control treatments. **(B)** CPS concentrations in non-autoclaved lake water (NA) with observed data points and fitted exponential decay of CPS with modeled degradation curves overlaid on individual data points. Degradation rates (k) were calculated

from the modeled degradation curves for RMNE (k=0.081, p=0.0021; $N(t)=1651.21 \cdot e^{-0.081 \cdot t}$, N = CPS concentration at timepoint t in hours) and FS (k=0.043, p<0.01; $N(t)=325.82 \cdot e^{-0.043 \cdot t}$, N = CPS concentration at timepoint t in hours). Each data point represents an individual measurement, and curves represent the modeled fit. N = 4 replicates for all treatments.

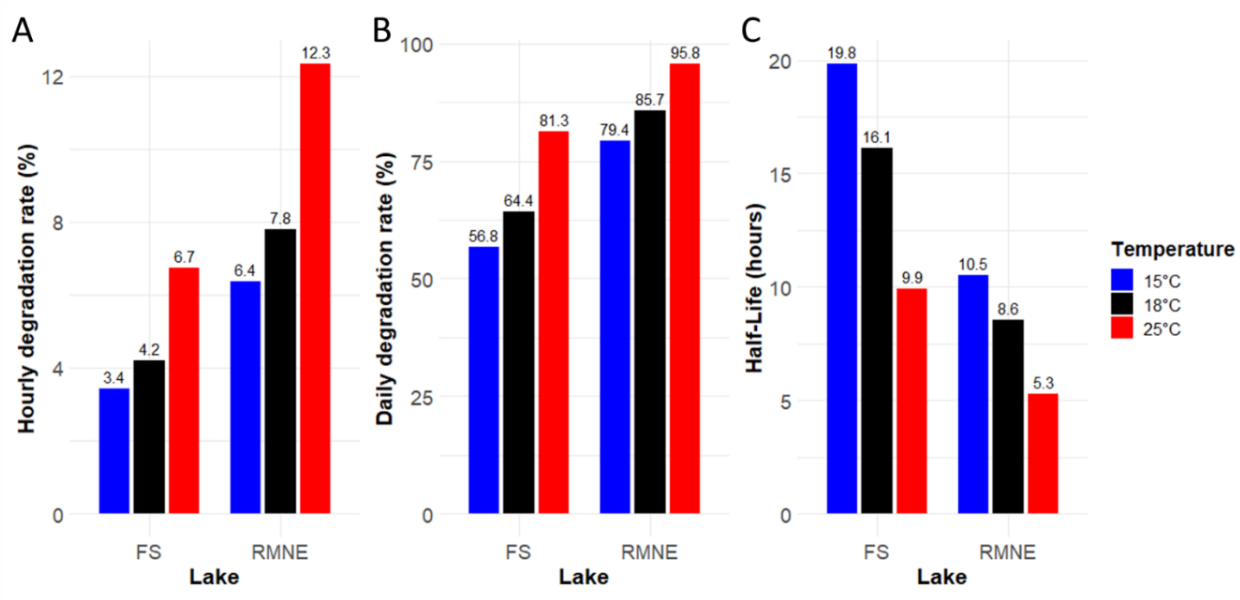


Figure 2: Hourly degradation rates (%), daily degradation rates (%), and half-life (hours) of 5α-cyprinol sulfate (CPS) at different temperatures in two lakes (FS and RMNE) in non-autoclaved lake water. (A) Percentage of CPS degraded per hour. **(B)** Percentage of CPS degraded per day. **(C)** CPS half-life in hours. Bars represent modeled values at 15°C (blue) and 25°C (red), calculated using Q10 scaling based on bacterial cell multiplication (BCM) as described by Simon and Wünsch (1998), alongside determined values at 18°C (black) derived from experimental data (n = 4). Percentage values are displayed above the bars for clarity.

The modeled impact of temperature and microbial activity on CPS degradation is shown in Figures 2 and SI Figure 1. CPS degradation in both lakes followed clear temperature-dependent trends, with higher temperatures leading to higher degradation rates, as predicted by Q10

scaling based on bacterial cell multiplication (BCM, Q10 ~2) as described by Simon and Wünsch (1998). In FS (Figure 2, SI Figure 1B), the observed degradation rate at 18°C falls between the modeled predictions for 15°C and 25°C. The predicted hourly degradation rate increased from 3.4% at 15°C to 6.7% at 25°C (Figure 2A), corresponding to daily degradation rates of 56.8% and 81.3%, respectively (Figure 2B). The half-life of CPS decreased notably from 19.8 hours at 15°C to 9.9 hours at 25°C (Figure 2C). In RNME (Figure 2, SI Figure 1A), CPS degradation was faster overall, with hourly degradation rates of 6.4% at 15°C, increasing to 12.3% at 25°C (Figure 2A). This translated to daily degradation rates of 79.4% and 95.8% (Figure 2B), with half-life values declining from 10.5 hours at 15°C to 5.3 hours at 25°C (Figure 2C).

The CPS concentrations at timepoint 0 h were not directly measured but were estimated using the model developed for data from 20–80 h. This model, fitted to the observed CPS degradation rates, was used to calculate the initial concentrations by extrapolating back to 0 h. In FS, the predicted CPS concentration at 0 h was 325.82 ng/L (SI Figure 1B), while in RNME, it was significantly higher at 1651.21 ng/L ($p=0.0069$) (SI Figure 1A). These estimates provide valuable insight into the initial in-situ CPS concentrations and their differences between the two lakes.

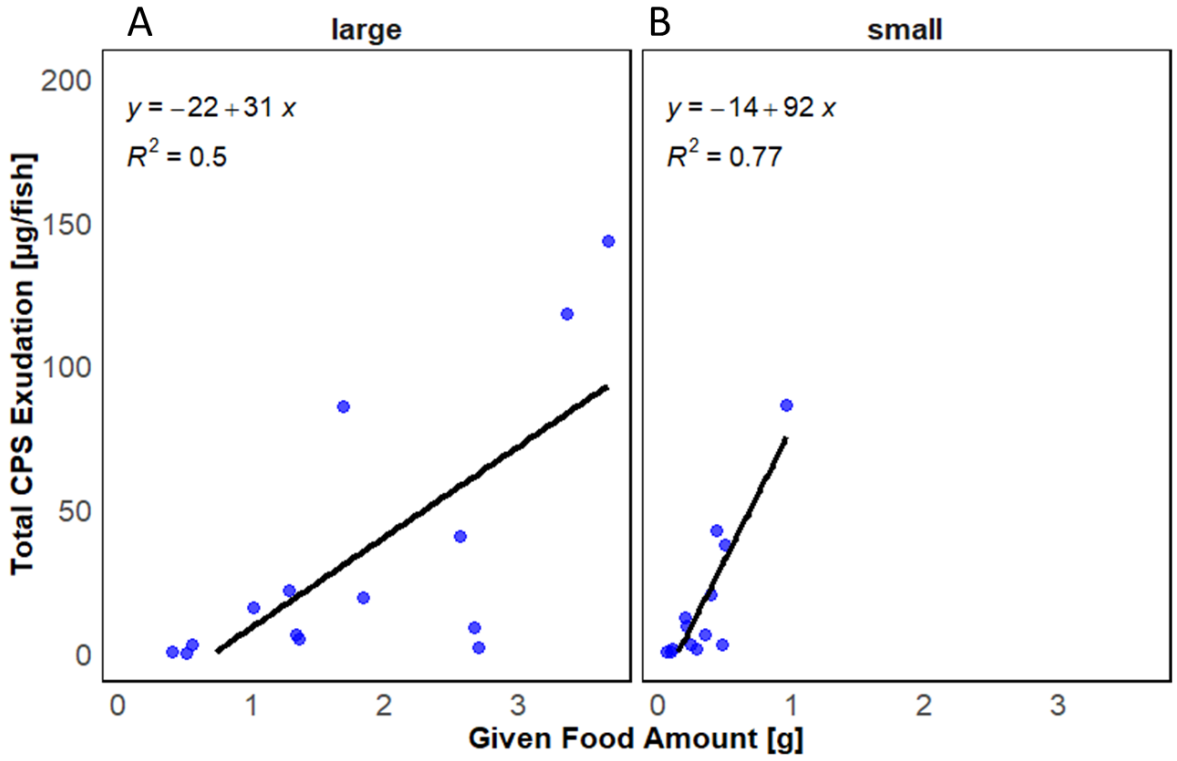


Figure 3: **Relationship between 5α-cyprinol sulfate (CPS) exudation (µg/fish) and food amount (g) for two fish size categories. (A)** Large fish (mean body mass 89.9 ± 13.5 g). **(B)** Small fish (mean body mass 18.2 ± 6.7 g). The x-axis represents the given food amount (g), and the y-axis indicates the total CPS exudation (µg/fish) 96 hours after the feeding event. Linear regression lines are fitted to the data, with corresponding equations and R^2 values provided in each panel to illustrate the fit of the regression models.

In order to determine rates of CPS exudation by fish, a controlled laboratory experiment was performed with different amounts of food being fed to individual fish (*Rutilus rutilus*) kept in aquaria. CPS exudation (µg/fish) was measured over four consecutive days, and the cumulative amount of exuded CPS was plotted against the food amount (g) (Figure 3). CPS-exudation rates deviated from normality (Shapiro–Wilk $W = 0.40$, $p < 0.001$), yet variances did not violate the assumption of homogeneity across food treatments (Levene $F_{(25,\ 80)} = 1.28$, $p = 0.20$). A multiple

linear regression model confirmed food amount as a significant predictor of CPS exudation ($p<0.001$), while fish size (i.e. body mass) had no significant effect ($p=0.268$). As fish size had no significant effect, it was excluded from the linear model, and only food amount was included as a predictor of CPS exudation. This led to a simplified model based solely on food amount. While the total CPS exudation per fish over 96 hours (Figure 3) accounts for the full digestion process across different fish sizes, we calculated exudation rates per hour to better capture the direct relationship between food intake and CPS release dynamics. Since a rate rather than a total value was required for further integration into the model, the CPS exudation rate per hour was derived by fitting a simplified model: $y=-0.8164+64.4952x$, where x represents the food amount (g) and y is the predicted CPS exudation (ng/h per fish). This model shows that for every additional gram of food, CPS exudation increased by approximately 64.5 ng/h per fish ($p<0.001$).

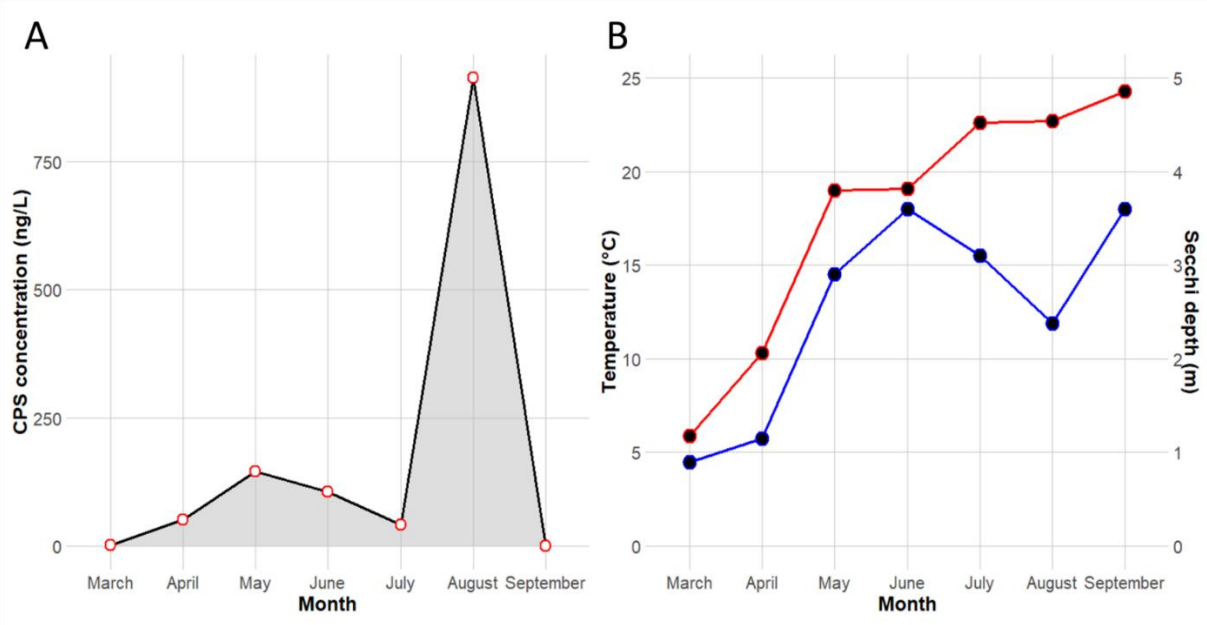


Figure 4: Seasonal dynamics of 5α-cyprinol sulfate (CPS) concentrations, water temperature, and Secchi depth in lake Reeser Meer Nord Erweiterung (RMNE) during 2023. (A) CPS concentrations (ng/L) from March to September, with the shaded area highlighting the seasonal trend. Points represent mean CPS concentrations derived from technical replicates (n = 4). **(B)** Temperature profile of the epilimnion (°C, red line) and Secchi depth (m, blue line) over the same period, illustrating seasonal variations in water transparency.

The seasonal dynamics of CPS concentrations and *Daphnia* abundances in RMNE were analyzed from March to September 2023. CPS concentrations (Figure 4A) were below detection limit in March and September and ranged from 40 ng/L up to a peak concentration of 900 ng/L in August. Additionally, the seasonal temperature profile (Figure 4B) revealed a progressive increase from March to August, peaking at 25°C, while water transparency measured as Secchi depth showed an inverse trend with reduced transparency during the warmer months. *Daphnia* ssp. were not detectable in March and nearly absent in April (0.3 Ind/L) (Figure 5). Relative abundances increased sharply in May (37.1 Ind/L) peaked in June

(80 Ind/L), and declined sharply in July (5 Ind/L) and August (2.3 Ind/L), with a resurgence in September (54.2 Ind/L).

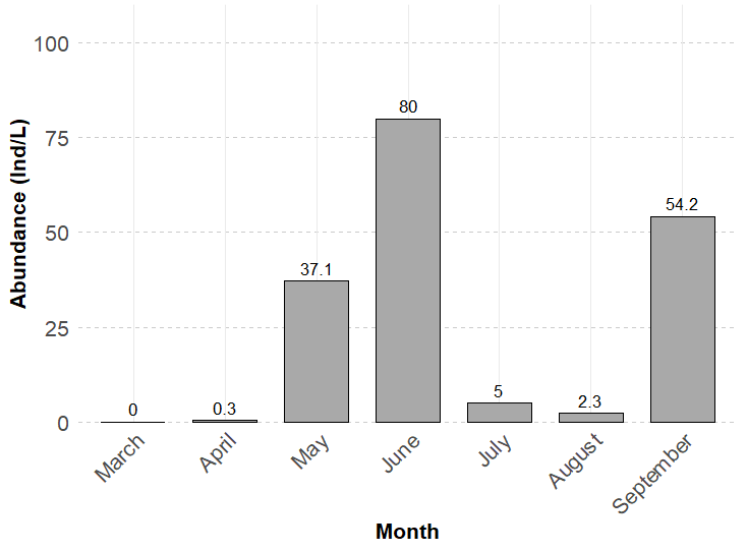


Figure 5: Abundance (Ind/L) of *Daphnia* in lake Reeser Meer Nord Erweiterung (RMNE) from March to September 2023. The values represent combined data from both the hypolimnion and epilimnion. Abundance is expressed in individuals per liter (Ind/L) for each month, with values displayed directly above each bar. (Data source: J. Borcherding, K. Scharnweber; pers. comm.)

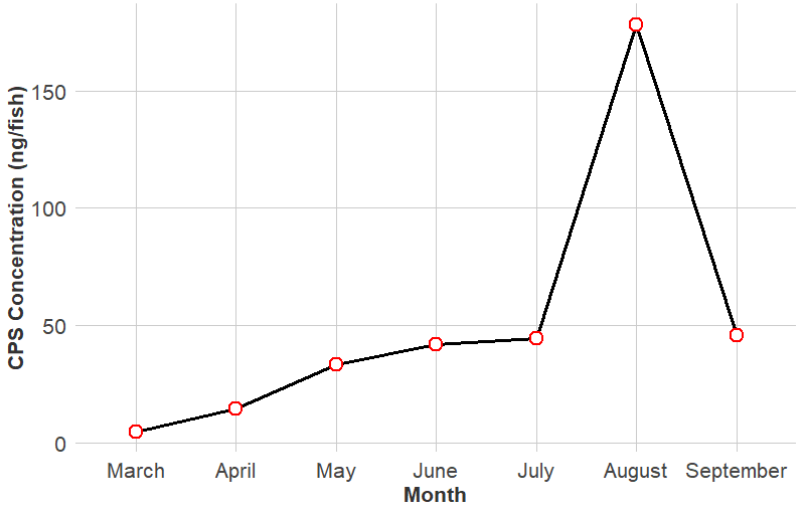


Figure 6: Modeled net exudation of 5*α*-cyprinol sulfate (CPS) per individual fish (ng/fish) from March to September. The model incorporates monthly temperature data from lake Reeser Meer Nord Erweiterung (RMNE) in 2023 and food consumption data derived from Persson (1983). The model accounts for temperature-dependent exudation and degradation rates alongside food intake, illustrating seasonal metabolic dynamics influenced by environmental conditions.

Modeled CPS exudation per fish in lake RMNE showed a gradual increase from March to July, peaking in August, followed by a decline in September (Figure 6). The model for CPS exudation incorporates not only the seasonal temperature profile but also daily zooplankton food rations of fish based on the study by Persson (1983). Including daily food rations in the model allows us to capture the combined effects of seasonal variations in food availability and metabolic processes, providing a more comprehensive understanding of CPS dynamics. By integrating both exudation and degradation processes, we aimed to investigate the balance between CPS release and microbial breakdown, enabling a more accurate prediction of in-situ CPS concentrations under shifting environmental conditions.

3.5 Discussion

Microbial CPS degradation

The bacterial degradation of the diel vertical migration (DVM)-inducing kairomone exuded by cyprinids was first demonstrated in the laboratory study by Loose et al. (1993). However, this proof-of-concept study did not provide insights into the relevance of this process under natural conditions. More recent mesocosm experiments (Ahlers and Hahn et al. 2024) indicated potential in-situ CPS degradation, though microbial involvement was not conclusively established.

In our study, we provide robust evidence that microbial degradation is the primary driver of CPS breakdown in both lakes that we have investigated here, as demonstrated by the absence of degradation in autoclaved control samples. The determined half-lives at 18°C were 8.6 hours in RMNE and 16.1 hours in FS, indicating that, on average, approximately 85.7% and 64.4% of the CPS compound is degraded daily, respectively. These differences in degradation rates suggest variations in microbial community composition, activity, or environmental conditions influencing CPS dynamics. The faster degradation in RMNE likely reflects a more specialized microbial community, potentially adapted to utilizing CPS as a carbon source while mitigating its inherent toxicity due to its amphiphilic nature (Philipp 2011; Feller et al. 2021; Müller et al. 2021). Furthermore, higher initial CPS concentrations in RMNE may have stimulated microbial activity through substrate-induced enzymatic activation, a well-documented phenomenon in microbial ecology (Allison et al. 2014; Boetius and Lochte 1994; Hernández et al. 2012). These results underscore the intricate relationship between microbial communities and environmental factors in regulating CPS degradation.

Temperature as a key modulator of microbial degradation

Temperature has emerged as a critical factor influencing degradation rates, as demonstrated by the Q10 modeling approach. Bacteria play a key role in dissolved organic carbon degradation, with studies showing that microbial activity drives a significant amount of carbon breakdown in freshwater systems (Tranvik et al. 2009; Kawasaki et al. 2013). For this reason, the Q10 values used to model CPS degradation rates were derived from bacterial growth rates under varying temperature conditions, as reported by (Simon and Wünsch 1998; Beveridge et al. 2010). Temperature affects microbial metabolism and community dynamics by regulating cellular processes such as enzyme activity, metabolic rates, and trophic interactions (Beveridge et al. 2010; Moon et al. 2023). These effects, in turn, shape broader ecosystem functions, emphasizing the critical role of temperature in microbial-mediated degradation processes. For instance, in RMNE, degradation rates increased from 6.4% at 15°C to 12.3% at 25°C per hour, with the half-life of the CPS-molecule effectively halving with this increase of temperature. This rapid degradation of CPS mirrors findings by Mendelski et al. (2019), who observed complete degradation of the bile salt chenodeoxycholic acid in soil environments within 20 hours at room temperature. The rapid microbial breakdown observed in our study challenges previous assumptions about persistence of bile salts (and thus as well of CPS) in aquatic environments, emphasizing the transient nature of this infochemical. (Wyatt 2014; Buchinger et al. 2014; Hofmann and Mysels 1987).

Linking CPS exudation to feeding activity

Zooplankton populations fluctuate seasonally, strongly influencing the feeding rates of zooplanktivorous fish (Persson 1983b). Persson's study demonstrated significant seasonal fluctuations in fish food intake, with higher consumption rates observed during warmer months

due to increased metabolic demands and greater resource availability. Our exudation experiments demonstrated that CPS release is directly proportional to food intake. According to the Plankton Ecology Group (PEG) model (Sommer et al. 1986; Sommer et al. 2012) fish feeding rates closely follow seasonal shifts in prey availability, which, according to our results, in turn will influence CPS excretion. This suggests that natural CPS release is governed primarily by feeding intensity rather than by fish size or body mass. This challenges traditional metabolic scaling principles, which propose that excretion rates scale non-linearly with body size (Vanni and Gephart 2011; Morgan and Hicks 2013).

Instead, our findings indicate that CPS excretion follows a different pattern, likely driven by feeding frequency rather than metabolic constraints. Bile compounds are secreted into the gut lumen in response to food intake through complex physiological mechanisms (Maldonado-Valderrama et al. 2011; Buchinger et al. 2014; Di Ciaula et al. 2017). CPS constitutes the major bile compound in cyprinid fish (Hagey et al. 2010), and consequently, periods of increased feeding, such as during zooplankton blooms, are expected to result in significant CPS excretion peaks. The constancy of factorial aerobic scope (FAS) across fish sizes suggests that metabolic efficiency remains tightly regulated regardless of body size, further supporting the conclusion that food intake is the primary driver of CPS release (Huang et al. 2013).

Our results further demonstrate that, while larger fish can ingest greater amounts of food and thus excrete higher absolute quantities of CPS, size-normalized excretion rates are remarkably similar across different fish sizes. This finding aligns with (Persson 1983b), who observed that older roach have higher predicted daily food rations than younger ones, reinforcing the conclusion that food consumption is the primary driver of CPS exudation. As a consequence,

seasonal dynamics of planktonic organisms play a fundamental role in shaping CPS exudation patterns in lakes.

CPS has been demonstrated to induce two types of defenses in *Daphnia*, i.e. DVM and morphological changes (Hahn et al. 2019; Hahn & von Elert 2022; Ahlers and Hahn et al. 2024). We here show that the release of CPS by cyprinid fish is linearly related to the ingested food amount, which is in accordance with the function of bile salts as emulsifiers of lipids in the gut lumen. Accordingly, we expect that the identity of the prey is less important, so that the rate of kairomone release would not change greatly if a fish were fed *Daphnia* instead of mosquito larvae. However, it should be noted that for inducible changes in life history of *Daphnia*, for which the chemical nature of the kairomone released by fish is yet unknown (Von Elert & Stibor 2006), it has recently been demonstrated that the release of the kairomone depends on that the prey is phylogenetically closely related to *Daphnia* (Gu et al 2023).

Seasonal interplay of CPS and environmental factors

The seasonal dynamics of CPS concentrations in RMNE provide valuable insights into the interconnected roles of fish feeding, environmental conditions, and prey availability. CPS concentrations fluctuated throughout the season (from 40 ng/L up to a peak concentration of 900 ng/L), with a pronounced peak in August, likely driven by increased fish feeding activity during this period (Sommer et al. 2012).

Furthermore, experimental studies have demonstrated that CPS concentrations must exceed specific thresholds to induce behavioral and morphological responses in *Daphnia* species. Specifically, concentrations above 4-17 µg/L were required to trigger diel vertical migration (DVM) in *Daphnia longispina* in a mesocosm experiment (Ahlers and Hahn et al. 2024) and in

D. magna in an indoor setup DVM was induced already with 53 ng/L (Hahn et al. 2019). Morphological defenses such as helmet and spine elongation in the invasive species *Daphnia lumholtzi* have been observed at even lower concentrations, with significant changes occurring already at 5.31 ng/L (Hahn & von Elert, 2022). These findings highlight the ecological relevance of CPS exudation, demonstrating that even minimal concentrations can elicit profound biological effects.

When comparing seasonal CPS profiles with *Daphnia* abundance data, it becomes evident that the latter alone does not fully explain the observed CPS dynamics in RMNE. Although *Daphnia* populations peaked in June, CPS concentrations remained relatively low, suggesting that fish predation on *Daphnia* alone cannot fully account for kairomone levels. As *Daphnia* abundances declined in July and August, fish likely shifted their diet to alternative prey, such as *Chaoborus*, other zooplankton, or phytoplankton, as suggested by previous studies (Persson 1982; Brabrand 1985; Haertel and Eckmann 2002; Persson 1983b). During this time of the year, young fish have increased in body size and gape size, enabling them to target larger prey items, further diversifying their diet. Therefore, it seems reasonable to assume that this dietary flexibility allows fish to sustain CPS excretion even when *Daphnia* populations are reduced.

Interestingly, in August, water transparency reached its seasonal minimum, coinciding with the peak in CPS concentrations. The simultaneous occurrence of high CPS concentrations and decreased water transparency supports the hypothesis that elevated fish activity, particularly in response to increased temperatures, intensifies predation pressure on zooplankton, indirectly leading to higher phytoplankton biomass and reduced water clarity.

Rapid turnover of CPS in aquatic systems

One of the key findings of this study is the exceptionally rapid turnover of CPS in aquatic systems. Despite degradation rates of up to 85.7% per day in RMNE, in-situ CPS concentrations remained relatively stable, indicating a dynamic equilibrium between degradation and continuous exudation from cyprinid fish. At 18°C, over 85% of CPS molecules are degraded daily, yet the steady concentrations suggest a finely tuned balance capable of rapidly responding to environmental fluctuations.

This high turnover challenges the previously held assumption of CPS stability in aquatic environments and instead suggests that in-situ concentrations are highly dynamic and responsive to biotic and abiotic changes. Previously, CPS was considered a reliable indicator of predation risk, with DVM amplitudes in *Daphnia* increasing in response to CPS concentrations (Hahn and von Elert 2022). However, our findings suggest a more nuanced perspective: CPS concentrations do not solely reflect predator abundance but are also strongly influenced by predator feeding activity and microbial degradation. This underscores the need to reinterpret CPS as a highly dynamic chemical signal, modulated by ecological and environmental conditions rather than being a stable proxy for predation pressure alone.

Advancing predictive models for CPS and fish dynamics

The model for prediction of net CPS exudation represents a first step towards integrating biotic and abiotic factors into a predictive framework. Notably, the model successfully reflects the seasonal pattern of the observed CPS concentrations in RMNE, underscoring the critical role of fish feeding activity in shaping the CPS dynamics over time. However, the pronounced decline in CPS concentrations observed in June cannot be accounted for by the current model, which strongly suggests that additional factors, such as prey availability, shifts in fish diet, or

abiotic influences, must be incorporated to improve the model's predictive accuracy. Furthermore, the current model does not fully account for the dynamic nature of CPS concentrations, as it primarily reflects long-term (monthly) shifts in biotic and abiotic factors. The model may overlook short-term (daily) fluctuations that could play a crucial role in CPS turnover and ecosystem signaling. Incorporating variables like diel feeding rhythms, prey-specific exudation rates, and broader ecosystem interactions would offer a more comprehensive understanding of CPS dynamics in aquatic systems. Additionally, the model could serve as a useful tool for indirectly estimating fish populations, addressing the scarcity of reliable data on fish abundance in natural environments. By integrating key factors such as temperature, food intake, and exudation patterns, this model has the potential to bridge critical knowledge gaps and provide a novel framework for understanding fish-mediated ecological processes in complex aquatic ecosystems.

3.6 Author contribution statement

Johanna Ahlers and Eric von Elert conceptualized the study and developed the methods; Johanna Ahlers analyzed the data and prepared all figures and tables; and Johanna Ahlers together with Eric von Elert conducted the research, interpreted the data, and wrote the manuscript.

3.7 Acknowledgements

We extend our sincere gratitude to Jost Borcherding, Ann-Marie Waldvogel, Kristin Scharnweber and Alexander Popov from the Ökologische Forschungsstation Rees for their invaluable expertise, support, and provision of *Daphnia* abundance data and lake water samples throughout the season at Lake RMNE. We also thank Patrick Fink and Andrea Hoff from the

UFZ Water Analytics Laboratory (GEWANA) for their assistance in conducting the phosphorus measurements. We thank Marie Olbrich who performed the indoor fish exudation experiments. This research was generously supported by the German Science Foundation (DFG) through a grant awarded to EVE (EL 179/16-1). Open Access funding was partly provided by the University of Cologne and facilitated through Projekt DEAL.

3.8 References

1. Ahlers, J. and Hahn, M. A.; Stockenreiter, M.; Stibor, H.; von Elert, E. (2024): Mesocosm experiments validate induction of *Daphnia* vertical migration by the fish-derived kairomone 5α-cyprinol sulfate. *Limnol Oceanogr Letters* 9 (3), pp. 307–315.
2. Allison, S. D.; Chacon, S. S.; German, D. P. (2014): Substrate concentration constraints on microbial decomposition. *Soil Biology and Biochemistry* 79, pp. 43–49.
3. Beklioglu, M.; Cetin, A.G.; Zorlu, P.; Ay-Zog, D. (2006): Role of planktonic bacteria in biodegradation of fish-exuded kairomone in laboratory bioassays of diel vertical migration. *Archiv für Hydrobiologie* (1), pp. 89–104.
4. Beveridge, O.S.; Petchey, O. L.; Humphries, S. (2010): Direct and indirect effects of temperature on the population dynamics and ecosystem functioning of aquatic microbial ecosystems. *The Journal of Animal Ecology* 79 (6), pp. 1324–1331.
5. Boetius, A.; Lochte, K. (1994): Regulation of microbial enzymatic degradation of organic matter in deep-sea sediments. *Mar. Ecol. Prog. Ser.* 104, pp. 299–307.
6. Brabrand, Å. (1985): Food of roach (*Rutilus rutilus*) and ide (*Leusiscus idus*): significance of diet shift for interspecific competition in omnivorous fishes. In *Oecologia 66* (4), pp. 461–467.
7. Buchinger, T. J.; Li, W.; Johnson, N. S. (2014): Bile salts as semiochemicals in fish. *Chemical Senses* 39 (8), pp. 647–654.
8. Di Ciaula, A.; Garruti, G.; Lunardi Baccetto, R.; Molina-Molina, E.; Bonfrate, L.; Wang, D. Q-H; Portincasa, P. (2017): Bile acid physiology. *Annals of Hepatology* 16 (Suppl. 1: s3-105), s4-s14. DOI: 10.5604/01.3001.0010.5493.
9. Feller, F. M.; Holert, J.; Yücel, O.; Philipp, B. (2021): Degradation of bile acids by soil and water bacteria. *Microorganisms* 9 (8). DOI: 10.3390/microorganisms9081759.

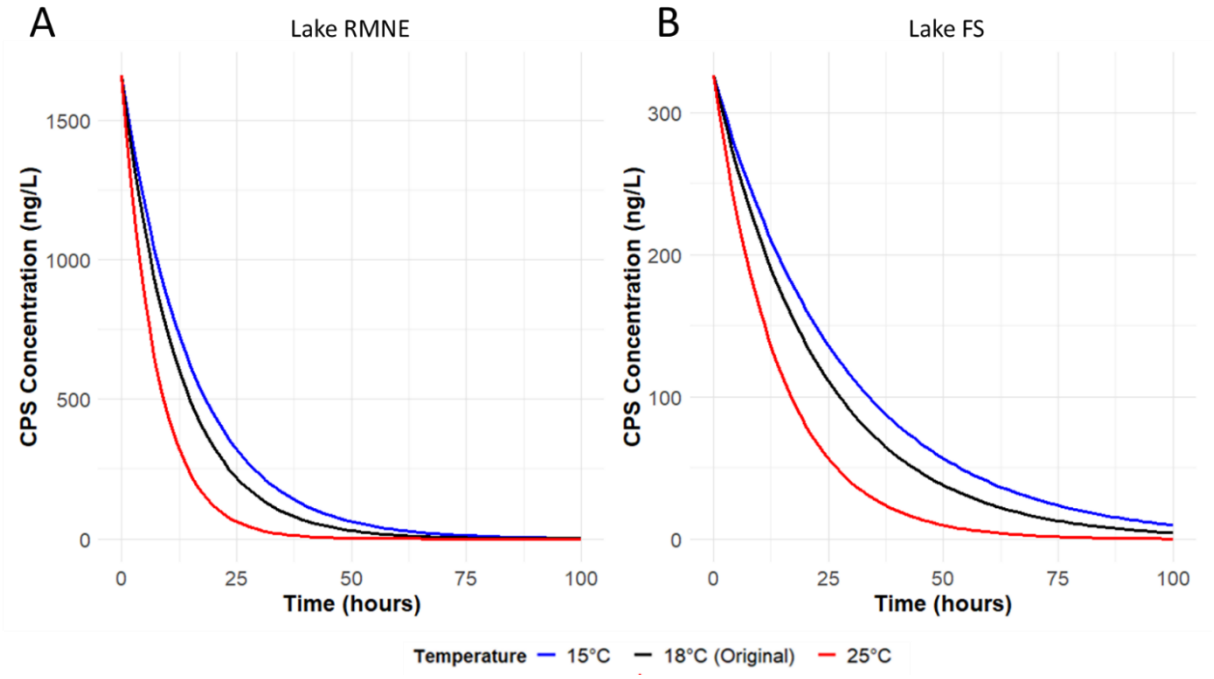
10. Ghuneim, L. J.; Distaso, M. A.; Chernikova, T. N.; Bargiela, R.; Lunev, E. A.; Korzhenkov, A. A. et al. (2021): Utilization of low-molecular-weight organic compounds by the filterable fraction of a lotic microbiome. *FEMS Microbiology Ecology* 97 (2). DOI: 10.1093/femsec/fiaa244.
11. Gorsky, G.; Ohman, M. D.; Picheral, M.; Gasparini, S.; Stemmann, L.; Romagnan, J. et al. (2010): Digital zooplankton image analysis using the ZooScan integrated system. *Journal of Plankton Research* 32 (3), pp. 285–303. DOI: 10.1093/plank
12. Gu, L.; de Meester, L.; Yang, Z. (2023): The role of prey and predator identity in eliciting inducible defenses of *Daphnia*. *Ecology* 104 (5), e4033. DOI: 10.1002/ecy.4033. t/fbp124.
13. Haertel, S. S.; Eckmann, R. (2002): Diel diet shift of roach and its implications for the estimation of daily rations. *Journal of Fish Biology* 60 (4), pp. 876–892. DOI: 10.1111/j.1095-8649.2002.tb02415.x.
14. Hagey, L. R.; Møller, P. R.; Hofmann, A. F.; Krasowski, M. D. (2010): Diversity of bile salts in fish and amphibians: evolution of a complex biochemical pathway. *Physiological and Biochemical Zoology*: PBZ 83 (2), pp. 308–321. DOI: 10.1086/649966.
15. Hahn, M. A.; Effertz, C.; Bigler, L.; von Elert, E. (2019): 5α-cyprinol sulfate, a bile salt from fish, induces diel vertical migration in *Daphnia*. *eLife* 8.
16. Hahn, M. A.; von Elert, E. (2022): One kairomone and multiple effects in *Daphnia* species—5α-Cyprinol sulfate induces morphological defenses in the invasive species *Daphnia lumholtzi*. *Front. Ecol. Evol.* 10, Article 804521.
17. Hernández, S. B.; Cota, I.; Ducret, A.; Aussel, L.; Casadesús, J. (2012): Adaptation and preadaptation of *Salmonella enterica* to bile. *PLoS Genetics* 8 (1), e1002459.

18. Hölker, F. (2003): The metabolic rate of roach in relation to body size and temperature. *Journal of Fish Biology* 62 (3), pp. 565–579.
19. Hölker, F. (2006): Effects of body size and temperature on metabolism of bream compared to sympatric roach. *Animal Biol* 56 (1), pp. 23–37.
20. Hofmann, A. F.; Mysels, K. J. (1987): Bile salts as biological surfactants. *Colloids and Surfaces* 30 (1), pp. 145–173.
21. Kawasaki, N.; Komatsu, K.; Kohzu, A.; Tomioka, N.; Shinohara, R.; Satou, T. et al. (2013): Bacterial contribution to dissolved organic matter in eutrophic Lake Kasumigaura, Japan. *Applied and Environmental Microbiology* 79 (23), pp. 7160–7168.
22. Loose, C. J.; von Elert, E.; Dawidowicz, P. (1993): Chemically-induced diel vertical migration in *Daphnia*: a new bioassay for kairomones exuded by fish. *Archiv_Hydrobiologie* 126 (3), pp. 329–337.
23. Maldonado-Valderrama, J.; Wilde, P.; Macierzanka, A.; Mackie, A. (2011): The role of bile salts in digestion. *Advances in Colloid and Interface Science* 165 (1), pp. 36–46.
24. Mendelski, M. N.; Dölling, R.; Feller, F. M.; Hoffmann, D.; Ramos Fangmeier, L.; Ludwig, K. C. et al. (2019): Steroids originating from bacterial bile acid degradation affect *Caenorhabditis elegans* and indicate potential risks for the fauna of manured soils. *Sci Rep* 9 (1), p. 11120.
25. Miner, B. E.; de Meester, L.; Pfrender, M. E.; Lampert, W.; Hairston, N. G. (2012): Linking genes to communities and ecosystems: *Daphnia* as an ecogenomic model. *Proc R Soc B* 279 (1735), pp. 1873–1882.
26. Moon, S.; Ham, S.; Jeong, J.; Ku, H.; Kim, H.; Lee, C. (2023): Temperature matters: bacterial response to temperature change. *Journal of Microbiology* 61 (3), pp. 343–357.

27. Morgan, D. K. J.; Hicks, B. J. (2013): A metabolic theory of ecology applied to temperature and mass dependence of N and P excretion by common carp. *Hydrobiologia* 705 (1), pp. 135–145.
28. Müller, F. M.; Holert, J.; Yücel, O.; Philipp, B. (2021): Degradation of bile acids by soil and water bacteria. *Microorganisms* 9 (8)
29. Persson, L. (1982): Rate of food evacuation in roach (*Rutilus rutilus*) in relation to temperature, and the application of evacuation rate estimates for studies on the rate of food consumption. *Freshwater Biology* 12 (3), pp. 203–210.
30. Persson, L. (1983): Food consumption and the significance of detritus and algae to intraspecific competition in roach (*Rutilus rutilus*) in a shallow eutrophic lake. *Oikos* 41 (1), p. 118.
31. Philipp, B. (2011): Bacterial degradation of bile salts. *Applied Microbiology and Biotechnology* 89 (4), pp. 903–915.
32. R . (2015) R: A Language and Environment for Statistical Computing. R Foundation for Statistical Computing: Vienna, Austria, http://www.R-project.org/.
33. Simon, M.; Wünsch, C. (1998): Temperature control of bacterioplankton growth in a temperate large lake. *Aquat. Microb. Ecol.* 16 (2), pp. 119–130.
34. Sommer, U.; Gliwicz, Z. M.; Lampert, W.; Duncan, A. (1986): The PEG-model of seasonal succession of planktonic events in fresh waters. *Arch. Hydrobiol.* 106 (4), pp. 433–471.
35. Sommer, U.; Adrian, R.; de Senerpont Domis, Lisette; Elser, J. J.; Gaedke, U.; Ibelings, B. et al. (2012): Beyond the plankton ecology group (PEG) model: mechanisms driving plankton succession. *Annu. Rev. Ecol. Evol. Syst.* 43 (1), pp. 429–448.

36. Sterr, B.; Sommaruga, R. (2008): Does ultraviolet radiation alter kairomones? An experimental test with *Chaoborus obscuripes* and *Daphnia pulex*. *Journal of Plankton Research* 30 (12), pp. 1343–1350.
37. Tranvik, L. J.; Downing, J. A.; Cotner, J. B.; Loiselle, S.A.; Striegl, R. G.; Ballatore, T. J. et al. (2009): Lakes and reservoirs as regulators of carbon cycling and climate. *Limnology and Oceanography* 54 (6part2), pp. 2298–2314.
38. Vanni, J. M.; Gephart, J. A. and the Ecological Society of America (2011): Metabolic ecology: how do body size and temperature affect nutrient cycling rates? *Teaching Issues and Experiments in Ecology (TIEE),* v. 7.
39. Vogelmann, C.; Teichert, M.; Schubert, M.; Martens, A.; Schultes, S.; Stibor, H. (2022): The usage of a zooplankton digitization software to study plankton dynamics in freshwater fisheries. *Fisheries Research* 251, p. 106326.
40. Von Elert, E.; Loose, C. J. (1996): Predator-induced diel vertical migration in *Daphnia*: enrichment and preliminary chemical characterization of a kairomone exuded by fish. *Journal of Chemical Ecology* 22 (5), pp. 885–895.
41. Von Elert, E.; Stibor, H. (2006): Predator-mediated life history shifts in *Daphnia*: enrichment and preliminary chemical characterisation of a kairomone exuded by fish. *Archiv Hydrobiologie* 167 (1-4), S. 21–35.
42. Von Elert, E. (2012): Information conveyed by chemical cues, Chemical ecology in aquatic systems. [eds.] C. Brönmark and L.-A. Hansson, Oxford Univ. Press. p. 19–38.
43. Vrede, K. (2005): Nutrient and temperature limitation of bacterioplankton growth in temperate lakes. *Microbial Ecology* 49 (2), pp. 245–256.
44. Wyatt, T. D. (2014): Pheromones and Animal Behavior. Chemical Signals and Signatures: Cambridge University Press.

3.9 Supporting information



SI Figure 1: Modeled exponential decay of 5α-cyprinol sulfate (CPS) concentrations over time (ng/L) for non-autoclaved lake water from two lakes sampled in June 2024. (A) CPS concentrations in lake RMNE. (B) CPS concentrations in lake FS. The black line represents modeled CPS concentrations at 18°C based on determined data. The blue and red lines represent modeled CPS concentrations adjusted to 15°C and 25°C, respectively, using Q10 scaling based on bacterial cell multiplication (BCM) as described by Simon and Wünsch (1998). The modeled curves span the time interval from 0 to 100 hours.

Effect	*Estimate*	*Std. Error*	*t-value*	*p-value*	*Interpretation*
(Intercept)	*5,78678*	*0,37333*	*15,501*	*<0.001*	*Log-transformed initial CPS concentration for FS (reference lake).*
time	*-0,04301*	*0,00631*	*-6,816*	*<0.001*	*Significant degradation rate (k) for FS.*
LakeRMNE	*1,62809*	*0,52549*	*3,098*	*0.00687*	*RMNE has a significantly higher initial CPS concentration compared to*
time:LakeRMNE	*-0,038*	*0,01039*	*-3,658*	*0.00211*	*RMNE has a significantly faster degradation rate compared to FS.*

SI Table 1: Results of a linear mixed-effects model (lme) used to analyze log-transformed CPS concentrations of autoclaved water (Control) over time in degradation experiments.

Effect	*Estimate*	*Std. Error*	*t-value*	*p-value*	*Interpretation*
(Intercept)	5.493	0.127	43.415	<0.001	Log-transformed initial CPS concentration for FS (reference lake).
time	0.0002	0.002	0.091	0.929	No significant degradation rate (k) for FS.
RMNE	0.490	0.188	2.604	0.017	RMNE has a significantly higher initial CPS concentration compared to FS.
time:RMNE	-0.003	0.004	-0.716	0.483	No significant difference in degradation rates between RMNE and FS.

SI Table 2: Results of a linear mixed-effects model (lme) used to analyze log-transformed CPS concentrations of non-autoclaved water (NA treatment) over time in degradation experiments.

Effect	*Estimate*	*Std. Error*	*t-value*	*p-value*	*Interpretation*

(Intercept)	5.787	0.373	15.501	<0.001	Log-transformed initial CPS concentration for FS (reference lake).
time	-0.043	0.006	-6.816	<0.001	Significant degradation rate (k) for FS.
RMNE	1.628	0.525	3.098	0.007	RMNE has a significantly higher initial CPS concentration compared to FS.
time:RMNE	-0.038	0.0104	-3.658	0.002	RMNE has a significantly faster degradation rate compared to FS.

General Discussion

The present dissertation explored the ecological significance, behavioral consequences, and dynamic nature of the fish-derived kairomone, 5α-cyprinol sulfate (CPS), with a particular focus on its role in driving diel vertical migration (DVM) in *Daphnia*. Understanding predator-prey interactions has long been central to ecological research (Lima and Dill 1990; Abrams 2000), as these interactions profoundly influence population dynamics, community structures, and ecosystem functioning. Within this framework, chemically mediated interactions are especially intriguing because kairomones as the underlying infochemicals, provide prey with critical information about predator presence and predation risk without direct encounters (Kats and Dill 1998; Ferrari et al. 2010). DVM is a well-studied behavioral adaptation characterized by daily vertical shifts in zooplankton positioning within the water column, significantly influencing nutrient cycling, primary productivity, and energy transfer through trophic levels. However, DVM is just one component of a diverse spectrum of predator-induced phenotypic changes in *Daphnia*, which also include life-history shifts, altered growth rates, changes in reproductive timing, and morphology (Boersma et al. 1998; Stoks et al. 2016). Understanding the extent to which CPS contributes to this full defensive phenotype remains an important and open question.

Despite extensive research into DVM, the chemical signals triggering this behavior under natural conditions remain insufficiently explored, particularly concerning their spatial and temporal dynamics in natural ecosystems. Therefore, by investigating CPS, a recently identified kairomone excreted by cyprinid fish known to induce DVM in laboratory settings, this research aimed to address crucial gaps between experimental studies and field realities. The motivation behind Chapter 1 was specifically to test the ecological relevance and effectiveness of CPS-

induced DVM in natural zooplankton communities under realistic conditions, employing field mesocosms to validate laboratory-based predictions. Chapter 2 aimed to move beyond confirming kairomone effectiveness by examining how CPS concentrations fluctuate in natural ecosystems, thereby developing a nuanced understanding of chemically mediated predation risk as a dynamic "landscape of fear." This concept, adapted from terrestrial ecology, considers spatial and temporal variations in predation risk as drivers of prey behavior and ecosystem processes (Gaynor et al. 2019; Laundré et al. 2010).

Further expanding on these interactions, Chapter 3 delved into the microbial degradation controlling CPS persistence and turnover in natural aquatic environments. Kairomone availability is a balance between continuous predator excretion and microbial degradation, yet the latter process remains poorly understood. Addressing this knowledge gap provides essential insights into the stability and reliability of chemical signals in aquatic ecosystems. Through an integrative approach involving field mesocosm experiments, comprehensive in-situ kairomone quantification, controlled laboratory bioassays, and detailed microbial degradation analyses, this dissertation substantially enhances our comprehension of chemically mediated interactions and their broader ecological implications. This work underscores the complexity of predator-prey dynamics and emphasizes the necessity of considering chemical signaling within environmental contexts, including microbial community interactions, evolutionary responses, and the broader implications of these processes in the context of environmental and climate changes.

Validation of CPS as a kairomone under near-natural conditions

Chapter 1 provided crucial evidence demonstrating that CPS effectively induces DVM in natural zooplankton communities under near-natural conditions. Previous laboratory studies

had identified CPS as an inducer of normal DVM patterns in *Daphnia magna* at concentrations as low as 100 pmol/L (Hahn et al. 2019). However, the mesocosm experiments presented here significantly advanced this knowledge by demonstrating that *Daphnia longispina* responded to CPS at environmentally realistic concentrations exceeding 2 nmol/L. These results confirm that CPS functions as an ecologically relevant cue, with in-situ concentrations being sufficiently high to trigger predator-avoidance behavior in natural communities.

Interestingly, a notable differential response between species was observed, with *Daphnia cucullata* exhibiting minimal responsiveness to CPS. This aligns with previous research indicating a preference by fish for larger prey, thus explaining the selective pressure on larger-bodied *Daphnia* species like *D. longispina* (Gliwicz and Pijanowska 1989; Tollrian and Harvell 1999). Additionally, the absence of pronounced upward migration at night observed in mesocosms and in Lake Klostersee can be attributed to multiple factors, such as suboptimal food conditions at the surface and elevated food quality at the deep chlorophyll maximum (DCM), as well as meteorological conditions, notably moonlight (Ringelberg 2010; Williamson et al. 2011). This complex interplay of factors highlights that DVM expression is not solely driven by CPS but is modulated by food availability and abiotic conditions, reflecting an adaptive trade-off strategy.

The establishment of a reliable method for CPS quantification in natural systems represents another significant advancement. This methodological progress enables the analysis of the kairomone's temporal and spatial dynamics, laying the groundwork for exploring predator-prey interactions through chemically mediated "landscapes of fear."

Expanding the landscape of fear concept to aquatic systems

Chapter 2 extends the chemical ecology perspective by conceptualizing CPS as a measurable component of the aquatic "landscape of fear." Drawing parallels with terrestrial ecosystems (Hopcraft et al. 2014; Kohl et al. 2018), this study showed that CPS concentrations in Lake Klostersee in Bavaria exhibit distinct diel and seasonal fluctuations, reflecting real-time shifts in predation risk perception by *Daphnia*. Seasonal variations in CPS, peaking in the warmer months, likely coincide with increased fish metabolic rates and intensified feeding, supporting the role of CPS as a dynamic indicator of predation pressure.

Investigations of the diel fluctuations of CPS concentrations were equally enlightening. Higher CPS concentrations in surface waters at night strongly suggested diel vertical movements of fish, influencing prey positioning. *Daphnia* adjusted their vertical distribution according to these CPS gradients, strategically exploiting the intermediate layers near the thermocline and thereby balancing predator avoidance and access to putatively high-quality food at the DCM. Notably, the rapid reduction in CPS concentrations following storm events underscores the sensitivity of this chemical landscape to abiotic disturbances, highlighting the dynamic nature of chemically mediated predator-prey interactions.

Genotypic variability among *Daphnia* clones in their CPS sensitivity thresholds emerged as a significant finding, suggesting that genetic diversity allows different clones to exploit varying temporal niches across seasons. This genetic variation within populations explains observed seasonal shifts in DVM amplitudes (de Meester et al. 1995), thereby influencing nutrient cycling and energy transfer within the lake ecosystem (Haupt et al. 2010). Such intra-population variability reinforces the notion that chemically mediated behaviors are subject to evolutionary

pressures and ecological trade-offs, further enriching the complexity of predator-prey dynamics.

Microbial dynamics and biogeochemical turnover of CPS

Chapter 3 provided compelling evidence for the rapid microbial degradation of CPS in natural waters, challenging previous assumptions about the chemical stability of bile salts. Degradation experiments demonstrated significant microbial-driven CPS turnover, with daily degradation rates ranging from 64% to 86%. This microbial activity varied significantly between lakes, suggesting distinct microbial community structures and adaptive strategies in response to CPS availability.

The rapid turnover of CPS underscores its role as a short-lived chemical cue, ideally suited for conveying real-time information about predator presence and feeding activity. Moreover, temperature emerged as a critical modulator of microbial degradation, with degradation rates increasing markedly at higher temperatures. This temperature dependency highlights the sensitivity of CPS dynamics to global warming, emphasizing the need to incorporate microbial processes into predictive ecological models.

Linking CPS exudation directly to fish feeding activity further reinforced the dynamic nature of this kairomone. Contrary to traditional metabolic scaling, CPS excretion rates correlated linearly with food intake, irrespective of fish size. This result emphasizes the metabolic linkage between predator foraging behavior and CPS production, providing a mechanistic understanding of how CPS concentrations reflect predator feeding intensity rather than merely predator abundance.

The predictive model developed for CPS dynamics integrated exudation and degradation processes, successfully capturing the seasonal fluctuations observed in natural systems. However, limitations identified in the model underscore the necessity for incorporating additional factors, such as shifts in prey availability and fish diet composition, and short-term environmental variability, to enhance its accuracy and ecological relevance.

Perspectives and future directions

Collectively, these findings further elucidate and extend the role of CPS as a pivotal infochemical mediating predator-prey interactions in freshwater ecosystems. By integrating mesocosm experiments, high-resolution in-situ analyses, and detailed microbial studies, this dissertation establishes CPS as a dynamic and ecologically significant cue that orchestrates behavioral adaptations in prey and shapes ecosystem structure and function.

Future research should further explore the interaction between CPS dynamics, environmental conditions, and ecological trade-offs governing DVM expression. Studies could incorporate additional environmental stressors such as UV radiation, hypoxia, and nutrient fluctuations, providing a comprehensive view of how chemically mediated behaviors adapt to multiple stressors. Furthermore, expanding the predictive modeling framework to incorporate finer-scale temporal dynamics, predator-prey feedbacks, and microbial community composition would enhance its robustness and applicability across diverse freshwater ecosystems. Such integrative models could also serve as valuable tools for indirectly assessing fish population dynamics, addressing current challenges in aquatic ecosystem monitoring.

This dissertation also opens new perspectives for understanding how chemically mediated defenses in *Daphnia* are shaped by cue diversity and complexity. Future studies should

investigate whether different predator species produce structurally distinct kairomones, and whether *Daphnia* integrates these signals in an additive or hierarchical fashion. Exploring whether threshold sensitivity to CPS shifts in the presence of other fish cues could reveal flexible risk assessment strategies. Additionally, more work is needed to understand how many traits beyond DVM are influenced by CPS. Since *Daphnia* exhibits predator-induced changes across life-history, morphological, and physiological traits, determining whether CPS alone can elicit this full spectrum of defenses is key to understanding its role as a generalizable risk cue. Finally, following the insights of Gu et al. (2023), future studies should explore more deeply how the identity of prey species shapes kairomone production. If feeding on *Daphnia* induces additional alarm cues, the resulting blend of signals may enhance the perception of predation risk, potentially interacting with CPS to modulate prey responses. This could reshape the chemical landscape of fear and add further complexity to predator-prey dynamics.

In conclusion, this dissertation significantly advances our understanding of chemical communication in aquatic predator-prey systems. By characterizing the complex interplay between CPS production, microbial degradation, prey genotype variability, and environmental context, this work provides a robust foundation for future explorations into the ecological and evolutionary dynamics of chemically mediated interactions. The insights gained here offer profound implications for managing freshwater ecosystems in the face of environmental change, underscoring the critical role of chemical ecology in ecological research and conservation strategies.

General References

1. Abrams, P. A. (2000). The evolution of predator-prey interactions: theory and evidence. *Annu. Rev. Ecol. Syst.* 31: 79–105.
2. Ahlers, J. and Hahn, M. A.; Stockenreiter, M.; H. Stibor; von Elert, E. (2024). Mesocosm experiments validate induction of *Daphnia* vertical migration by the fish-derived kairomone 5α-cyprinol sulfate. *Limnol. Oceanogr. Letters* 9: 307–315.
3. Boersma, M.; Spaak P.; de Meester, L. (1998). Predator-mediated plasticity in morphology, life history, and behavior of *Daphnia*: the uncoupling of responses. *Am. Nat.* 152: 237–248.
4. Brant, C. O.; Chung-Davidson, Y.-W.; Li, K.; Scott, A. M.; Li, W. (2013). Biosynthesis and release of pheromonal bile salts in mature male sea lamprey. *BMC Biochem*. 14: 30.
5. Brönmark, C. and Hansson, L.-A. [Eds.] (2012). *Chemical Ecology in Aquatic Systems.* Oxford University Press.
6. Brooks, J. L. and Dodson, S. I. (1965). Predation, body size, and composition of plankton. Science 150: 28–35.
7. Brown, W. L.; Eisner, T.; Whittaker, R. H. (1970). Allomones and kairomones: transspecific chemical messengers. *BioScience* 20: 21–22.
8. Cousyn, C.; de Meester, L.; Colbourne, J. K.; Brendonck, L.; Verschuren, D.; Volckaert, F. (2001). Rapid, local adaptation of zooplankton behavior to changes in predation pressure in the absence of neutral genetic changes. *Proc. Natl. Acad. Sci. U.S.A.* 98: 6256–6260.
9. de Meester, L.; Boersma, M.; Spaak, P. (1999). Environmental stress and local adaptation in *Daphnia magna. Limnol. Oceanogr.* 44: 393–402.

10. de Meester, L.; Weider, L. J.; Tollrian, R. (1995). Alternative antipredator defences and genetic polymorphism in a pelagic predator–prey system. *Nature* 378: 483–485.
11. Diel, P.; Keine, M.; Martin-Creuzburg, D.; Laforsch, C. (2020). Knowing the enemy: inducible defences in freshwater zooplankton. *Diversity* 12: 147.
12. Dodson, S. (1988). The ecological role of chemical stimuli for the zooplankton: predator-avoidance behavior in *Daphnia*. Limnol. *Oceanogr*. 33: 1431–1439.
13. Draper, A. M. and Weissburg, M. J. (2019). Impacts of global warming and elevated CO2 on sensory behavior in predator-prey interactions: a review and synthesis. *Front. Ecol. Evol.* 7: 72.
14. Ebert, D. (2022). *Daphnia* as a versatile model system in ecology and evolution. *EvoDevo* 13: 16.
15. Engel, K.; Schreder, T.; Tollrian, R. (2014). Morphological defences of invasive *Daphnia lumholtzi* protect against vertebrate and invertebrate predators. *J. Plankton Res.* 36: 1140–1145.
16. Ferrari, M. C. O.; Wisenden, B. D.; Chivers, D. P. (2010). Chemical ecology of predator–prey interactions in aquatic ecosystems: a review and prospectus. *Can. J. Zool.* 88: 698–724.
17. Gaynor, K. M.; Brown, J. S.; Middleton, A. D.; Power, M. E.; Brashares, J. S. (2019). Landscapes of fear: spatial patterns of risk perception and response. Trends *Ecol. Evol.* 34: 355–368.
18. Gliwicz, M. Z. (1986). Predation and the evolution of vertical migration in zooplankton. *Nature* 320: 746–748.
19. Gliwicz, Z. M and Pijanowska, J. (1989). The role of predation in zooplankton succession. *Plankton Ecology*, Springer, Berlin, Heidelberg: 253–296.

20. Gu, L.; de Meester, L.; Yang. Z. (2023). The role of prey and predator identity in eliciting inducible defenses of *Daphnia*. *Ecology* 104: e4033.
21. Hahn, M.A. and von Elert, E. (2022). One kairomone and multiple effects in *Daphnia* species—5α-Cyprinol sulfate induces morphological defenses in the invasive species *Daphnia lumholtzi*. *Front. Ecol. Evol.* 10: 804521.
22. Hahn, M. A.; Effertz C.; Bigler L.; von Elert, E. (2019). 5α-cyprinol sulfate, a bile salt from fish, induces diel vertical migration in *Daphnia*. *eLife* 8: e44791.
23. Haupt, F.; Stockenreiter, M.; Reichwaldt, E. S.; Baumgartner, M.; Lampert, W.; Boersma, M.; Stibor, H. (2010). Upward phosphorus transport by *Daphnia* diel vertical migration. *Limnol. Oceanogr.* 55: 529–534.
24. Hopcraft, J. G. C.; Morales, J. M.; Beyer, H. L.; Borner, M.; Mwangomo, E.; Sinclair, A. R. E. et al. (2014). Competition, predation, and migration: individual choice patterns of Serengeti migrants captured by hierarchical models. *Ecol. Monogr.* 84: 355–372.
25. Kats, L. B. and Dill, L. M. (1998). The scent of death: chemosensory assessment of predation risk by prey animals. *Écoscience* 5: 361–394.
26. Kohl, M. T.; Stahler, D. R.; Metz, M. C.; Forester, J. D.; Kauffman, M. J.; Varley, N. et al. (2018). Diel predator activity drives a dynamic landscape of fear. *Ecol. Monogr.* 88: 638–652.
27. Laforsch, C. and Tollrian, R. (2004). Inducible defenses in multipredator environments: cyclomorphosis in *Daphnia cucullata*. *Ecology* 85: 2302–2311.
28. Lass, S. and Spaak, P. (2003). Chemically induced anti-predator defences in plankton: a review. *Hydrobiologia* 491: 221–239.

29. Laundré, J. W.; Hernández, L.; Altendorf, K. B. (2001). Wolves, elk, and bison: reestablishing the "landscape of fear" in Yellowstone National Park, U.S.A. *Can. J. Zool*. 79: 1401–1409.

30. Laundré, J. W.; Hernández, L.; Ripple, W. J. (2010). The landscape of fear: ecological implications of being afraid. *Open Ecol*. J. 3: 1–7.

31. Lima, S. L. and Dill, L. M. (1990). Behavioral decisions made under the risk of predation: a review and prospectus. *Can. J. Zool.* 68: 619–640.

32. Loose, C. J. and Dawidowicz, P. (1994). Trade-offs in diel vertical migration by zooplankton: the costs of predator avoidance. *Ecology* 75: 2255–2263.

33. Miner, B. E.; de Meester, L.; Pfrender, M. E.; Lampert, W.; Hairston, N. G. (2012). Linking genes to communities and ecosystems: *Daphnia* as an ecogenomic model. *Proc. Biol. Sci.* 279: 1873–1882.

34. Müller, C.; Caspers, B. A.; Gadau, J.; Kaiser, S. (2020). The power of infochemicals in mediating individualized niches. *Trends Ecol. Evol.* 35: 981–989.

35. Ogorelec, Ž.; Wunsch, C., A; Kunzmann, J.; Octorina, P.; Navarro, J. I. (2021). Large daphniids are keystone species that link fish predation and phytoplankton in trophic cascades. *Fundam. Appl. Limnol.* 194: 297–309.

36. Pohnert, G.; Steinke, M.; Tollrian, R. (2007). Chemical cues, defence metabolites and the shaping of pelagic interspecific interactions. *Trends Ecol. Evol.* 22: 198–204.

37. Polkinghorne, C. N.; Olson, J. M.; Gallaher, D. G.; Sorensen; P. W. (2001). Larval sea lamprey release two unique bile acids to the water at a rate sufficient to produce detectable riverine pheromone plumes. *Fish Physiol. Biochem*. 24: 15–30.

38. Rajchard, J. (2013). Kairomones—important substances in interspecific communication in vertebrates: a review. *Vet. Med.* 58: 561–566.

39. Ringelberg, J. (2010). Diel vertical migration in lakes. *Diel Vertical Migration of Zooplankton in Lakes and Oceans*, Springer, Dordrecht: 171–215.

40. Roggatz, C. C.; Saha, M.; Blanchard, S.; Schirrmacher, P.; Fink, P.; Verheggen, F.; Hardege, J. D. (2022). Becoming nose-blind—climate change impacts on chemical communication. *Glob. Change Biol.* 28: 4495–4505.

41. Rose, K. C.; Williamson, C. E.; Fischer, J. M.; Connelly, S. J.; Olson, M.; Tucker, A. J.; Noe, D. A. (2012). The role of ultraviolet radiation and fish in regulating the vertical distribution of *Daphnia*. *Limnol. Oceanogr*. 57: 1867–1876.

42. Scrosati, R. A. (2021). Nonconsumptive predator effects on prey demography: recent advances using intertidal invertebrates. *Front. Ecol. Evol.* 9: 626869.

43. Stich, H.-B. and Lampert, W. (1981). Predator evasion as an explanation of diurnal vertical migration by zooplankton. *Nature* 293: 396–398.

44. Stoks, R.; Govaert, L.; Pauwels, K.; Jansen, B.; de Meester, L. (2016). Resurrecting complexity: the interplay of plasticity and rapid evolution in the multiple trait response to strong changes in predation pressure in the water flea *Daphnia magna*. *Ecol. Lett.* 19: 180–190.

45. Tollrian, R. and Harvell, C. D. (Eds.) (1999). The Ecology and Evolution of Inducible Defenses. *Princeton University Press.*

46. Tollrian, R. (1995). Predator-induced morphological defenses: costs, life history shifts, and maternal effects in *Daphnia pulex*. *Ecology* 76: 1691–1705.

47. von Elert, E. and Loose, C. J. (1996). Predator-induced diel vertical migration in *Daphnia*: enrichment and preliminary chemical characterization of a kairomone exuded by fish. *J. Chem. Ecol.* 22: 885–895.
48. von Elert, E. and Pohnert, G. (2000). Predator specificity of kairomones in diel vertical migration of *Daphnia*: a chemical approach. *Oikos 88:* 119–128.
49. Weider, L. J. and Pijanowska, J. (1993). Plasticity of *Daphnia* life histories in response to chemical cues from predators. *Oikos* 67: 385–392.
50. Williamson, C. E.; Fischer, J. M.; Bollens, S. M.; Overholt, E. P.; Breckenridge, J. K. (2011). Toward a more comprehensive theory of zooplankton diel vertical migration: integrating ultraviolet radiation and water transparency into the biotic paradigm. *Limnol. Oceanogr.* 56: 1603–1623.
51. Zhang, C.; Goitom, E.; Brans, K.; de Meester, L.; Stoks, R. (2022). Scared to evolve? Non-consumptive effects drive rapid adaptive evolution in a natural prey population. *Proc. Biol. Sci.* 289: 20220188.

List of Publications

[1]Ahlers, Johanna and Hahn, Meike A.; Stockenreiter, Maria; Stibor, Herwig; von Elert, Eric (2024): Mesocosm experiments validate induction of *Daphnia* vertical migration by the fish-derived kairomone 5α-cyprinol sulfate. *Limnol Oceanogr Letters* 9 (3), pp. 307–315.

[2]Ahlers, Johanna, von Elert, Eric (2025): Signals in flux: Investigating the seasonal turnover of the cyprinid kairomone 5α-cyprinol sulfate. *Freshwater Biology*. [manuscript in review]

[1] Corresponds to Chapter 1

[2] Corresponds to Chapter 3

Acknowledgements

First and foremost, I would like to express my deepest gratitude to **Prof. Dr. Eric von Elert** for his continuous support, guidance, and inspiring supervision throughout the course of this dissertation. His scientific insight and encouragement have been invaluable. I always felt very welcome and supported in his research group, which provided an inspiring and comfortable environment to grow both scientifically and personally. I will always remember how much I looked forward to our group's Christmas dinners, and I sincerely hope we will stay in touch long after this work is finished.

I would also like to thank **Prof. Dr. Patrick Fink**, my second examiner, for his interest in my work and his constructive feedback during the evaluation process.

Special thanks go to **Prof. Dr. Mathias Schäfer** and **Dr. Maja Ilić** for chairing and participating in my defense examination with kind support.

I am deeply grateful to **Dr. Maria Stockenreiter** for the great collaboration and assistance during our fieldwork at Lake Klostersee in Seeon. I will always fondly remember the beautiful days in the field and your warm hospitality.

My sincere thanks go to **Dr. Carlos Sanchez**, for introducing me to the world of metabolomics and for the dedicated collaboration and training on the LC-MS, both in the lab and in the field.

I also want to thank **Dr. Susanne Brodesser** and **Dr. Marlen Schmidtendorf** for their kind cooperation, technical expertise, and support with the LC-MS analyses at the CECAD.

A very warm thank you to **Prof. Dr. Jost Borcherding** and **Dr. Kristin Scharnweber** for their helpful insights and support regarding fish data and fish husbandry, as well as for kindly welcoming me to the Rees field station.

I am also truly thankful to my wonderful colleagues **Thomas von Einem**, **Sascha Dopf**, and **Kathrin Otte** for creating such a pleasant and supportive working environment and for the countless insightful and joyful conversations we shared along the way.

To my dear friends **Daniela Niedeggen** and **Angela Heisterkamp**, thank you for your unwavering support and companionship throughout our study journeys – and for all the coffee breaks, laughs, and heartfelt talks that made this time so special.

I would also like to thank the dedicated students who contributed their time and energy to my experimental work: **Marie Olbrich**, **Jakob Büssemaker**, **Bianca Heckman**, **Finja Kollorz**, **Jonas Lange**, and **Tom Leven**. Your support and team spirit made all the difference.

My deepest gratitude goes to my parents **Christiane** and **Norbert**, for their endless support, encouragement, and belief in me throughout my entire academic journey. Your love and guidance have been a constant source of strength and motivation. You have always been role models for me, and I am deeply proud of you.

Finally, my heartfelt thanks to my husband and best friend **Felix**, for standing by my side every step of the way, for his patience, support, and love. Thank you for everything and for the wonderful time we shared in Cologne during this chapter of our lives.